Ion-ion, ion-molecule, and ion-electron reactions affecting the response of the electron capture detector to resonance electron capturing compounds

by Cornelius Andrew Valkenburg

A thesis submitted in partial fulfillment of the requirements for the degree of Doctor of Philosophy in Chemistry
Montana State University

Abstract:
The electron capture detector (ECD) response to resonance electron capturing compounds is shown to be affected not only by the electron capture reaction, but also by the detailed nature of the subsequent competitive reaction dynamics. For aromatic molecules with a low electron affinity, two processes accompany the electron capture reaction. These additional processes are electron detachment from the molecular negative ion and the protonation of the analyte molecules. Results are presented in which the effects of these two undesired reactions are eliminated by the chemical doping of the detector make-up gas with a high proton affinity amine and an alkylmono-chloride. In the detector gas these dopants alter and stabilize the reaction dynamics and provide greatly increased sensitivity, linearity, and reproducibility of the ECD response to polycyclic aromatic molecules. For numerous PAH's, ECD responses were measured as a function of analyte concentration, detector temperature, dopant type, and dopant concentration. Identification of the charged species in the ECD plasma was accomplished by a specialized ECD interfaced to a quadrupole mass spectrometer.

Theoretical modeling of the constant current ECD response to resonance electron capturing compounds includes a kinetic model to explain the mechanism of response with the amine and alkyl monochloride dopants. The existing theoretical models of resonance electron capture in the ECD are Improved and supported by the results presented here.

Utilizing two ECD cells in series, experiments are described in which the tendency for regeneration of the parent molecule from the molecular anion by recombination with positive ions was investigated. The efficiency of molecular regeneration for molecules with a high electron affinity is determined from the ratio of the response in the tandem cells and the compound's known electron attachment rate. Theoretical models and results for compounds responding by a resonance and a dissociative electron capture mechanism are presented. Differences in the molecular anion behavior in the recombination reaction are discussed, as well as the application of this technique to tandem cell coulometry.

ION-ION, ION-MOLECULE, AND ION-ELECTRON REACTIONS AFFECTING THE RESPONSE OF THE ELECTRON CAPTURE DETECTOR TO RESONANCE ELECTRON CAPTURING COMPOUNDS

by

Cornelius Andrew Valkenburg

A thesis submitted in partial fulfillment
of the requirements for the degree

of

Doctor of Philosophy

in

Chemistry

MONTANA STATE UNIVERSITY
Bozeman, Montana

May 1987

APPROVAL

of a thesis submitted by

Cornelius Andrew Valkenburg

This thesis has been read by each member of the thesis committee and has been found to be satisfactory regarding content, English usage, format, citations, bibliographic style, and consistency, and is ready for submission to the College of Graduate Studies.

6/23/87
Date

Eric Dumsrud
Chairperson, Graduate Committee

Approved for the Major Department

6/23/87
Date

Edwin H Abbott
Head, Major Department

Approved for the College of Graduate Studies

6/24/87
Date

Henry L Parsons
Graduate Dean

STATEMENT OF PERMISSION TO USE

In presenting this thesis in partial fulfillment of the requirements for a doctoral degree at Montana State University, I agree that the Library shall make it available to borrowers under rules of the Library. I further agree that copying of this thesis is allowable only for scholarly purposes, consistent with "fair use" as prescribed in the U.S. Copyright Law. Requests for extensive copying or reproduction of this thesis should be referred to University Microfilms International, 300 North Zeeb Road, Ann Arbor, Michigan 48106, to whom I have granted "the exclusive right to reproduce and distribute copies of the dissertation in and from microfilm and the right to reproduce and distribute by abstract in any format."

Signature Cornelius A. Vallenburg Jr.

Date 6-12-1987

To my wife Linda, and son Casey, for the joy and optimism in life they have given me, and the hopes and dreams we share for the future. To my parents, for their unwavering support and faith in me.

VITA

Cornelius Andrew Valkenburg was born November 28, 1957 in Hamilton, Ontario, Canada, the son of Dutch immigrants, Cornelis and Johanna Valkenburg. He graduated in 1975 from Stevenson High School, Stevenson, Washington.

He majored in Biology at Carroll College in Helena, Montana, and graduated with honors in May of 1979. He then worked for one year as a chemical research technician with Oregon Graduate Center in Beaverton, Oregon. The year following was spent in research and development with Falls Chemicals in Great Falls, Montana.

In December of 1980 he was married to Linda Doig and they now have one child, Casey.

In September, 1981 he joined the chemistry graduate school at Montana State University. In 1983, he entered the doctoral program in Analytical Chemistry under the supervision of professor Eric Grimsrud.

He has accepted a position as a Senior Scientist with Lockheed, Las Vegas, Nevada, beginning February 1987.

ACKNOWLEDGMENT

I would like to thank all those who made this thesis possible, for without them I could not have completed this work. I would like specifically to thank Dr. Eric Grimsrud, my research advisor and director, for his patience, support, interest, and guidance. His technical expertise, suggestions and constructive criticism have resulted in a job successfully done. I consider him a true educator. Also thanks to my readers, Dr. John Cardellina, Dr. Ed Dratz, Dr. Reed Howald, Dr. John Amend, and Dr. Tim E. Lewis for offering their helpful suggestions and assistance. Special acknowledgment to those people in my research group and the Chemistry Department that have made Montana State University an enjoyable work place throughout these past years. A deep gratitude goes to my family for their love, prayers, encouragement, and confidence in me. To all those people not acknowledged but complementary to the production of this work, my special thanks.

TABLE OF CONTENTS

Table of Contents - Continued

LIST OF TABLES

LIST OF FIGURES

List of Figures - Continued

List of Figures - Continued

List of Figures - Continued

List of Figures - Continued

List of Figures - Continued

ABSTRACT

The electron capture detector (ECD) response to resonance electron capturing compounds is shown to be affected not only by the electron capture reaction, but also by the detailed nature of the subsequent competitive reaction dynamics. For aromatic molecules with a low electron affinity, two processes accompany the electron capture reaction. These additional processes are electron detachment from the molecular negative ion and the protonation of the analyte molecules. Results are presented in which the effects of these two undesired reactions are eliminated by the chemical doping of the detector make-up gas with a high proton affinity amine and an alkylmonochloride. In the detector gas these dopants alter and stabilize the reaction dynamics and provide greatly increased sensitivity, linearity, and reproducibility of the ECD response to polycyclic aromatic molecules. For numerous PAH's, ECD responses were measured as a function of analyte concentration, detector temperature, dopant type, and dopant concentration. Identification of the charged species in the ECD plasma was accomplished by a specialized ECD interfaced to a quadrupole mass spectrometer.

Theoretical modeling of the constant current ECD response to resonance electron capturing compounds includes a kinetic model to explain the mechanism of response with the amine and alkyl monochloride dopants. The existing theoretical models of resonance electron capture in the ECD are improved and supported by the results presented here.

Utilizing two ECD cells in series, experiments are described in which the tendency for regeneration of the parent molecule from the molecular anion by recombination with positive ions was investigated. The efficiency of molecular regeneration for molecules with a high electron affinity is determined from the ratio of the response in the tandem cells and the compound's known electron attachment rate. Theoretical models and results for compounds responding by a resonance and a dissociative electron capture mechanism are presented. Differences in the molecular anion behavior in the recombination reaction are discussed, as well as the application of this technique to tandem cell coulometry.

INTRODUCTION

Historical Review

The electron capture detector (ECD) for gas chromatography has seen considerable development in the last 30 years since its discovery by Dr. James E. Lovelock[1]. The detector is simple in construction and operation, is extremely sensitive to many compound classes, and has only recently been challenged by mass spectrometry in regards to detection limits for compounds to which it is sensitive. It is interesting to note that of those compounds to which the ECD is sensitive many are environmentally important pollutants of anthropogenic origin. The detector was pressed into service early in its stage of development because of its unparalleled sensitivity to compounds that were undetectable by the existing techniques of the time. Compounds of anthropogenic sources, particularly the halogenated pesticides, could be detected in sample concentrations as low as the parts per trillion level. The detector was instrumental in showing the ubiquity of pesticides and other man-made compounds throughout the biosphere. The effects of environmental contamination discussed in Rachel Carson's book, Silent Spring[2], could then be supported by an analytical method which was able to detect trace levels of persistent

pesticides such as DDT and their bioaccumulation in food chains.

A schematic design of a typical detector with a concentric coaxial anode is shown in Figure 1. It consists of a cylindrical volume through which gas chromatographic column effluents are passed. The walls of the detector are lined by a beta emitting radioactive source. Today, the most common radiation source is ^{63}Ni on platinum foil. The high energy beta particles ionize the detector gas, typically N_2 or Ar/10% methane, to produce positive ions and thermalized electrons. An electrically isolated electrode is placed within the detector and is biased to a positive electrical potential to collect the thermalized electrons within the cylinder. The flow of electrons (current) is then measured. The analytical signal is the decrease in current due to the removal of electrons by an analyte molecule capturing the thermalized electrons to produce a stable negative ion.

The sensitivity of the detector is related to the rate at which electron attachment to analyte molecules occurs. The attachment of an electron to a solute molecule is related to the electron affinity (EA) and the activation energy of the reaction. The larger the activation energy for attachment, slower is the attachment reaction. For those molecules with a significant activation barrier, higher detector temperatures will facilitate the attachment

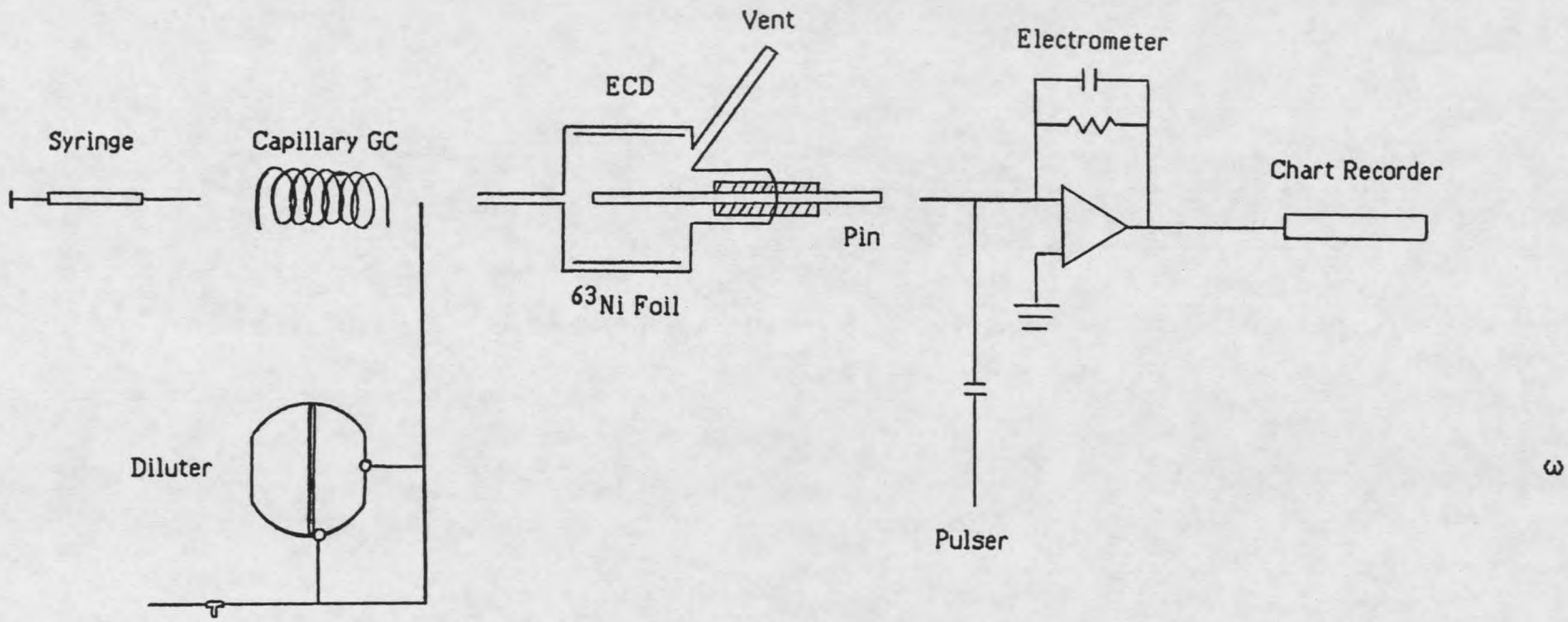

Fig. 1. Schematic illustration of a fixed frequency electron capture detector (ECD) configured for chemical doping experiments.

of an electron. Therefore, at higher detector temperatures higher sensitivity is expected for molecules with a large EA, and a selective detector for compounds in this class is provided.

The first reported description and application of the ECD was by Lovelock in 1957[3]. This detector used a tritium embedded metal foil as a radiation source and was operated with a continuous +50 volts applied to the electrode. The direct current (DC) ECD was plagued with unusual responses, non-reproducibility, and non-linear calibration curves. Despite these limitations, the exceptional sensitivity of the detector propelled it into commercial development by instrument manufacturers, and it was widely used for trace residue analysis within a few years. The first reported application of the ECD to environmental problems was in 1961[4].

In the early 1960's Lovelock continued work on the development of the ECD and other ionization detectors. He suggested that the problems of reproducibility with the DC-ECD responses could be explained by contact potentials and space charge effects, and that a pulsed waveform potential should eliminate these effects[5]. He proposed that a pulsed ECD would allow for the electron capture reactions to occur under field free conditions and that the collection of negative ions would not complicate the response when pulse widths of small duration and amplitude were used.

Previous experiments on the amplitude of the voltage levels revealed that moderate voltages would collect the electrons and, with further increase in voltage levels, the less mobile negative ions would also be measured at the detector electrode[6]. Therefore, particularly with the pulsed ECD, the appropriate selection of voltage levels would result in the collection only of electrons. Developmental research was also conducted to determine possible types of carrier gases. Nitrogen or argon with 10% methane were selected as detector gases, because the electron capture response would not be perturbed by metastable reactions as found to occur with pure helium or pure argon gases. The pulsed ECD, where the response was taken as the difference in current (ΔI) with and without sample present, was found to improve the reproducibility of the detector, and gave linear responses over the first 10% of the dynamic range of the instrument.

In the mid 60's, Wentworth et al.[7] developed the first detailed explanation of the reaction dynamics occurring within the ECD, and improved the method of signal processing by using the response function, $(I-I^{o})/I^{o}$, where I is the instantaneous current and I^{o} is the current in the absence of sample. This mode of signal processing gave linear ranges up to 90% of detector saturation, and facilitated the modeling of the reactions occurring within the EC cell. At pulse periods greater than 500 µsec the dynamics of the

reactions within the ECD were then described as a series of kinetically competitive reactions at equilibrium. However, this mode of signal processing required that the chromatographic conditions be quite clean, since only a small amount of an electron capturing impurity would significantly diminish the baseline standing current in the absence of sample.

Maggs et al.[6] greatly improved the method of signal processing for the pulsed ECD by developing the constant current (CC) ECD. In this mode of operation the cell current is held constant by a feedback loop to the pulsing portion of the circuit. The frequency of pulsing is increased to compensate for the electron loss processes due to analyte entering the cell. The signal measured is thus proportional to the pulse frequency. With this mode of signal processing the linearity of response is extended to 99% of detector saturation. The constant-current pulsed ECD is the one mode available on commercial GC-ECD systems used today.

Even with the improvements in the development of pulsed ECD signal processing, non-linear response versus concentration plots continued to be observed for some compounds. Within this group of compounds are the monochloroalkanes, the polyhalogenated hydrocarbons, and some of the polycyclic aromatic hydrocarbons (PAH's).

Polyhalogenated hydrocarbons are the compounds best suited for ECD detection since they have the fastest electron attachment rates and subsequently the highest molar sensitivities for the ECD. For these compounds non-linear calibration is caused by the significant proportion of sample destruction through the reaction with reagent electrons. This results in a detector concentration which is no longer proportional to the concentration of analyte eluting from the column. In 1983, Knighton and Grimsrud accounted for this effect with a new response function for the CC-ECD[9].

Monochloroalkanes were found to have high sensitivity in the low concentration region, but would quickly reach a limiting response which would not increase with larger concentration of sample[10]. Because they have moderate to small electron attachment rates, linear calibration was expected. Numerous explanations have been offered for the cause of this unusual behavior, yet the causative factor remains unknown. Studies on this interesting class of compounds will be presented in this investigation.

The PAH's are an environmentally important class of compounds due to man's uses of fossil fuels and their continual increased loading on the environment. Unfortunately, many of the PAH's, when analyzed in low concentration and/or with high detector temperatures, exhibit unusual peak shapes that are opposite to the normal

electron capture response, or have a complicated "W" shaped character to them[11,12]. These unusual peak shapes prevent accurate quantitation and unpredictable and non-linear calibration curves result. Since many of the PAH's have a low EA and poor sensitivity accompanied with the unusual responses, EC detection for these compounds is generally not favored.

Theoretical Modeling

Developments of theoretical models to explain the chemical dynamics within the ECD have paralleled the improvements in the processing of the detector signal. Wentworth et al.[7] were the first to give a detailed explanation of the chemical dynamics occurring within the pulsed ECD. The reaction models that will be presented here are based on reaction dynamics that were originally proposed by Wentworth, and will incorporate the most recent understanding of the reaction processes in the ECD.

These recently developed kinetic models have been applied to the responses of numerous compounds and explain the dynamics of the detector's responses for most compounds satisfactorily. However, for compounds which exhibit unusual responses and non-linear calibration curves, the current theoretical models are not effective in describing the reaction dynamics involved in the detector's response.

Two of the important issues in the debate concerning the ECD have been the distribution of charge density and whether or not charge neutrality exists. The current understanding of the charge distribution has been addressed by the use of a specialized ECD interfaced to a mass spectrometer[13,14]. The use of the atmospheric pressure ionization mass spectrometer (APIMS) has allowed the measurement of the positive and negative ions formed within the detector. The model favored here is that offered in 1980 by Gobby, Grimsrud, and Warden[15] and further supported by the work of Grimsrud and Connolly[16]. Their work was built on the understanding and observations of Wentworth et al.[7,17] and the APIMS observations of Siegel and Mckeown[18].

A summary of the current space charge model developed by Grimsrud et al. for the pulsed ECD is as follows. When ^{63}Ni radiation sources are used relatively uniform ionization throughout the cell is expected[16]. The application of short voltage pulses clears the cell of all electrons[7]. Positive ions left after a pulse are thought to create a space charge potential which is dissipated in time by space-charge-migration of the positive ions to the cell walls. The pulse itself does not measurably perturb the location of positive or negative ions in space. Over the range of pulse periods used in the CC-ECD, the total positive ion density remains relatively constant, since recombination of positive ions with electrons and negative

ions is approximately equal to losses by migration to the walls. The contribution of positive ion collection at the electrode is dependent on cell geometry and is not affected by pulsing or pulse polarity. It is dependent only on space-charge-driven-migration. Negatively charged species will be drawn towards the region of highest positive charge potential (in the center of the EC cell) to form a neutral plasma which contains an equal number of positive ions and negative ions. The plasma grows with time until the next pulse. Pulse periods less than 1000 µsec for normal cell geometry will be sufficient to prevent the charge-neutral plasma from expanding to the walls. The total number of negatively charged species within the detector at time "T" of the pulse will be a constant value. For example, a 50-volt pulse of 1 µsec duration, though sufficient to clear the detector of all electrons, will not remove the negatively charged ions from the charge neutral plasma. The kinetic equations modeling these reactions require that the negatively charged species be considered as populations rather than concentrations within the detector, since the negatively charged species are localized in the region within the charge neutral plasma.

From these studies on charge densities, better ECD geometries have been designed and improved interpretations of EC reaction dynamics were possible. With a better understanding of the ECD, limits for the frequency of

response in the CC-ECD could be established for optimum sensitivity and linear calibration curves.

The detector designed by Patterson[19] for the Varian 3700 series Gas Chromatographs, is an example of an ECD designed for small-bore capillary chromatography using the knowledge from this type of basic research to improve the detector's mode of operation. This small-volume detector was designed with a displaced coaxial anode so that the signal measured would only reflect the electron density. This was done by minimizing the collection of positive and negative ions at the electrode, normally a concern with a small-volume ECD necessary for capillary chromatography.

The reactions that are considered to be the most important in affecting the electron density within the electron capture detector are:

$$\text{Beta particles} + N_2 \xrightarrow{S} P^+ + \text{electrons} + \text{Radicals} \qquad (1)$$

$$AB + e^- \xrightarrow{k_1} AB^- \qquad (2)$$

$$AB^- \xrightarrow{k_{-1}} AB + e- \qquad (3)$$

$$AB + e^- \xrightarrow{k_d} A + B^- \text{ or } A^- + B \qquad (4)$$

$$AB^- + P^+ \xrightarrow{R_1} \text{Neutrals} \qquad (5)$$

$$AB^- + X \xrightarrow{R_2} R^- + AB \qquad (6)$$

$$e^- + P^+ \xrightarrow{R_3} \text{Neutrals} \qquad (7)$$

$$e^- + \text{Impurity} \xrightarrow{k_b} \text{Impurity}^- \qquad (8)$$

In reaction (1) beta particles react with carrier gas molecules to produce positive ions, radicals, and electrons. S is the rate of ion pair production. The positive ions formed are initially characteristic of the carrier gas but, through a series of rapid charge and proton transfer reactions, will eventually produce a terminal set of positive ions. These positive ions are characteristic of other neutrals with higher proton affinities than the carrier gas molecules[18]. About 35 ion pairs are formed per beta particle[15]. Reaction (2) is the attachment of a thermalized electron by analyte molecule AB, with k_1 as the second order rate constant of electron attachment. Reaction (3) is the electron detachment from the negative ion AB^-, with its rate of reaction denoted as k_{-1}. Reaction (4) represents the unimolecular dissociative electron capture of analyte AB to form a stable negative ion fragment with reaction rate k_d. Reaction (5) represents the recombination of negative ions with positive ions to produce neutrals with a recombination rate R_1. Reaction (6) is the loss of AB^- ions to compound X with a reaction rate R_2. Compound X will

include any compound or radical that may be reactive with the negative ion. It is included here to represent chemical dopants that will be discussed later in this investigation. Reaction (7) is the recombination of electrons with positive ions by recombination rate R_3. Reaction (8) is the loss of electrons due to column bleed and other carrier gas impurities with a reaction rate k_b. In the current theoretical models as applied to all of the above reactions, S, K_b, R_1, R_2, and R_3 are assigned constant values when the detector operating conditions are specified and stabilized.

The response of the detector is related to the ability of a molecule to capture an electron, and the stability of the negative ion formed. Because only the electron density is measured and the total number of negatively charged species is a constant value at time "T" of the pulse, the response of the detector's signal becomes a function of the number of negative ions relative to the number of electrons. This is assuming that the negative species in the detector each have the same rate of loss by recombination with positive ions. Therefore, the detector's sensitivity, which has been related to the electron attachment rate, must also include the fate and stability of the negative ion produced.

With the resonance electron capture of an electron, the system moves to a lower energy state, Delta G of this reaction is approximately equal to the EA of the molecule. The ion formed can dissipate this energy by collision with

buffer gas molecules within the detector. If the EA of the molecules is not large, the negative ion formed by reaction (2) can undergo simple electron detachment as depicted in reaction (3). This process of detachment, if it proceeds at a rate competitive with reaction (2), would result in a weak and very small molar response for that particular compound. The overall production of negative ions and the response of the detector by this resonance electron capture process has been related to the equilibrium of reaction (2) and (3) combined[7,18,20]. For other systems, where reaction (3) is not significant, the negative ion must be stable or otherwise a dissociative electron capture mechanism, as depicted in reaction (4), would occur. Typically, high sensitivity and large molar responses are seen when dissociative electron capture is operating. The major loss process for a stable negative ion as depicted in reaction (5) is the recombination of positive ions with negative ions. Diffusion to the walls and ventilation out of the cell can be neglected for all negatively charged species in the space charge model, because these processes are slow relative to recombination with positive ions.

The sum of the electron production and electron loss process can be mathematically represented by these two differential equations:

$$dN_{e^-}/dt = S + k_{-1}N_{A^-} - (k_1 n_A + R_3 n_{p+} + R_4 n_B)N_{e^-} \qquad (9)$$

$$dN_{A-}/dt = k_1 n_A N_{e-} - (k_{-1} + R_1 n_{p+} R_2 n_{Rad} + k_d) N_{A-} \quad (10)$$

A capital N denotes a population and a small n denotes concentration. To obtain a numerical solution, the rates of the reactions, and the ion and molecule densities must be known.

Experimentation on the electron capture responses of CH_3I and CCl_4, for example, illustrates the importance of other reactions occurring within the ECD in addition to the direct electron capture process[21]. Indirect electron capture processes are important in interpreting the response differences between these two compounds.

The behavior of CCl_4 in the ECD is explained by a dissociative electron capture mechanism[22], with negative ion APIMS studies demonstrating the formation of Cl^-. The production of the stable Cl^- ion will, upon recombination with positive ions, produce a neutral species (HCl) which does not undergo further electron attachment[23]. The remaining neutral radical, $\cdot CCl_3$, is not believed to be reactive to electrons based on the APIMS studies of CCl_3Br [24]. The reaction of a CCl_4 molecule with an electron should then occur only once. Measuring the numbers of electrons reacted with a quantity of analyte molecules, along with the efficiency of the reaction, has been the basis for using the ECD as a coulometric cell[22,25,27]. Up to 90% efficiency can be expected from the reaction of CCl_4 with electrons, and

reasonably accurate analytical results have been obtained using tandem cell coulometry[22,26].

The molecule CH_3I has a smaller k_1 value[28] than CCl_4 [29] and therefore would be expected to have a slower electron attachment rate and smaller molar response sensitivities based on the above mechanism. However, hypercoulometric results were found by tandem ECD cell coulometry. This hypercoulometric result has been explained by the occurrence of an additional reaction sequence[21]. The APIMS study showed that CH_3I produces the stable negative ion I^- by dissociative electron capture. Upon recombination with positive ions, I^- produces HI which is thermodynamically capable of undergoing further electron attachment and regeneration of the I^- ion for recycling by the recombination/electron attachment process. This unusual reaction sequence allows for an additional source of electron loss to each analyte molecule and demonstrates the significant impact that reactions other than electron capture may have on the sensitivity of the ECD. Numerous studies, including this investigation, have been done to determine the importance of individual reactions and mechanisms involved in the response of the detector.

Part of this study will examine a similar recombination/regeneration sequence to that just mentioned. It will differ in that it will examine the importance of parent molecule regeneration, where the molecular species being

studied is regenerated from the molecular anion by recombination with positive ions. Also to be examined in this investigation is the relationship between reactions (6) and (7) and the "W"-shaped peaks of low-EA PAH's. To understand these relationships a detailed examination of the existing theories as applied to resonance electron capture will be made.

A recent publication by Zlatkis et al.[20] discusses how the mechanism of response can be determined from the molar response of a compound relative to the operating detector temperature. Generally, for a compound responding by a resonance electron capture mechanism, highest molar responses are favored by the lowest detector temperature. This results from the higher electron detachment rates (reaction 3) as temperature is increased. A dissociative process is implied by an increase in molar sensitivity with increasing temperature.

In their model, Zlatkis et al. describe three different regions that can be observed when the molar response, (R), for compounds is plotted as ln $RT^{3/2}$ against 1000/T, where T is the temperature in degrees Kelvin. They describe an alpha, beta, and a gamma region in these plots; the alpha is where $k_{-1} > R_1[+] > k_d$, the beta region is where $R_1[+] > k_{-1} > k_d$, and the gamma region is where $R_1[+] > k_d > k_{-1}$. The alpha region describes resonance electron capture, and when plotted, gives a positive slope with a common Y-intercept

for compounds of similar structure[7,30]. The beta region describes the process where electron detachment is not competitive with the rate of recombination between positive and negative ions. That is, resonance electron capture is occurring, yet the negative ion is considered to be stable to detachment relative to the negative ion loss rate by recombination with positive ions. The beta region is expected to give a negative slope. The gamma region describes the dissociative electron capture process as the dominant force in affecting the detector's response. An increase in detector temperature tends to increase the molecules instability, and favors further dissociation of chemical bonds. Often, the fragment ion is more stable than the molecular negative ion and plots with very steep negative slopes are then observed. When steep negative slopes are not seen, thermodynamic calculations or results from APIMS studies must be used to distinguish between stable resonance electron capture and dissociative electron capture processes.

Though the Zlatkis model requires a number of assumptions, it has aided in the understanding of the mechanisms of response and, indeed, the modeling does agree with the experimental observations. Some of the assumptions used are as follows:

1) The pulse frequency is directly proportional to the electron density and equations derived for electron density will apply to the CC-ECD.

2) Those observations and assumptions previously discussed for the space charge model are also applied here.

3) A steady state is reached for all charged species and the reactions can be described by kinetically competitive reactions at equilibrium.

4) The only temperature dependent rates of reaction are k_{-1} and k_d. All of the other reaction rates, including the electron attachment rate, k_1, are temperature independent. The electron attachment rate is considered temperature independent, since molecules with a positive EA would have a very low energy of activation for ionization to occur Therefore, ionization should not be assisted by temperature.

Selectivity and Chemical Doping

Recent advances in capillary gas chromatography and the use of selective detectors with high sensitivity have been a great aid to analysts. The advantages of selective detectors for gas chromatography are especially evident in environmental analyses. Complex environmental samples can produce extremely complicated chromatograms with a universal detector such as the flame ionization detector (FID), making

detection of a low-concentration target compound very difficult if the baseline is complicated with coeluting compounds. The simplicity of the ECD and its associated electronics, as well as its sensitivity and selectivity to many compounds of environmental interest, have brought about its widespread use in trace residue analysis. The fact that many environmentally important compounds are both mutagenically active and sensitive to ECD detection make this detector particularly important to trace residue monitoring.

The selectivity of the ECD has also limited its application to those areas of trace environmental analysis for compounds in which the ECD is sensitive. For those compounds to which the ECD is not sensitive, other selective gas chromatographic detectors must be used. Other selective detectors such as the photoionization, flame photometric, flameless alkali, and alkali-flame ionization detectors have been successfully used in environmental laboratories, each being selective to particular classes of compounds. These selective detectors, including the ECD, and others, have recently been reviewed and their detection abilities and limitations have been well described[31].

None of the other detectors, with the exception of mass spectrometers, have the ultimate detection limits of the ECD. The mass spectrometer approaches the sensitivity and detection limits that the ECD has for certain high EA compounds, but these limits are only being realized by

efficient research grade instruments operated by trained technicians applying some of the more recent developments in alternate ionization techniques. With its capability of mass filtering and various chemical ionization procedures, the mass spectrometer is considered to be the most universal and selective detector. Application of the mass spectrometer to environmental analyses has been extremely useful, although under its normal mode of operation with electron impact ionization (as currently required by the U.S. EPA), it too is limited in distinguishing isomers for some classes of compounds. The other selective detectors are more cost effective than the highly sophisticated mass spectrometer and for this reason their use is often preferred.

One of the requirements for the proper operation of the electron capture detector has been the need for high purity detector gases free from electron capturing impurities. Oxygen, commonly found in many carrier gases, was noted to destroy the standing current of the ECD. Therefore the carrier gas and make-up gas required effective oxygen scrubbers for normal ECD operation. In the early 1970's Van de Wiel and Tommassen[32] noted that when oxygen was present in the detector gas, not only was there a loss in baseline standing current, but the compound n-butyl bromide gave a response of larger magnitude. Grimsrud and Stebbins[33], capitalizing on this observation, intentionally doped the ECD with O_2 to cause alterations in the

selectivity of the detector and reported significantly enhanced response values for a number of compounds. In their mechanism proposed to explain these responses they found that in addition to the reactions already occurring within the ECD they could rationalize the enhancements by adding these reactions:

$$O_2 + e^- \rightleftharpoons O_2^- \qquad (11)$$

$$O_2^- + AB \text{ ----> Stable negative ions and Neutrals} \qquad (12)$$

Reaction (11) depicts the resonance electron capture of O_2 to produce the superoxide anion O_2^-. In reaction (12), O_2^- is reacting with neutral unreacted solute molecules to produce stable negative ions. This happens in addition to the normal electron capture reaction. One ion commonly observed in the APIMS spectrum of O_2-doped PAH's is the $(AB + O)^-$ ion[34]. The O_2^- lost by reaction with analyte is replaced by the kinetic equilibrium depicted in reaction (11). The overall effect is that an increased rate of electron loss is observed and a larger response is predicted for some types of analytes in the ECD. It is interesting to note that the sensitized response to analyte does not involve direct reaction with the electron, but rather is an indirect electron capture process. Though the overall response to analyte is quite complicated for the O_2 sensitized response, the kinetic theory and its mathematical

derivations have been worked out[35]. Briefly discussed, the normal electron capture response will remain effective in the presence of O_2 with the sensitization dependent on the remaining amount of unreacted neutrals and their rate of reaction with O_2^-. Grimsrud et al., presented thermodynamic considerations on the reactions of different AB-type molecules with O_2^- [34].

With O_2 doping, the selectivity of the detector has been altered to include an even larger number of compounds. Some of these compounds previously exhibited little or no detection sensitivity. Linear and near-linear calibration curves have resulted, and an improved sensitivity for many compounds is easily seen in their chromatograms. The fact that compounds and their isomers are unique in their enhancement values, identification based on GC retention times and the enhancement levels is possible[36,37]. This doping scheme has been manipulated in a variety of ways, with isomer identification made possible even for coeluting peaks[37]. The O_2 sensitized ECD has been applied to the monitoring of methyl chloride in the atmosphere[38], and has also demonstrated its applicability to the analysis of many low concentration PAH's and their isomers[36,37].

Realizing that the reaction chemistry occurring within the ECD could be altered by chemical doping of the detector gas, and that responses could be generated by indirect electron capture, Phillips et al. developed N_2O doping of

the ECD[39]. They termed this selective electron capture sensitization (SECS). Nitrous oxide doping works in a very similar manner as O_2 doping and is explained by an equilibrium reaction sequence involving electrons. The reaction is driven to the right when the reagent ions produced react with the analyte molecules. The reagent ion thought to be of primary importance in the reaction with analyte is the O^- ion. Because the reagent ion is different than the one theorized for O_2 doping, the N_2O doping scheme predicts sensitization to differing types of compounds. The level of sensitization is highly dependent upon the neutral's ability to react with the O^- ion.

The ECD has been very important to trace residue analysis in environmental applications and through selective sensitization it has been able to respond to additional compound classes. Many difficult problems have been overcome with this simple, yet sensitive detector. Through careful characterization of the reaction dynamics and chemical doping possibilities, it is possible that many more compounds can continue to be analyzed by this increasingly versatile detector.

RESEARCH OBJECTIVES

This study was developed to give further consideration to the chemical dynamics occurring within the pulsed ECD. Numerous others have studied the resonance electron capture process and reasonable working models have been developed for many compounds as was summarized in the previous section [7,17,20,30]. The models previously generated for resonance electron capture were successful in explaining the temperature dependence and the mechanism of response[20,30]. These models utilized simplifying assumptions concerning the effects of the recombination processes to describe mathematically the signals observed, however these assumptions may not necessarily be valid for all cases. The present investigation will evaluate the assumptions that were previously made by testing the theoretical models against chemical systems which do not agree with the predicted linear calibration curves.

To determine how these anomalous results come about for some compounds, all of the reactions known to be occurring within the ECD were individually reviewed. Compounds were analyzed and chemical dopants were selected to demonstrate the various reactions in relation to the measured response of the ECD. Previously derived mathematical models required

steady-state approximations of the negative ion density to calculate the expected electron density. The calculated electron density was then related to a pulse frequency in the CC-ECD[8]. Because the normal response of the CC-ECD to an analyte is measured by means of an increase in the pulsing frequency, steady-state approximations as applied to long pulse periods may no longer be valid at higher frequency responses. Computer modeling of the resonance electron capture theories was done to examine the assumptions regarding the validity of steady-state approximations. Computer modeling was chosen to examine this relationship since the variables can easily be changed. The reiterations in the calculations necessary would otherwise be quite tedious by hand.

Another of the objectives of this study was the examination of positive ion/electron recombinations in the ECD reaction dynamics. The "W"-shaped response observed for some PAH's is believed to be the result of a competition between the positive ion/electron recombination reaction with the weak electron capture response. Anthracene and several other low EA PAH's, were carefully characterized according to their effect on the positive ion nature of the ECD. Using APIMS instrumentation, the response of the ECD to PAH's was examined relative to the positive ion composition of the ECD. Alterations in the positive ion

nature were through the use of chemical dopants with any changes in the measured ECD response noted.

A survey of chemical dopants was also done to see if some of these may possibly eliminate, enhance, or stabilize the reactions and/or the rates of the reaction that might affect the electron density during the elution of a sample. With the use of chemical dopants, it was hoped that the response of the ECD could be made to reflect only the electron capture reaction of the analyte by preventing any indirect electron loss or production reactions involving the analyte molecule. For example, a dopant that would preferentially react with trace O_2 rather than with the analyte should eliminate any sensitization of the analyte response caused by trace O_2.

In the last portion of this study, the importance of positive-negative ion recombinations was examined. This investigation, in particular, looked at the fate of a resonance electron capturing molecule after it had undergone electron capture followed by a positive ion recombination. The requirements for this analysis differed, in that tandem ECD cells were used, and the responses of higher EA compounds were measured. The tandem cells are two matched ECD cells hooked in series with one another. The signals from each cell are individually measured. Interpretations of the signal intensity and the ratios between the two cells are compared to literature values of the electron capture

rate constants. In theory, if the parent molecule is regenerated from its anion by the recombination with a positive ion, a response similar to that of CH_3I, should be observed in these detectors that have been used and characterized for coulometric analysis.

EXPERIMENTAL

Varian Instrumentation

A Varian 3700 gas chromatograph equipped with a flame ionization detector and a ^{63}Ni constant current electron capture detector was used to survey the aromatic hydrocarbons and determine their sensitivity to chemical doping schemes. The commercial EC cell on the Varian 3700 utilizes a displaced coaxial anode and is a Patterson engineering design. It has been well described elsewhere[19]. Design advantages of the Varian Aerograph ECD over conventional coaxial electrode geometry give it decreased levels of background currents from positive and negative ions, an increase in sensitivity through a smaller cell volume, and improved enhancement values to chemical doping techniques[40].

Analytical signals from the electrometer were recorded on a Varian 9176 strip chart recorder. Peak heights were measured with a ruler and converted to a frequency response $(f-f^{o})$. Baseline levels of frequency were constantly monitored, and only when conditions were optimized with acceptable baseline levels would experiments be logged.

The ECD make-up gas was high purity nitrogen which was first passed through a water removing ($CaSO_4$ and molecular sieve 5A) trap followed by an oxygen removing (Alltech Oxy

Trap) trap. The cleaned N_2 gas was then sent through a flow controlling needle valve (Swagelock Flow controllers) before entering a 3.3-liter stainless steel dilution vessel. The output of the dilution vessel was connected to the make-up gas lines at the base of the detector housing. Overall flow rate of the gases through the detector was monitored by a soap-bubble meter connected to the exhaust of the detector, the flow rate being generally set to 40 ml/min.

For the gas chromatographic analysis of the aromatic hydrocarbons, samples were injected via a splitless injection port into a 30 meter, 0.32 mm ID., DB-1 fused silica capillary column (J & W Scientific). Carrier gas velocity through the column was maintained by measuring the time for the elution of the oxygen and solvent peak. This elution time was set to a fixed value by varying the pressure at the head of the column. The capillary column was necessary for the separation of the compound's response from other EC sensitive impurities in the sample. The splitless injection port temperature was generally held at 210° C for most of the PAH's. Detector temperatures were varied according to the nature of the experiment, but were always higher than the maximum column temperature to prevent contamination of the ^{63}Ni foil by condensation of column effluents.

Samples were first run with a flame ionization detector to determine the best chromatographic operating conditions.

FID retention times were characterized for a number of compounds and relative retention times were used to assign a signal in the ECD chromatogram to the response of the compound. It was necessary to use the FID first, since the normal ECD chromatogram observed for many of the PAH's studied were complicated by ECD responsive trace impurities in the weakly responding compound standards. Sample sizes of approximately 100 ng were used for the FID analysis. Chromatographic conditions chosen were those that gave good separation from the solvent, gaussian shaped peaks, and reasonable retention times. Generally, temperature programming was found to be the most effective method.

Hewlett Packard Instrumentation

A Hewlett Packard 5890A gas chromatograph (HPGC) was equipped with a ^{63}Ni constant current pulsed ECD using a conventional coaxial anode design. An EC cell of conventional design and geometry was chosen since fundamental studies on the physical processes and reaction dynamics have been predominately done with detectors of this design. Response enhancement values and their temperature dependence could then be better interpreted using a detector of conventional design. Information about the EC cell used in the HP-5890A was revealed through personal communications with Hewlett Packard engineers. The detector has a cell volume of 2.8 cm^3 and is lined with a ^{63}Ni foil of 12 ± 0.5

millicuries which produces a standing current of 8.1 to 9.9 nanoamps. The electrometer is a constant current design and uses a pulse width of 0.75 μsec. The reference current is set to obtain a baseline pulse frequency of 400 hz for either N_2 or Ar/CH_4.

The HP gas chromatographic system consisted of carrier and make-up gases of ultra high purity N_2 or Ar/10% CH_4 mixtures. Oxygen and H_2O were removed by conventional techniques as previously described. The column used was a 6-ft., .57 mm ID., SE-30 column (Hewlett Packard). The column flow rate was set to 10 ml/min using the same gas that was used for the make-up gas in the detector. Overall flow rate through the detector with the make-up and carrier gas was generally set to 40 ml/min. The glass-lined splitless injection port and make-up gas lines were adapted to the large-bore capillary column with a kit provided by the instrument manufacturer. The installation of the dilution vessel and carrier gas scrubbers were the same as described for the Varian GC system. When using the N_2 or Ar/CH_4 detector gases, reference currents for the commercial electrometer were adjusted to compensate for the differences in the carrier gases. Retention times of the samples analyzed on the HP GC-ECD system were identified by their chemically enhanced responses as determined for compounds that were enhanced on the Varian GC-ECD system.

Analytical signals from the HP commercial electrometer were measured with an Omniscribe 1 mv strip chart recorder and peak areas were integrated with an Apple II+ computer fitted with an Issacs Cyborg A to D interface. Control of the A to D interface and digitization of the data was accomplished with an Appligration software program. Range and attenuation of the electrometer was set for maximum sensitivity of the response.

Atmospheric Pressure Ionization Mass Spectrometer (APIMS)

The APIMS is a specialized ECD capable of measuring an ECD function as well as the positive and negative ions existing within the detector. This particular system has been completely described elsewhere[14], and only a brief review relative to the experiments in this study is presented here. A schematic diagram of the EC ionization source is given in Figure 2. The walls of the detector are lined with a 6-mCi ^{63}Ni foil which emits beta radiations producing positive ions, negative ions, and thermalized electrons. The ions are sampled in the source at a flow rate of 4 ml/min by a 20-µm aperture into a differentially pumped vacuum region containing a quadrupole mass filter with a channeltron ion counting detector. Differences in voltage potential biases allow the mass filter and channeltron detector to be set for positive or negative ion

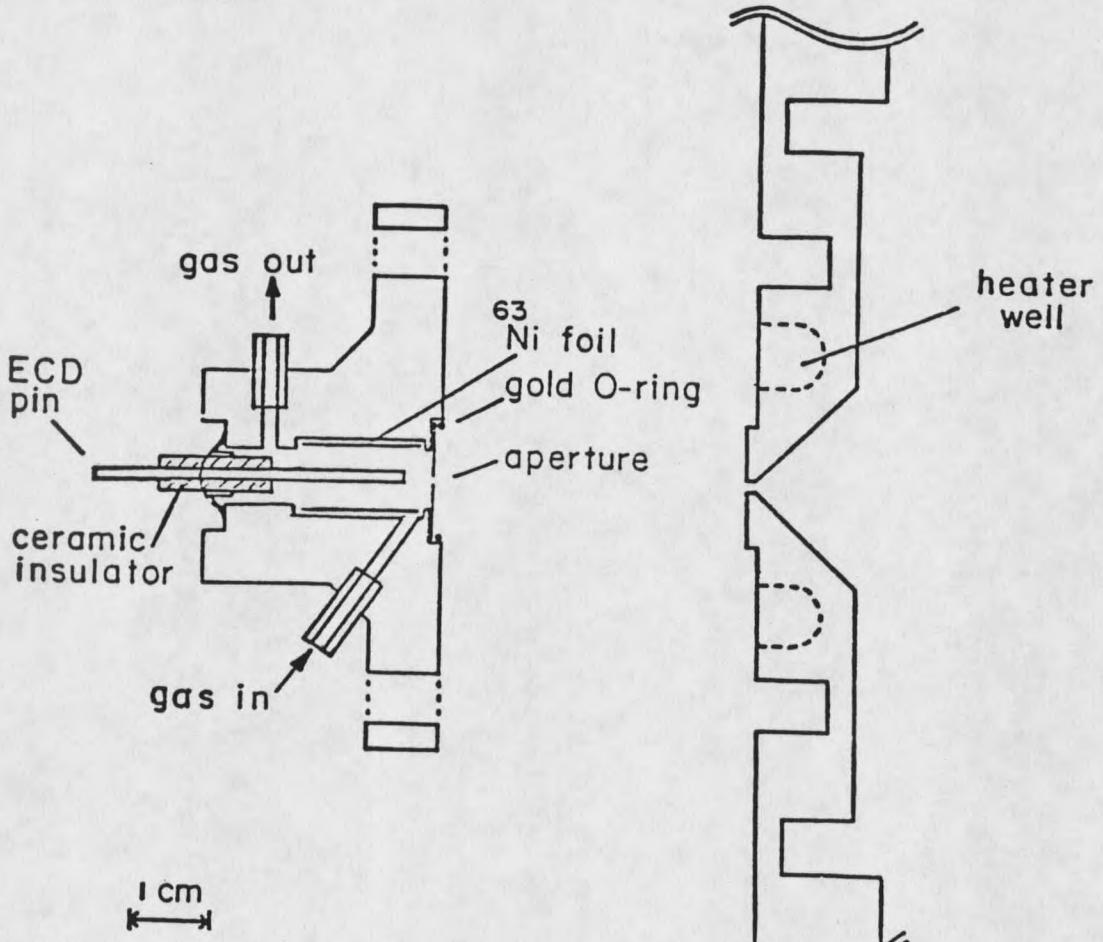

Fig. 2. Specialized ECD/atmospheric pressure ionization mass spectrometer (APIMS) source used for the ECD signal and ion measurements.

detection. The stainless steel pin that protrudes through the center of the source in Figure 2 is the electrode by which the ECD function is obtained. Pulses of +50-volts and 1 μsec duration are applied to the pin with a constant frequency of 200 msec using an electrometer circuit designed by Grimsrud et al.[41]. The analytical signals from the source and the ion detector were recorded on a 2-pen Omniscribe strip chart recorder.

Positive ion signals were measured simultaneously with the ECD function, but the pulser was turned off for measurements of the negative ion signals[42]. Mass spectra were obtained by scanning of the quadrupole mass filter with identification of each mass by single ion monitoring.

To introduce samples into the ion source a simple isothermal gas chromatograph was utilized. The gas chromatograph was equipped with a standard injection port and a 1/8 in. x 1.5 ft. stainless steel column packed with 4% OV-101 on Chromosorb W. High purity N_2 was passed through O_2 and H_2O removing traps and then through a 3.3-liter stainless steel dilution sphere. This arrangement was then connected to the head of the column. No make-up gas lines were necessary since flow rates through the packed column were adequate. The effluent from the GC was introduced into the APIMS ion source by means of a heated 1/8 in. x 6 in. glass lined stainless steel transfer line.

Tandem ECD Cells

Briefly described, the tandem cells are two well-matched electron capture detectors hooked in series to the end of a chromatographic system. In this study the tandem cells were used for the determination of relative electron attachments rates and the importance of ion-ion recombination reactions in the overall response of the ECD. Compounds chosen for this study were those which had known mechanisms of response and a high electron affinity.

The tandem ionization cells used in this study are schematically represented in Figure 3. They were fabricated from stainless steel and teflon insulators, and were of a concentric coaxial design. The internal length and diameter of each cell is 1.4 cm, with a volume for each of 2.2 cm^3. The cells were connected by a small aperture which separated the reaction chemistry in each, yet allowed the gas stream to flow from one cell to the other. The cell walls were lined with ^{63}Ni-on-platinum foils (New England Nuclear). Each foil had an activity of 15 mCi. The axial pins shown in Figure 3 were the electrodes by which the ECD functions were obtained.

An electronics package was assembled, using one fixed frequency pulser and two electrometers by which ECD functions for both cells could simultaneously be determined. The entire circuit design was based on work previously done

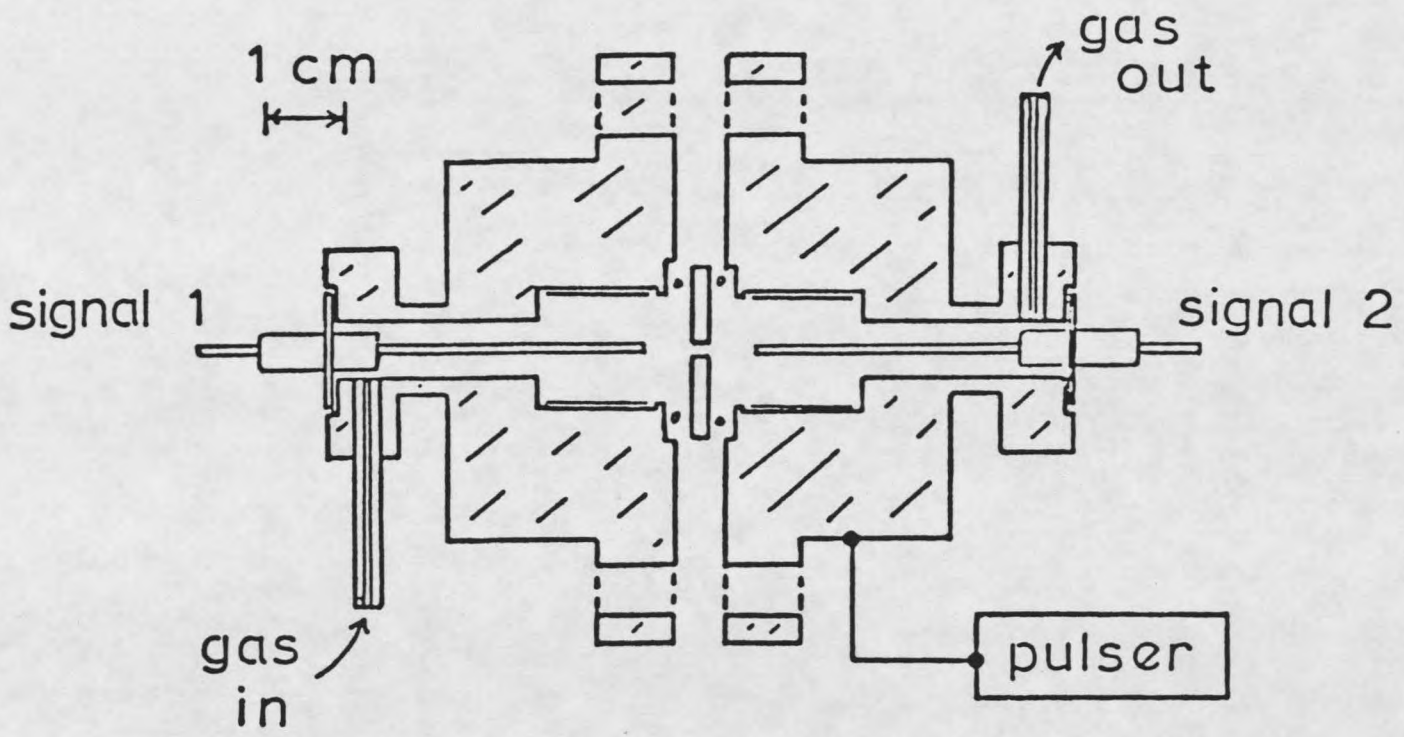

Fig. 3. Tandem ECD cells used in this study.

by Grimsrud et al.[41]. Pulses of +45 volts and 1 μsec duration were capacitively coupled to each electrode. Pulse period was adjusted according to the experimental design and was monitored with a Tecktronix model 91 oscilloscope. The cell currents were measured with two separate electrometers consisting of operational amplifiers (RCA CA3140) with 10^9 ohm precision (±1%) feedback resistors. The electrometers were calibrated by comparison with several commercial picoammeters. The analytical signals were recorded on a 2-pen Omniscribe strip chart recorder and peak areas were integrated (nanoamp-minutes) using the same system as described for the HP instrument. It was necessary to use peak areas since peak broadening was expected in the second cell and peak height measurements would thus introduce unwanted errors.

Exponential Diluter and Doping Methods

All four of the instrumental systems used an exponential diluter for chemical doping experiments. An exponential diluter was chosen since dopants and their concentrations could easily be changed according to the experiments being performed. Basically, the system is a large volume reservoir within the make-up gas line leading to the detector to which chemicals could be added. The diluter assembly was constructed of two stainless steel salad bowls welded together and having 1/8 in. stainless

steel tubing connections inserted for Swagelock fittings and valves. The diluter assembly is schematically illustrated in Figure 4. With this assembly, make-up gas to the detector could be routed through the diluter or, by switching valves, make-up gas could bypass the diluter system for clean carrier gas analysis. A third valve could also be opened for rapid flushing of the diluter with high gas flow rates to the outside atmosphere. It was important to vent gases from the ECD and diluter to the outside, since the chemicals chosen were often noxious and potentially hazardous compounds. Gaseous and liquid chemical dopants were added to the system through a Swagelock "Tee" fitted with an injection port septum. The "Tee" was located just prior to the entrance of the make-up gas line leading into the diluter. Gaseous dopants were added by a Hamilton 5 ml ground glass syringe and liquid dopants by a Hamilton 10 µl syringe. Initial concentrations in the diluter were calculated assuming ideal gas behavior. One to two ml of gaseous dopant and 1-2 µl of liquid dopants were found to give an initial concentration of 100 ppm in the dilution sphere. A similar system called a "Quantegg" has been described previously for the preparation of dilute gaseous standards using a flowing exponential diluter[43].

The concentration of dopant leading into the detector was then a simple function of the initial concentration, the

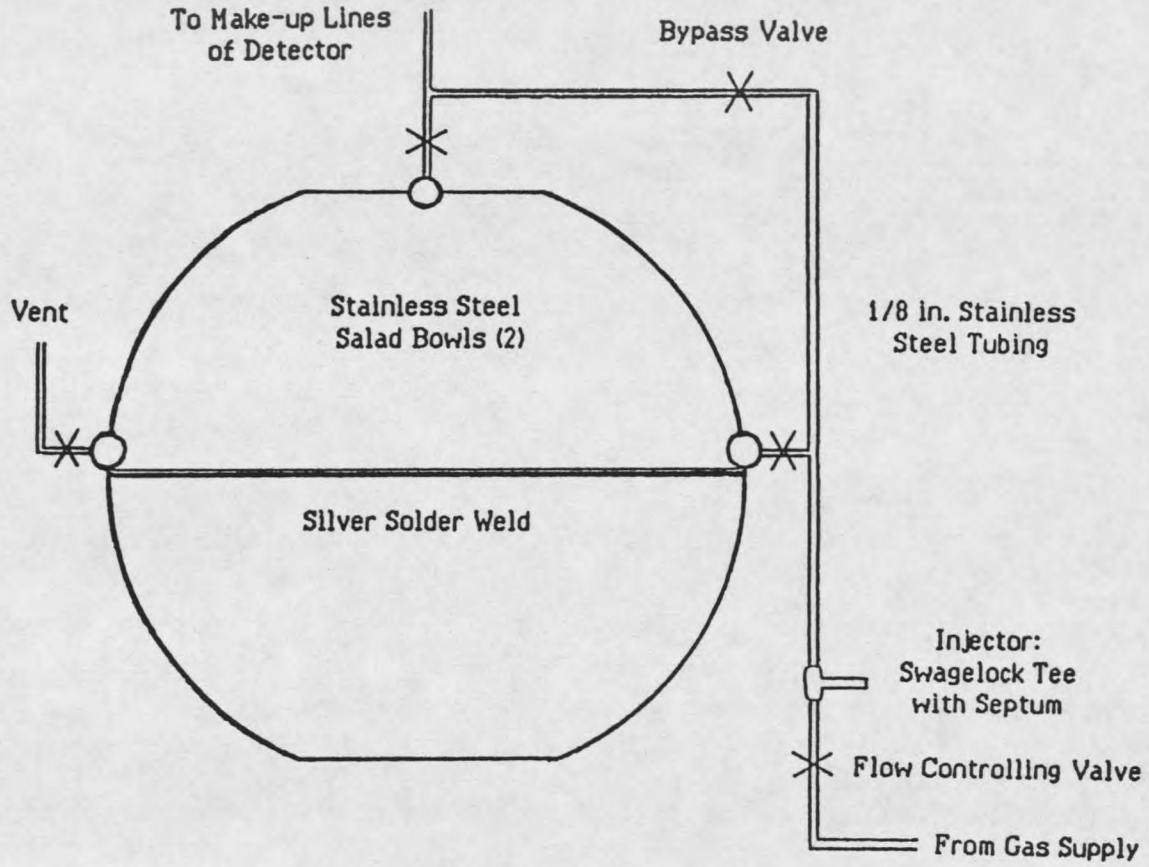

Fig. 4. Schematic illustration of the diluter assembly and valve switching system. (X) = valve and (O) = 1/8 inch stainless steel tubing welded into the sphere.

flow rate of gas out of the diluter, the volume of the diluter, and the elapsed time from which the initial concentration was introduced. The equation relating this is: $C = C_o e^{-(F \times T)/V}$, where C is the concentration at time T, C_o is the initial concentration within the diluter, F is the flow rate, V is the volume of the diluter converted to atmospheric pressure, and T is the difference in time from the initial concentration. The accuracy of standards prepared in this manner has previously been reviewed[43,44]. An accuracy to within 10% of the calculated value for a concentration as low as 0.1% of the original starting concentration is possible. Calculations of sample size at time T and the diluter half-life concentrations agreed very well with experiments done to test the half-life of the diluter. To measure the half-life of the diluter a compound which has been shown to capture electrons quite rapidly, SF_6 (Matheson Gas), and exhibits a linear calibration curve in the ECD over selected ranges in concentration, was added to the diluter. The response of the ECD to the exponential decrease in SF_6 was measured with time and flow rate. Thus, the volume and half-life of the diluter could then easily be determined.

The volume of the diluter gas was a function of the pressure above atmospheric pressure and the actual volume of the diluter. For some conditions, as was the case for the system coupled with the APIMS instrumentation, pressure was

necessary since the diluter was placed before the column. The calculated volume and half-life of the pressurized diluter also agreed with experimental values obtained by the exponential decrease of SF_6 measured by the ECD response. Calculated concentrations over large variations in dopant concentrations were also checked by the addition to the diluter of much smaller sample sizes. The results also agreed quite well, and no significant errors were noted.

Chemical Standard Preparation

All of the PAH's, amines, alkyl chlorides and hydrocarbons were purchased from commercial suppliers and used without additional purification. When the standards were used as samples, a chromatographic system would separate the impurities from the compound of interest. Detector response was then assigned to the "pure" compound according to its chromatographic retention time. However, when using the compounds as dopants within the diluter, it was important that the dopants themselves and their impurities did not capture electrons and destroy the baseline or standing current of the detector. Chemical dopants were selected that would not attach thermal electrons. These dopants were further tested for electron-capturing impurities by GC-ECD.

Respectively, the compounds, their sources, and purities found satisfactory for the doping schemes were: ethyl chloride (Matheson Gas, 99.7%), 1-chloropropane

(Aldrich, 99%), 1-chlorobutane (Aldrich, 97%), 2-chlorobutane (Aldrich, 99%), anhydrous trimethylamine (Aldrich, 99%), SF_6 (Matheson Gas, 99.8%), triethylamine (Aldrich, 99%), NH_3 (Matheson Gas, 99.99%), toluene, cyclohexane, diethylether, methanol, and acetone, (all reagent grade, J.T. Baker). The PAH's and other samples analyzed by GC-ECD were obtained from Aldrich, Alfa, and Chemical Services in Pennsylvania.

Gaseous CH_3NH_2 was obtained by combining 3 g of the pure hydrochloride salt of CH_3NH_2 (Aldrich, 98%) with about 3 ml of concentrated KOH in a 5-ml volumetric flask. The flask was sealed with a small rubber pipet bulb through which a small hole had been pierced with a needle. The flask was then heated until gas evolved. A period of continued gas evolution was allowed so that the oxygen content of the headspace gas became minimal. An aliquot of the CH_3NH_2 gas was then captured in a 5-ml glass syringe by inserting its needle through the bulb hole and allowing the pressure of the evolving gas to fill the syringe.

The semivolatile samples were prepared by weighing out approximately 4 mg to an accuracy of 0.1 mg and dissolving into them into 10 ml of pesticide grade benzene or toluene (MCB Omnisolve). This was followed by successive dilutions using volumetric flasks to obtain appropriate sample sizes for ECD detection. Injections of 0.5 - 1 µl were made into

the chromatographic system with a Hamilton 1 μl syringe fitted with a Chaney adapter.

The volatile samples of perfluoromethylcyclohexane (C_7F_{14}), SF_6, CCl_4, $CFCl_3$, and octofluorotoluene (C_7F_8) were prepared as gaseous standards by successive dilutions into pressurized airtight glass carboys. From the final carboy in the dilution series, gaseous samples were taken by a 100-ml ground-glass syringe and analyzed by a gas chromatographic system fitted with a Carle 8030 gas sampling valve having a 2 ml sampling loop. Samples prepared in this manner could be measured with a precision of ±1%.

RESULTS and DISCUSSION

Positive Ion-Electron Recombination

The temperature dependence of compounds responding by a resonance electron capture process was recently modeled by Wojnarovits and Foldiak[30]. Figure 5 presents the calculated rates of electron attachment and detachment that they obtained for anthracene. Also included in this Figure is the lifetime of the negative ion ($1/k_{-1}$) calculated for a number of temperatures. At the detector temperatures normally used in gas chromatography (200° C or greater), the lifetime of the anthracene negative ion was shown to be very short. For molecules known to respond by resonance electron capture, a small molar sensitivity is expected when the detachment rate of an electron is faster than the electron attachment rate. In the Wojnarovits and Foldiak model the forward rate of electron attachment was temperature independent. Furthermore, the value given for this rate constant was only two orders of magnitude smaller than the very rapid electron attachment rates given for the strongly responding compounds CCL_4 and SF_6 [29]. If electron attachment alone was the process by which the ECD response was obtained, a very sensitive response would be observed.

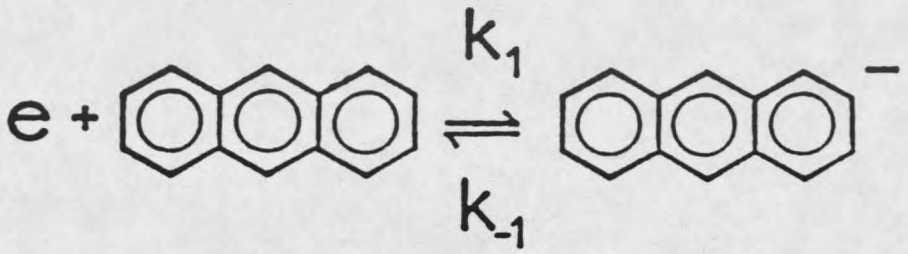

$$\frac{k_1}{k_{-1}} = \frac{5 \times 10^{-9}\ cc\ s^{-1}}{1.0 \times 10^{7} T^{3/2} e^{-(12\ kcal/RT)}\ s^{-1}}$$

	100°	150°	200°	250°	300°	350°C
τ_{-1}(us)	103	13	2.3	0.6	0.2	0.07

Fig. 5. Resonance electron capture mechanism of anthracene. Rate constants and lifetimes of the negative anthracene ion (k_{-1}) obtained from reference 30.

In Figure 6, the ECD chromatogram of anthracene on a commercial CC-GC-ECD system is shown. Not only was the response weak, as expected for the pure sample, but a very complicated and useless analytical signal was observed. These "W" shaped peaks have been reported before for many of the PAH's, including anthracene[11,12]. This effect was dependent on the compound type, concentration, and the operating detector temperature. In Figure 7, using the EC cell on the APIMS described in Figure 2, the responses to three different concentrations of anthracene are shown. The electronics package used for this detector was a fixed frequency pulser. A normal analytical signal in a fixed frequency pulse modulated ECD is reflected by a decrease in the level of standing current due to the loss of electron density.

In the chromatograms represented in Figure 7, the loss of baseline standing current for the first minute after injection corresponded to the benzene solvent. Two minutes after injection, anthracene eluted in a broad 1-minute wide peak. As can be seen in this Figure, as anthracene passes through the detector, an inverted response, reflecting an increase in electron density occured for all three sample sizes. Higher concentrations of anthracene produced a response similar to the one shown in Figure 6. With lower detector temperatures the EC response was favored by a reduction in the electron detachment rate and the subsequent

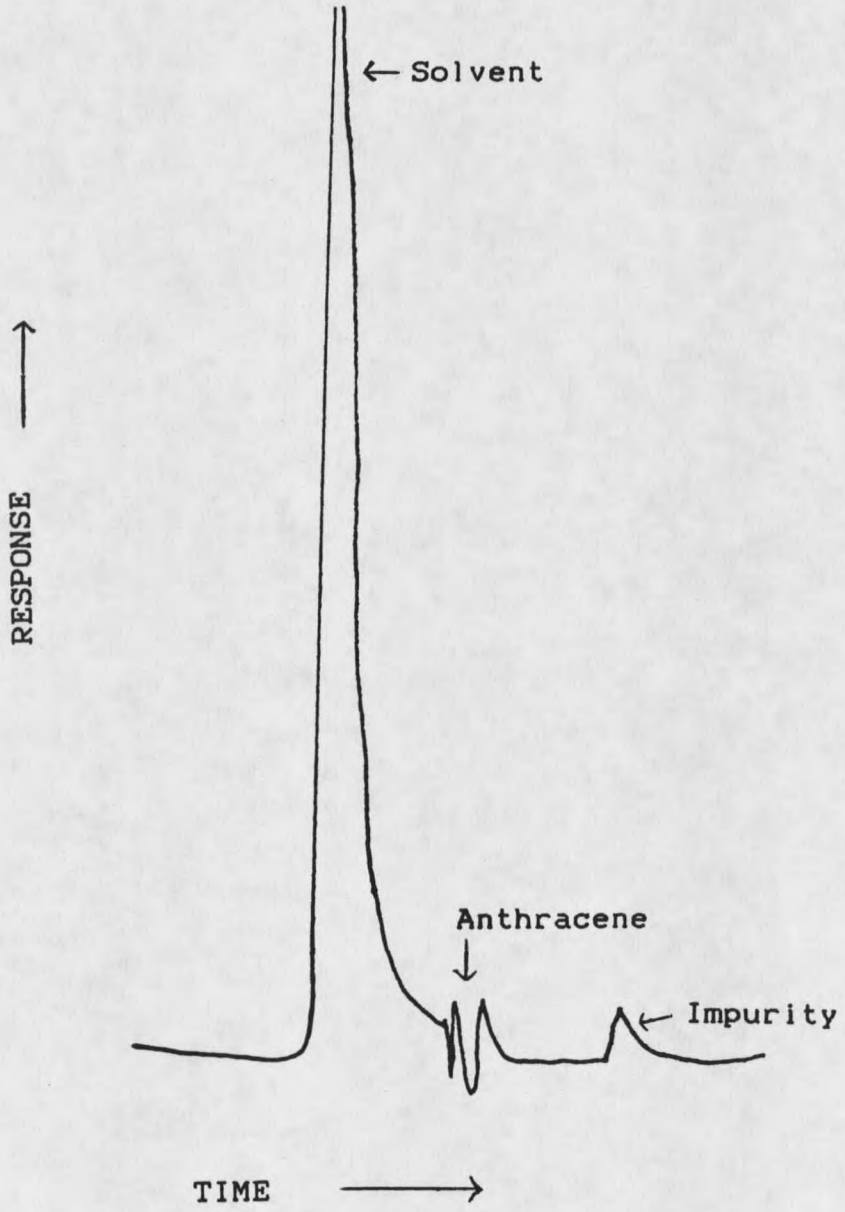

Fig. 6. Reconstructed chromatogram of anthracene from a Varian gas chromatograph equipped with a constant current ECD.

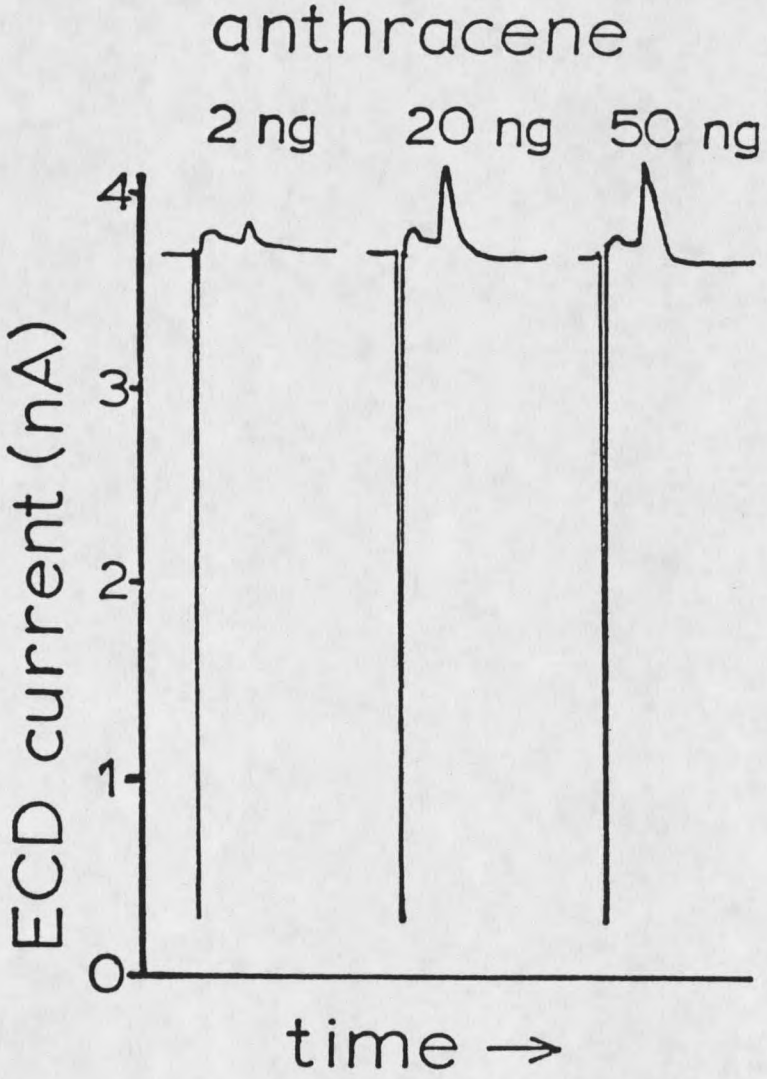

Fig. 7. ECD response of APIMS to three anthracene samples with N_2 as the carrier gas. Detector temperature was 250° C.

formation of a more stable negative ion. Figure 8 was produced under the same conditions as Figure 7 except that the detector temperature was lowered. In the case of the 2-ng sample, a completely inverted response was still observed. With the 20-ng sample, the response was still inverted but had a more complex shape. The electron density first increased, then decreased in the center of the peak; then increased again and finally decreased back to the baseline as the detector was cleared of anthracene. The 50-ng sample has a similar response, except at the center of the peak greater electron loss was seen. As has been demonstrated in Figures 6-8, the nature of the unusual response was dependent on analyte concentration and detector temperature, and this effect can be observed on more than one instrument. This anomolous response has been observed on various commercial and homebuilt GC-ECD systems (Valkenburg, unpublished data). Wizner et al.[11] also reported W-shape peaks for several other polynuclear aromatic hydrocarbons. It was concluded that these unusual responses are not due to the physical characteristics of the ECD, since different ECD geometries were used. Thus, some common characteristic in the ECD plasma is most probably the cause.

In a previous study it was suggested that the unusual responses to anthracene were due to positive ion chemistry[12]. With the use of the APIMS, the character of

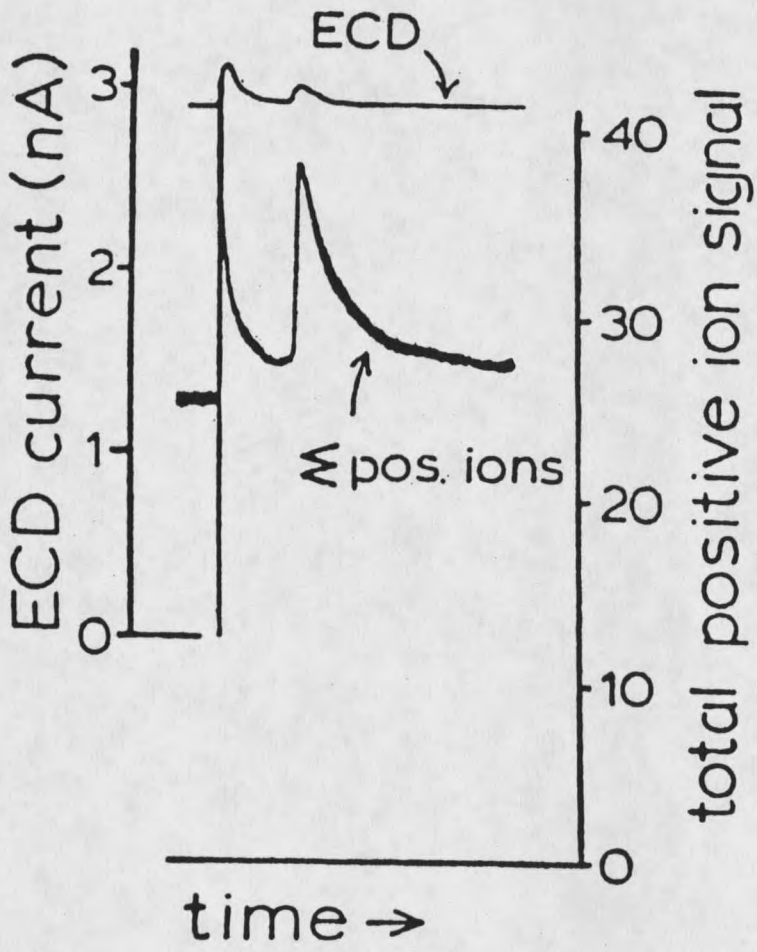

Fig. 8. Analysis of 2-ng anthracene sample using N_2 carrier gas with simultaneous measurement of the ECD current and the APIMS total positive ion signal.

positive ion chemistry dynamics occurring within the ECD was investigated for the condition of anthracene samples. In Figure 8, the mass filter analyzed the total positive ions during the chromatogram of anthracene, while, simultaneously, the ECD function was monitored. In mass spectrometry with quadrupole detection there is a bias towards higher masses when using the selected ion monitoring (SIM) or the total ion mode. Thus, the increase in the total positive ion signal may be attributed to three possible reasons. First, the total number of positive ions has increased; second, the mass of the positive ions within the detector has increased and the response was a function of the detector's bias towards larger masses; or third, a combination of these two.

In Figure 9 the positive ion spectra were recorded at various times during the chromatogram of anthracene. To aid in the interpretation of these chromatograms, the major ions observed in these chromatograms were monitored by setting the mass filter to SIM. The results are shown in Figure 10. The identification of the ions was based on the previous experiments with APIMS using ECD ion sources[13,18,45]. The intense ion at m/e 37 was commonly observed in the positive APIMS spectrum of nitrogen[45] and was assigned as $(H_2O)_2H^+$. The ion at m/e 224 is always observed in our system and has been attributed to a column bleed molecule because of its silicon isotope peaks, and probably originates from the

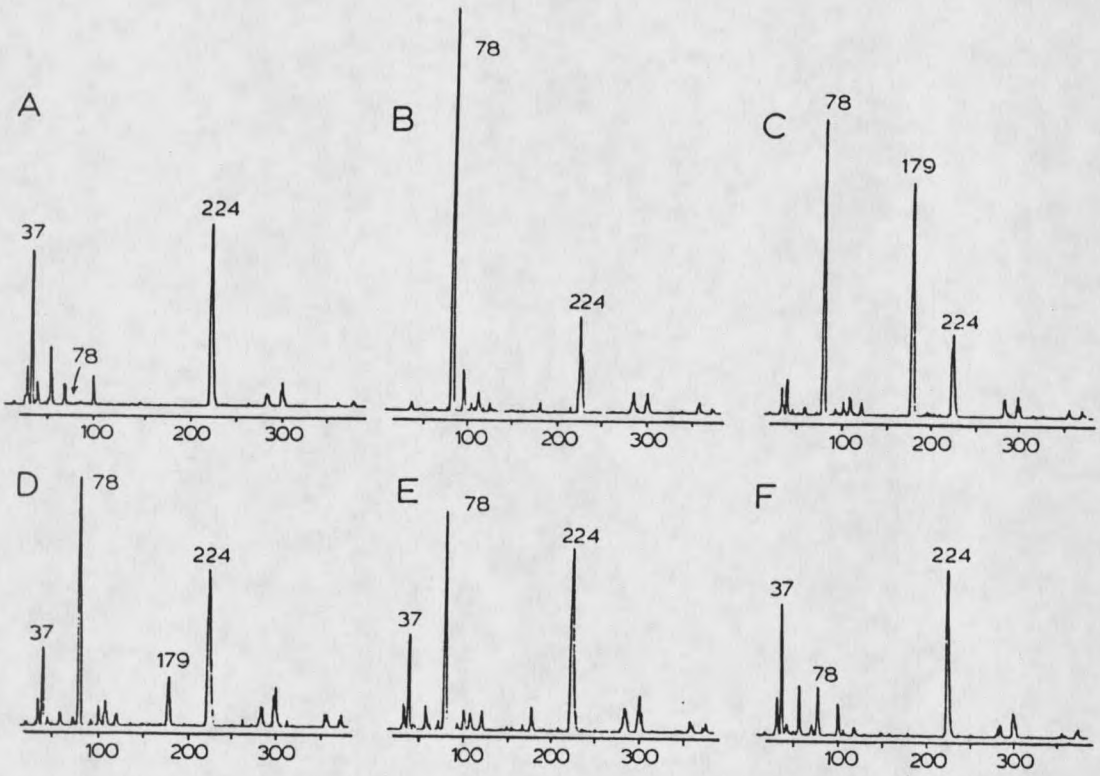

Fig. 9. Positive ion APIMS mass spectra recorded at various times during the analysis of a 2-ng anthracene sample using N_2 carrier gas: (A) just prior to the injection of sample, (B) just prior to the elution of anthracene, (C) during the elution of anthracene, (D) 2 minutes after the anthracene peak, (E) 1/2 hour later, and (F) 2 hours later.

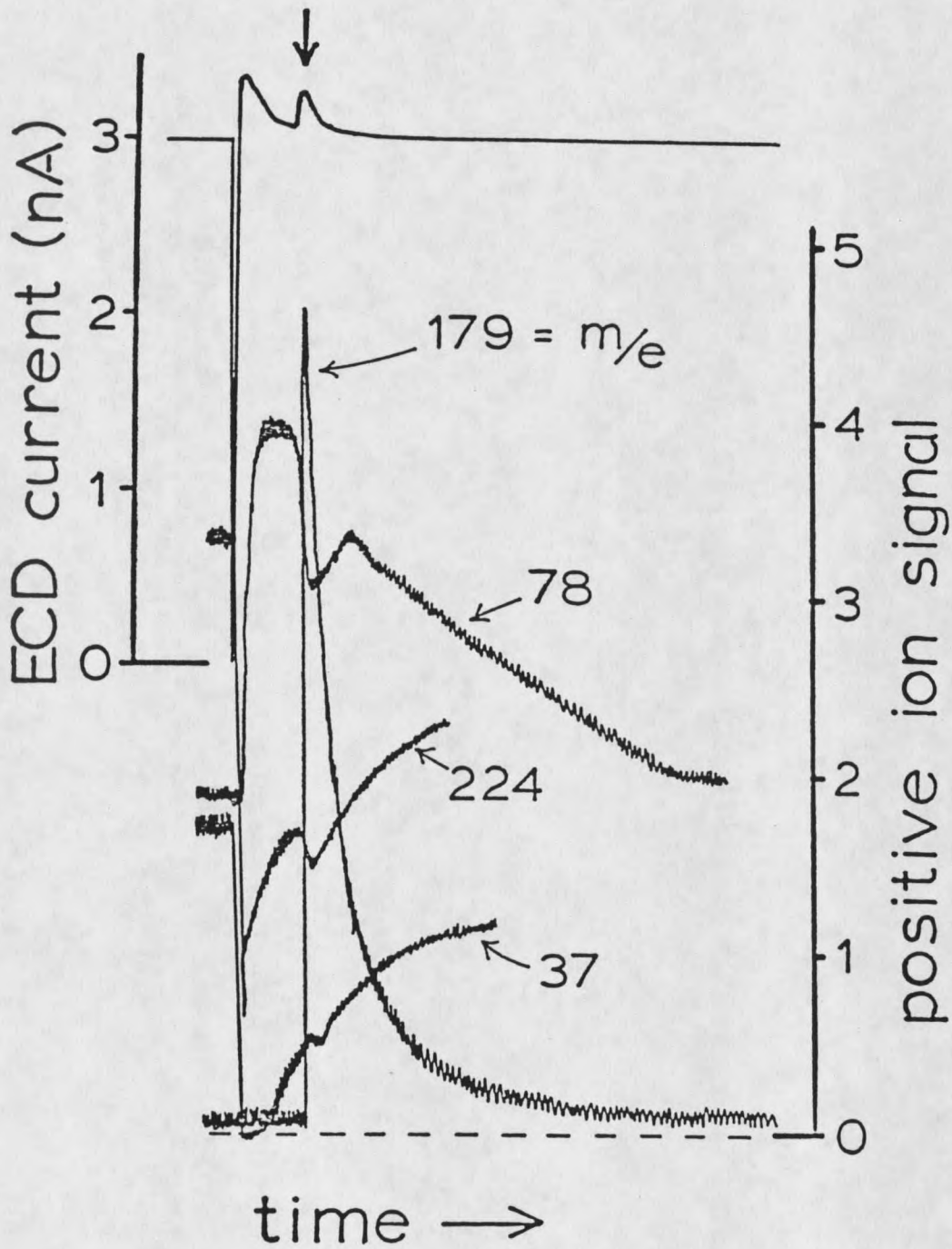

Fig. 10. Four repeated analyses of 2-ng anthracene samples with N_2 carrier gas and simultaneous measurement of the ECD current and the intensities of selected positive ions.

Si-based OV-101 column used in this study. The ion at m/e 78 was not seen until the solvent entered into the detector. This ion reflects the presence of the benzene solvent. This solvent ion persisted as an impurity within the system for many hours. Thus it was commonly observed between sample injections and was considered a stable impurity level for this discussion. These three terminal positive ions were the most stable when clean N_2 was used as the carrier gas. During the elution of anthracene the $(M + H)^+$ ion at m/e 179 was evident. Ideally, what can be seen in Figure 10 was that the positive ion nature of the ECD is dynamic and changing throughout the chromatogram of a sample.

From previous studies[45,46] the complicated positive ion spectra observed in APIMS studies were explained by rapid proton transfer reactions, with the terminal positive ion spectra dominated by those molecules with the highest proton affinity (PA). These points were addressed by Grimsrud[46] to explain the positive ions measured when a 99% pure sample of methylamine was doped into the detector. He suggested that the impurities of other alkylamines, particularly trimethylamine, were the cause of the positive ion spectra measured. He related the observed spectra to proton transfer reactions and considered the thermodynamics of this reaction:

$$CH_3NH_3^+ + (CH_3)_3N \overset{K_{eq}}{<----->} CH_3NH_2 + (CH_3)_3NH^+ \qquad (13)$$

The proton affinities of methylamine and trimethylamine were 212.3 kcal/mole and 222.1 kcal/mole respectively[47]. An approximate value for the equilibrium constant can be determined through this equation:

$$K_{eq} = \exp(222.1 - 212.3/RT) = 5 \times 10^4 \text{ at } 180^{\circ} C \qquad (14)$$

Thus, trimethylamine, as an impurity with a concentration as low as 0.1% of the methylamine dopant, could produce the terminal positive ions seen in the ECD ion source by APIMS. This experiment demonstrates that the terminal positive ions can be affected by the proton affinity of neutrals and their concentrations. The proton affinities of benzene, anthracene and H_2O are 188, 206.4, and 171, respectively[47,48]. These values are quite high and make their appearance in the positive ion spectra reasonable.

In view of these characteristics, it has been determined that during a chromatogram, the ECD plasma contains an uncontrolled set of positive ions. This is a dynamic and continuously changing system, which is dependent upon the existing neutral's proton affinity and its overall concentration within the detector. The changing set of positive ions within the detector could then affect the electron density through some chemical processes. Using this knowledge of positive ion formation within the ECD it was believed that the terminal positive ions could be stabilized by doping the ECD with compounds of high proton

affinity. The selection of a satisfactory chemical dopant with its accompanying impurities to control the positive ion character must meet these three criteria:

1) The dopant must be of a very high proton affinity and its concentration must be large enough relative to the analyte to satisfy the equilibrium mentioned in equation (13) and (14).

2) The dopant or its impurities must not react with the reagent electrons and destroy the baseline of the detector, ie., they must be compounds with a very low or negative EA.

3) The dopant must not facilitate any indirect electron capture by reacting with the analyte or the analyte negative ion, since this would complicate the interpretations of the effects by positive ion control.

If such a compound could be found then, in theory, the nature of the positive ions could be controlled, as well as their effects on electron density. The observed mass spectrum in Figure 11, indeed suggests such a case, where 100 ppm of the detector gas was trimethylamine (TMA), The intense ion at m/e 60 was assigned to the $(M + H)^+$ ion. The ion at m/e 58 was the $(M - H)^+$ ion and has previously been observed in the chemical ionization mass spectrum of TMA at 1-10 torr pressures[49]. The ions at m/e 117 and 119 are the cluster ions from an additional TMA molecule to ions m/e 58 and 60. Given the simple spectra from the TMA dopant and

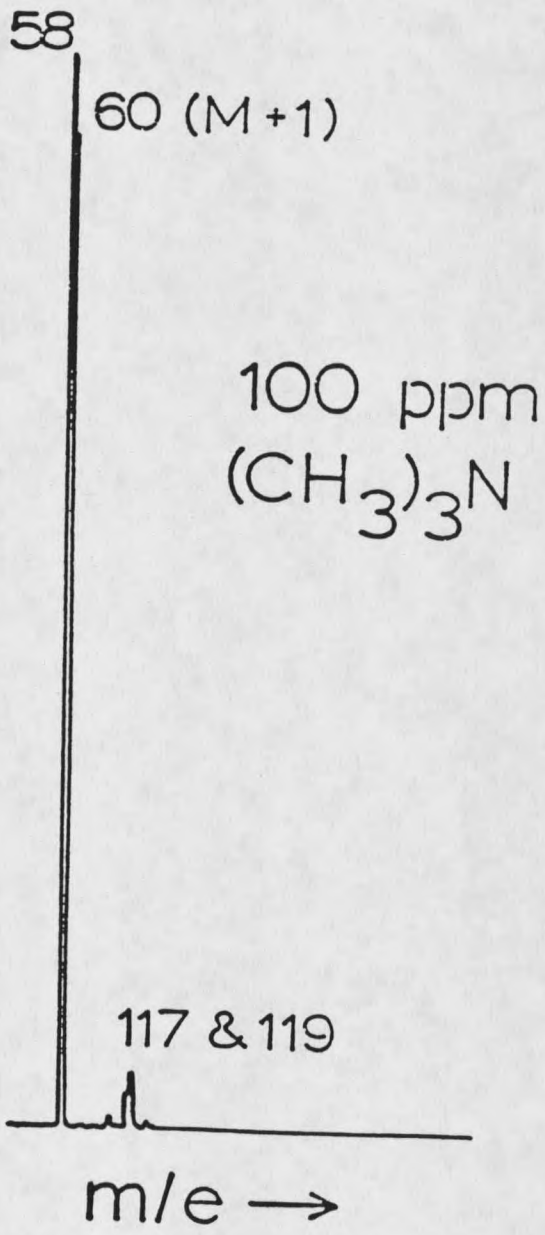

Fig. 11. Positive ion atmospheric pressure ionization mass spectrum of N_2 carrier gas doped with 100 ppm of $(CH_3)_3N$.

the absence of normal positive ions (Figure 9 (A) and 9 (F), respectively), suggest that the TMA dopant is dominating the positive ion nature of the ECD because of its proton affinity and concentration. The addition of 100 ppm TMA resulted in an insignificant decrease in detector baseline and, occasionally improvements in standing current were observed.

In Figure 12 the total positive ions and the characteristic ions for TMA (m/e 60) and anthracene (m/e 179) are monitored in addition to the normal ECD function for the same three samples and conditions used to produce Figure 10. The response illustrated in Figure 12, and the fact that the spectra observed throughout the chromatogram was that observed for TMA, indicates that the anthracene molecule was not protonated. The total number of positive ions is constant in composition and population. Additionally, the ECD function indicates a weak but normal electron capture response as anthracene passes through the detector.

These results indicate a relationship between positive ion stabilization with TMA and the response of the ECD for anthracene. If TMA is only affecting the positive character of the ECD, then a reasonable modification of the existing theories can be used to explain the relationship between positive ions and the anomalous results shown in Figures 6, 7, and 8. The mechanism used to explain these results is shown in Figure 13.

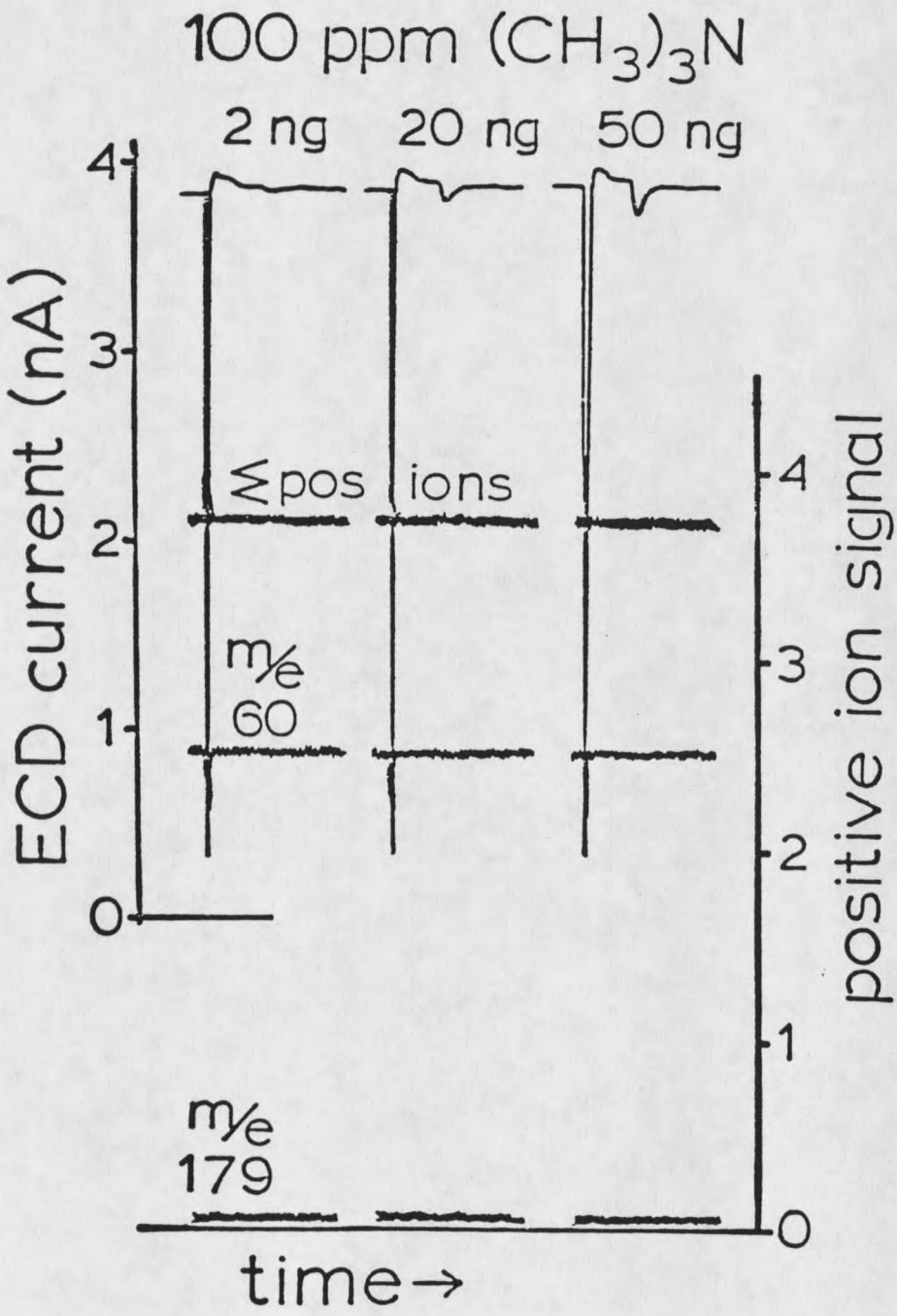

Fig. 12. Analyses of three anthracene samples using N_2 carrier gas doped with 100 ppm of $(CH_3)_3N$ and simultaneous measurements of ECD current and selected APIMS positive ion signals.

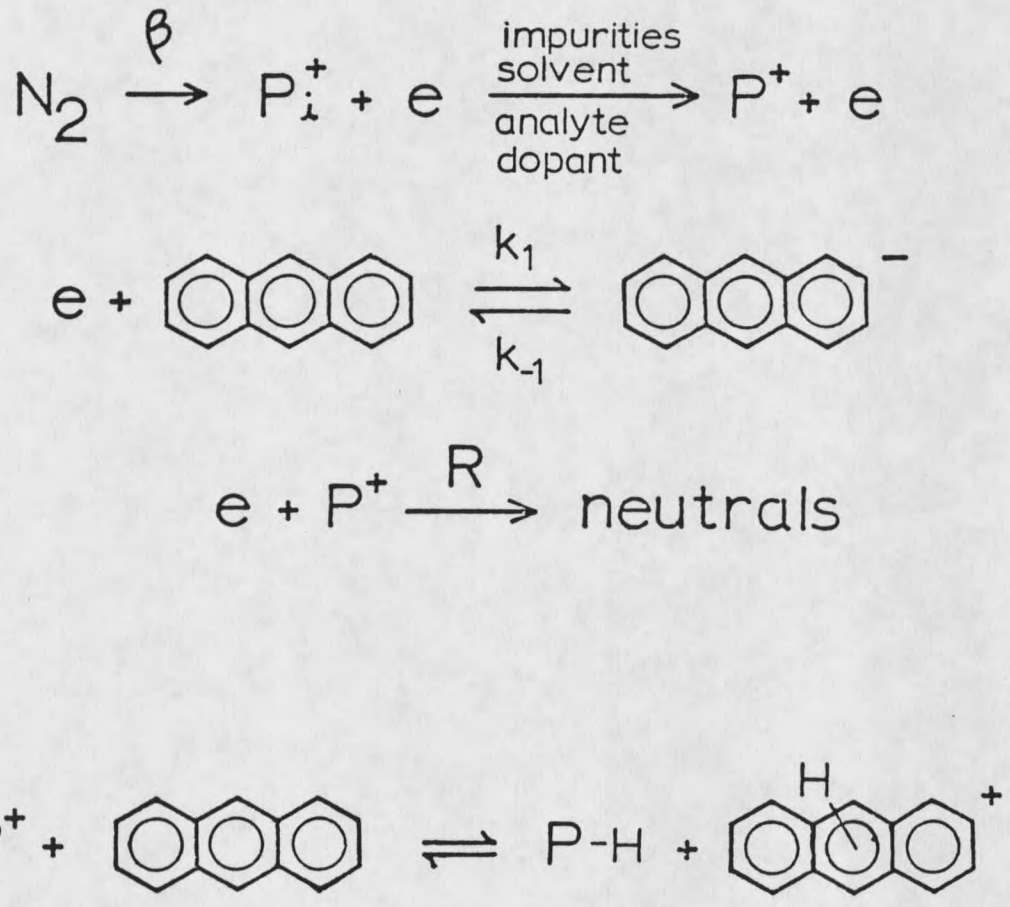

Fig. 13. The reaction sequence of positive ions produced from beta radiation in the ECD during the elution of anthracene.

The reactions shown in Figure 13 symbolize the formation of initial positive ions and electrons by beta radiation, the resonance electron capture by anthracene, the recombination of electrons with positive ions, and the protonation of anthracene by proton transfer. In N_2 detector gas the initial positive ions formed are the very reactive N_3^+ and N_4^+ ions which undergo further proton transfer to impurities and/or dopants in the N_2 detector gas (43). As shown in Figures 10 and 12, the normal positive ions in undoped carrier gas were reactive to the anthracene neutrals and, under the TMA doped conditions, this reaction was not favored. The recombination rate constant, R, in the reaction of positive ions with electrons could conceivably be dependent upon the nature of the positive ions within the detector. If this was the case, then the rate of reaction for the undoped condition may have been changing throughout the chromatogram. Thus, when the positive ions were stabilized by TMA doping, the rate could be given a fixed value.

During the elution of anthracene a very drastic change in the nature of the positive ions was noted. This large aromatic molecule could conceivably spread the positive charge throughout its π-resonance system and produce a very stable positive ion. It would be reasonable to expect that this type of stable positive ion could have a recombination rate constant significantly smaller than the

average rate constant expected for the impurities. A smaller recombination rate constant between the electrons and positive ions would shift the existing equilibrium and, consequently an increase in electron density and positive ions could then be accounted for. The ECD response for anthracene illutstrated in Figure 7, indicating the weak loss of electrons by resonance electron capture, was overwhelmed by the increase in electrons from the change in the average positive ion/electron recombination rate. If positive ion stabilization is considered, then the weak electron capture reaction observed for anthracene (Figure 12) can then be explained.

The above model could also be used to explain the W-shaped character of the peaks in Figures 6 and 8. The electron loss rate with larger sample sizes, or decreased temperatures, eventually exceeds the production of electrons by the anthracene positive ion chemistry. In Figure 10, a relationship emerges between the three negative responses for the increasing sample sizes and the measured level of positive ions for anthracene. Between the 20 and 50 ng sample masses only a small difference was noted in the quantity of anthracene positive ions and the negative EC responses. This non-linear relationship between sample size and the amount of anthracene protonation can be elucidated through an understanding of ECD plasmas.

The total number of positive ions is determined by the detector design, the activity of the radioactive foil, and the recombination loss rate[16]. With the 50-ng anthracene sample the majority of positive ions measured were those of anthracene. In the APIMS it has been noted that concentrations of TMA dopant as low as 0.1 ppm were sufficient to dominate the mass spectrum. Therefore, the production of electrons by a decrease in the average recombination rate is limited in amount and would involve only a specified quantity of analyte molecules. Any excess neutrals would then be available for electron capture reactions. An electron loss was seen only when a response value exceeded the finite amount of electron production allowed by a change in the recombination rate. In the case of the lower detector temperature (Figure 8) or if a larger sample size would be used, the unreacted neutrals had a larger electron capture response and this was reflected by the normal deflection in the center of the peaks where the largest amount of compound was present. On either shoulder of the peak, analyte concentration within the detector was a smaller concentration and the effects of the positive ion dynamics could then be seen.

To ensure that the proposed mechanism was correct and that the criteria for a successful positive ion dopant were met by TMA, a series of chemical dopants with various proton affinities were tested along with TMA. In Figure 14 the

results from these experiments are shown. The ECD function was monitored along with the SIM trace of the positive m/e 179 ion. The SIM of the positive m/e 179 was selected to indicate the degree of protonation of the anthracene ion. Compounds were chosen which gave only a small loss of baseline when 100 ppm was doped into the detector gas.

The important characteristics to be noted in Figure 14 are: (1) the standing current and its subsequent loss when the dopant was injected; (2) the degree of protonation of anthracene as indicated by the positive ion signal at m/e 179; and (3) the ECD response to the samples. In Figure 14 (A) the normal response in clean N_2 is shown as a reference. The positive ion signal observed at m/e 179 indicates substantial protonation of anthracene and near-saturation of the positive ion signal with the large sample size. In Figure 14 (B) the beneficial effects of TMA are again shown. In Figure 14 (C) and 14 (D) the effects of methylamine (PA =213 kcal/mole) and NH_3 (PA = 204 kcal/mole) indicate that these compounds can also control the positive ion character. Due to their lower PA's a slight amount of protonation of the anthracene ion was indicated with the larger sample sizes. The positive ion control attained by these compounds again yielded a weak electron capture response. It is postulated that the slightly improved ECD response for the methylamine doped condition may be due to the impurities within the dopant, quite possibly O_2 or H_2O from the dopant

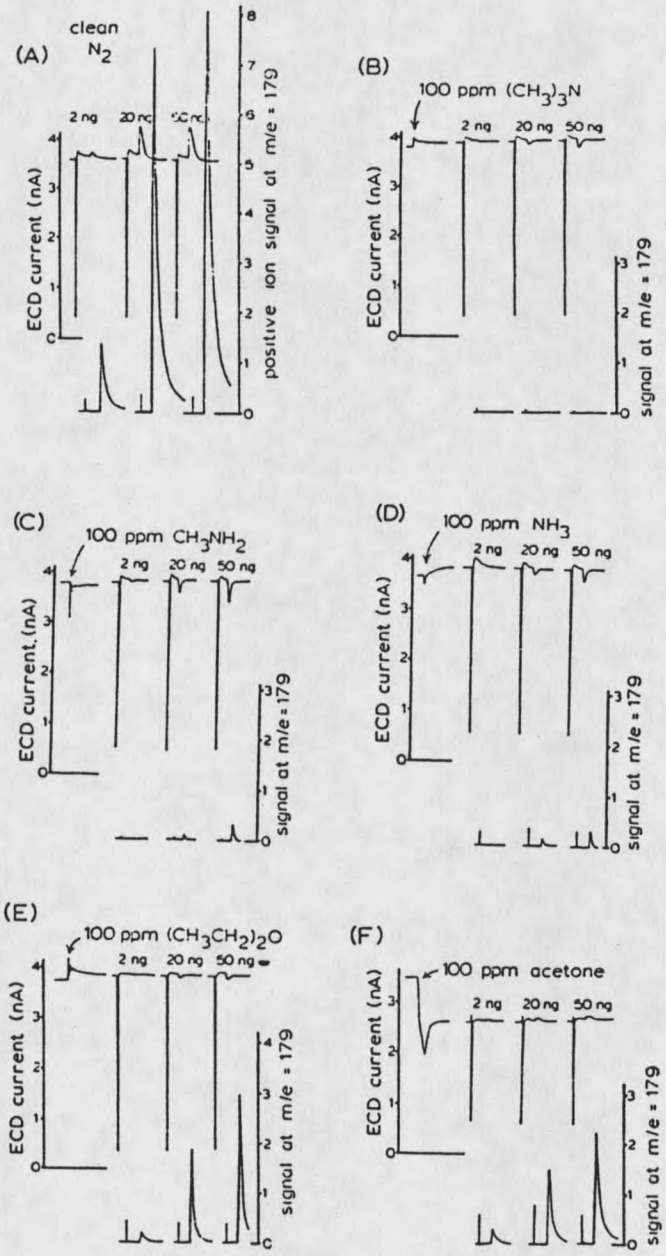

Fig. 14. Repeated analyses of anthracene samples with various chemical dopants added to the carrier gas. In addition to the ECD current, the positive ion intensity at m/e 179 was monitored. In each instance, the effect of addition of the dopant to the carrier gas on the ECD standing current is also shown.

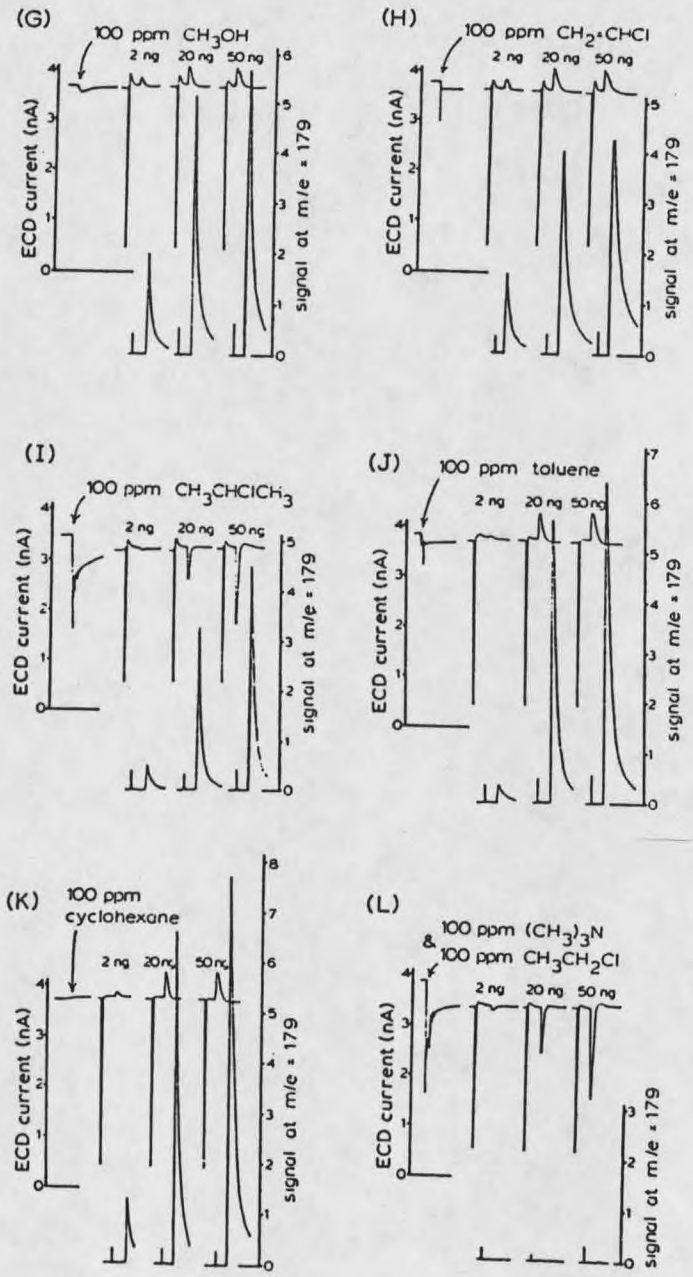

Fig. 14 - Continued

preparation method (See experimental section). In Figures 14 (E), (F), and (G), the responses to anthracene with the addition of dopants of decreasing PA are shown. In the presence of diethylether (PA = 199 kcal/mole), the total mass spectrum still retained characteristic ions of the diethylether, but now the proportion of positive ion at m/e 179 increased. Also the EC response of anthracene become less obvious. With acetone (PA = 194 kcal/mole) and methylalcohol (PA = 184), the positive ion control was no longer effective as manifested by the progressive negative response of the ECD function and the m/e 179 ion increase. With methylalcohol there were essentially, no beneficial positive ion effects, and the response appeared very similar to clean N_2. In the three cases shown in Figures 14 (H), (J), and (K) where non-basic hydrocarbons were used, no indication of positive ion stabilization or normal EC response was apparent.

Alkyl Chloride Doping

The monochloroalkanes used in Figures 14 (I) and 14 (L) were chosen as chemical dopants because any chemical species that may cause indirect electron capture were expected to be removed by the alkyl chloride dopant. This class of dopant was not expected to give any beneficial effect on positive ion chemistry stabilization due to its low proton affinity. The use of alkyl chlorides was based on the unusual response

that the monochloroalkanes had in the ECD, and the explanations given for these responses[28,44,50]. Figure 15 presents the response versus concentration curve obtained with a Varian CC-GC-ECD. This is shown for three monochloroalkanes. Also included in the Figure is the response of vinylchloride, a compound known to give linear response curves, to demonstrate that a linear calibration was possible and that the response was not an artifact of the experimental procedures or instrumentation. In Figure 15, it can be seen that the three alkyl chlorides all had large molar sensitivities in the very small concentration range and then quickly reached a limiting response that did not increase with larger concentrations of sample. It should be noted that the maximum level of response or, in this case, the baseline frequency of the constant current pulsed detector increased only slightly, about 1 kHz in this example. This is one property necessary for a suitable dopant.

The effect of detector temperature on the response of ethylchloride (EtCl) is shown in Figure 16. It can be seen that at lower detector temperatures response curves similar to those shown in Figure 15 were observed for EtCl. With the higher detector temperature (350° C), the same elevated molar responses were seen for the very small concentrations. With larger concentrations, however, the response became linear with concentration, although with a small molar

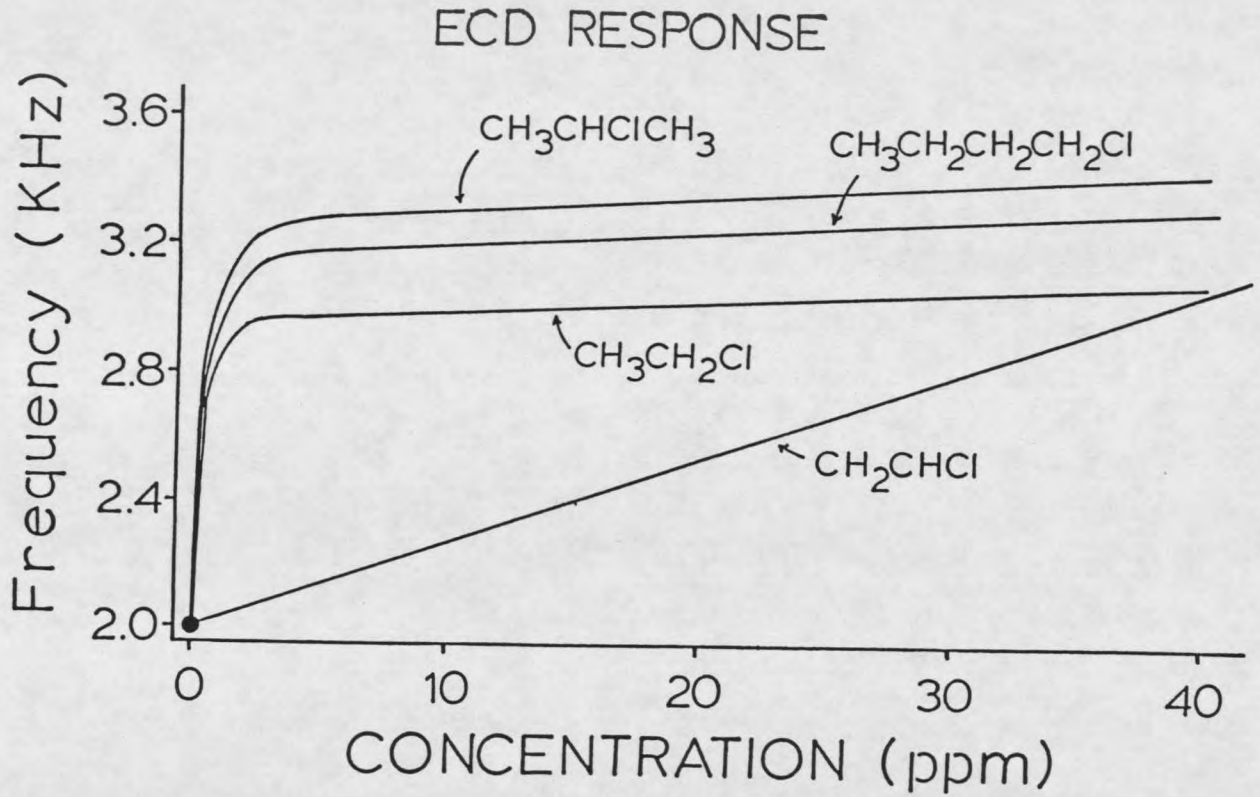

Fig. 15. Baseline frequency of the Varian CC-ECD as a function of the concentration of various monochlorohydrocarbons in N_2 detector gas at 250° C.

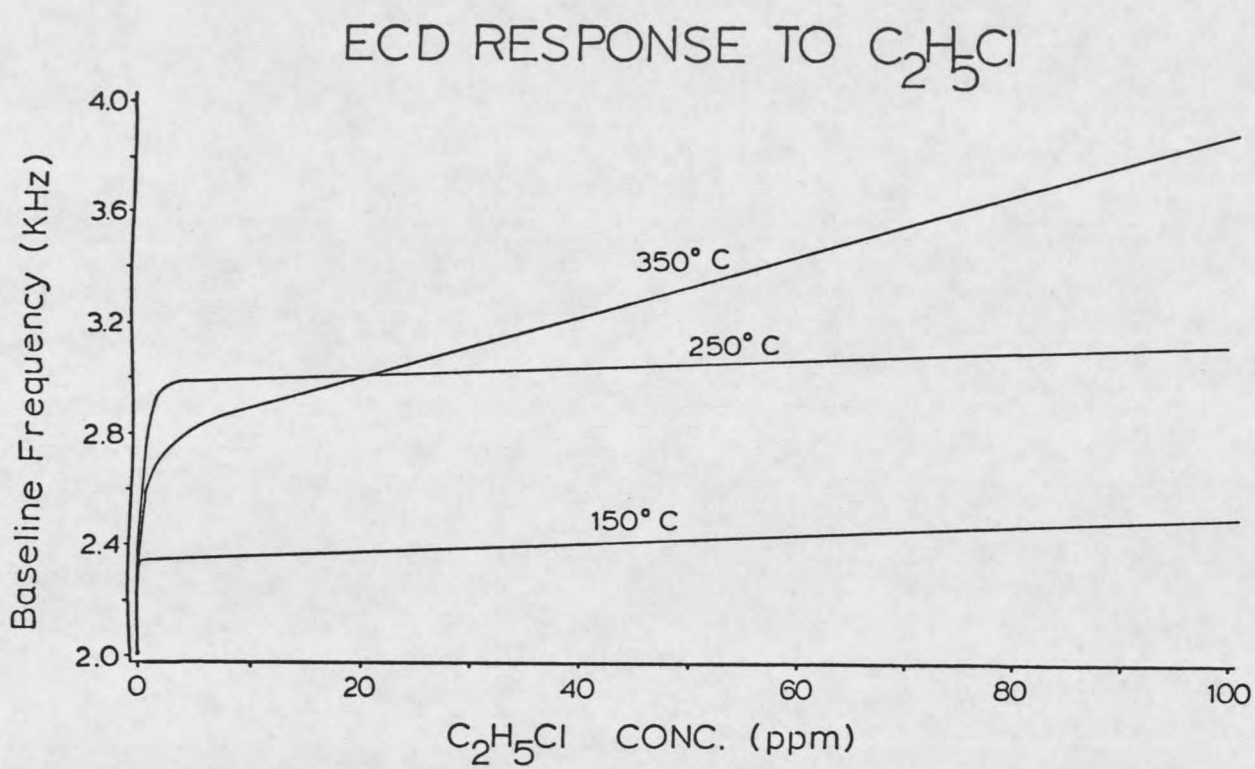

Fig. 16. Baseline frequency of the Varian CC-ECD as a function of the amount of ethyl chloride doped into the N_2 detector gas at three detector temperatures.

sensitivity. This type of temperature dependence was also observed for the other monochloroalkanes used in Figure 15. These two experiments with alkyl chlorides were conducted by measuring the baseline of the detector with sample introduced into the detector by an exponential diluter. Similar results have also been obtained when the sample was introduced into the detector as a chromatographic pulse via column chromatography.

In the interpretation of these unusual responses at low temperatures, it was thought that direct electron capture was not occurring with any of these alkyl chlorides. The response seen for the low concentration region was the result of an indirect electron capture process by some sensitizing reagent within the ECD plasma. This reagent, which was thought to be in limited quantity, was titrated and removed from the detector by a low concentration of sample. Once the sensitizing species was removed from the detector, there was no longer a basis for response with increased levels of the alkyl chlorides. At the detector temperature of 350° C, a dissociative capture mechanism was facilitated and was responsible for the linear increases in response to sample concentration with the larger sample sizes. A thermally assisted dissociative mechanism of response is reasonable for the monochloroalkanes since the polychloroalkanes are known to respond by this mechanism[51]. For these compounds detector temperatures in excess of

300° C were sufficient to cause an increasing degree of sensitivity and linearity by means of a dissociative mechanism.

Numerous investigations have been made to determine the chemical species responsible for the sensitized response in the low concentration range. Trace levels of O_2 were initially suspected as the causative reagent, yet tests to prove this hypothesis did not support this conclusion[10]. Later testing for hydroxyl radicals, H_2O, and NH_3, also gave inconclusive proof as to the species responsible[44,50]. For this study, the hypothesis was that a limited amount of sensitizing reagent may be present in the detector gas. The addition of an alkyl chloride as a dopant to the detector gas should titrate and remove these species. Thus, if an alkyl chloride were added along with the TMA dopant the ECD function should represent only the resonance electron capture of a low EA compound, since the positive ions would not be affecting the electron density. Furthermore any sensitizing species should be lost to reaction with the EtCl and unavailable to sensitize the response.

The results shown in Figures 14 (I) and 14 (L) do not support this hypothesis. In Figure 14 (I), with isopropyl-chloride as the dopant, the positive ions were not controlled as expected for this non-basic hydrocarbon. However, the ECD function yielded a normal electron capture response of even greater magnitude than any of the amine dopants.

This response was entirely unpredicted and without a reasonable explanation. Combining EtCl and TMA as the dopants in Figure 14 (L) shows that the positive ions were controlled by the TMA, but sensitized responses were again observed with a monochloroalkane present in the detector gas.

Further experiments were performed with the alkyl chloride dopants to determine a mechanism for the enhanced responses and to characterize the effectiveness of the sensitized response in general. In Figure 17, the response of two anthracene samples to differing concentrations of EtCl is shown. The response of the smaller anthracene sample rapidly increased with small concentrations of EtCl, and quickly reached a limiting value at 10 ppm of EtCl in the detector gas. The larger sample size was found to require a higher concentration of EtCl to reach the limiting value of sensitized response.

In another experiment, the APIMS was set to measure negative ions, and the entire mass spectrum was recorded at various times during the chromatogram for the clean and EtCl doped conditions. Throughout either of the chromatograms the only recorded negative ion signals of significant intensity were those of the background ions and those with EtCl doping at m/e 35 and 37. Comparisons between signal intensities of different ions was hampered by ion measurement biases[24]. The signal at m/e 178 for the anthracene molecular anion was very weak. In this mass

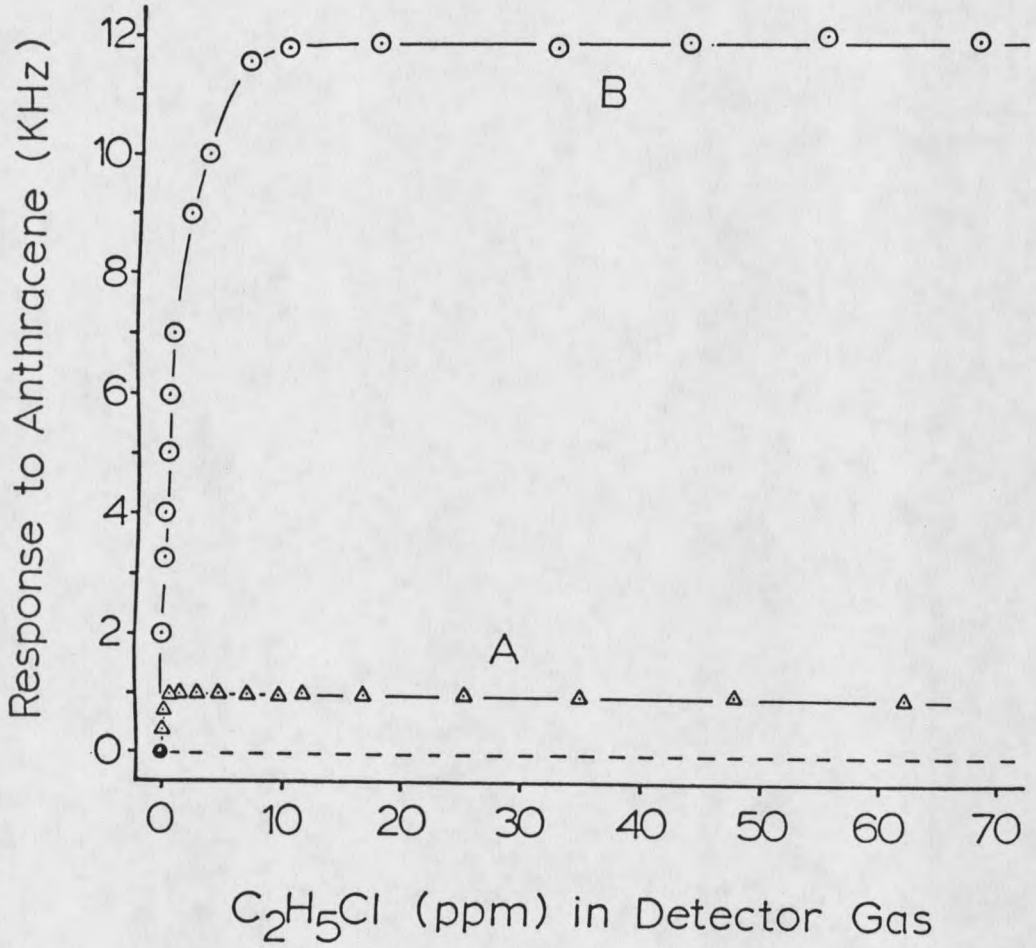

Fig. 17. Effect of ethyl chloride concentration in the carrier gas on the response to two anthracene samples (1x and 10x) on a Varian GC-CC-ECD system.

spectrometer only very stable negative ions were capable of being measured and the anthracene anion or any other anion susceptible to electron detachment does not usually survive the passage through the aperture and go on to the ion counting detector. Figure 18 is the SIM trace of the m/e 35 ion throughout the EtCl doped analysis of anthracene. The ion at m/e 35 was only significantly observed as anthracene passed through the detector. The very weak negative ion signal at m/e 178, normally seen with clean carrier gas, was not observed with EtCl doping. This information, along with the anthracene response versus EtCl concentration in Figure 17, was instrumental in forming the proposed mechanism of response which is given in Figure 19.

In this mechanism, the EtCl molecule is reactive to the analyte negative ion and through an electron transfer process the stable dissociative product, Cl^-, is yielded along with unknown neutrals. The summed effect by this mechanism is electron capture by an EtCl molecule. The resonance electron capture equilibrium of electron attachment and detachment is disturbed by this additional loss mechanism of anthracene anion, and subsequently more electrons are reacted with the analyte neutrals in an attempt to reestablish the equilibrium. The observed result is a sensitized response for anthracene. From the data in Figure 17, it appears that the negative ion trapping was quite effective. The rate limiting step is the production

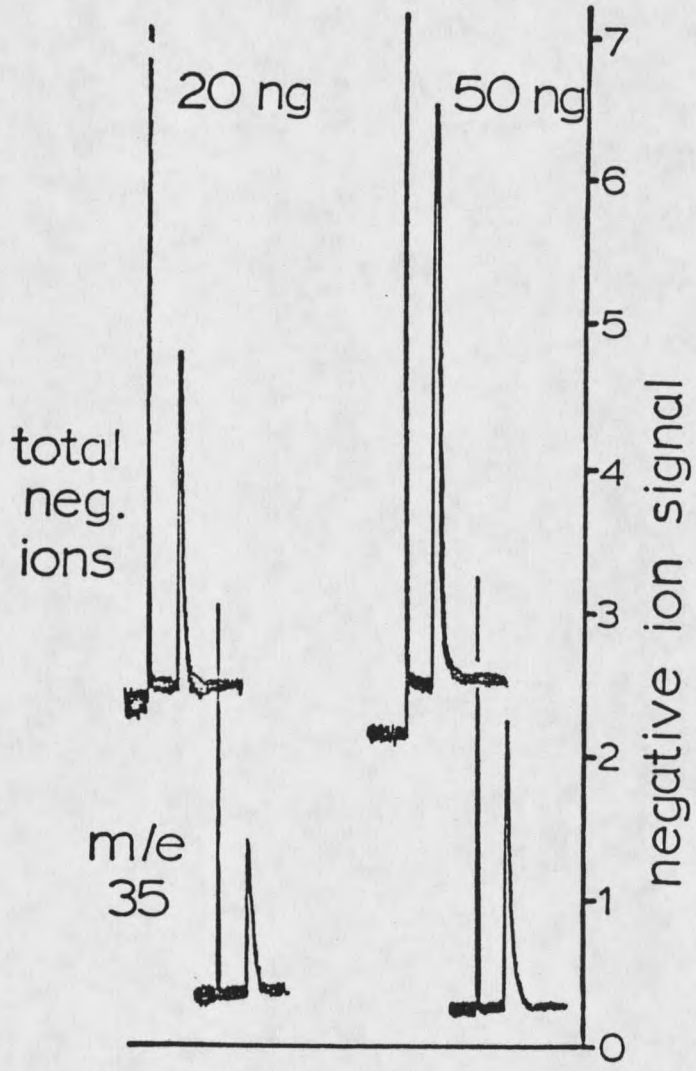

Fig. 18. APIMS total negative ion signal and Cl^- response at m/e 35 to two anthracene sample concentrations.

of the reagent analyte negative ion. Increases in the concentration of EtCl, greater than 10 ppm for the small sample, did not increase the degree of sensitization. If this was the case, where the limiting reagent was the analyte negative ion, then the rate of electron attachment should be dependent only on k_1, the forward rate constant of anthracene, which is of sufficient magnitude for a very sensitive response. The rate of reaction of the anthracene negative ion with EtCl was calculated at approximately the rate of an ion molecule reaction[52], 1×10^{-9} molecules cc sec^{-1}, from the data presented in Figure 17.

The mechanism proposed in Figure 19 is complimentary to the one that has been proposed for O_2 doping, except that the roles of analyte and dopant have been reversed. With EtCl doping, the analyte's electron attachment rate dictates the maximum sensitivity of the response. The resulting net reaction is the electron transfer from the unstable A^- ion to EtCl which dissociates to produce the stable Cl^- ion. The sum of the reactions indicates that the dopant provided the electron capture response. The degree of reaction with EtCl is dependent upon the production rate of the analyte negative ion, which is in turn dependent on the chromatographed analyte amount and the electron attachment rate. The ECD response is actually a function of the ratio of negative ions to electrons. The production of a more stable negative ion by electron transfer was the reason why a

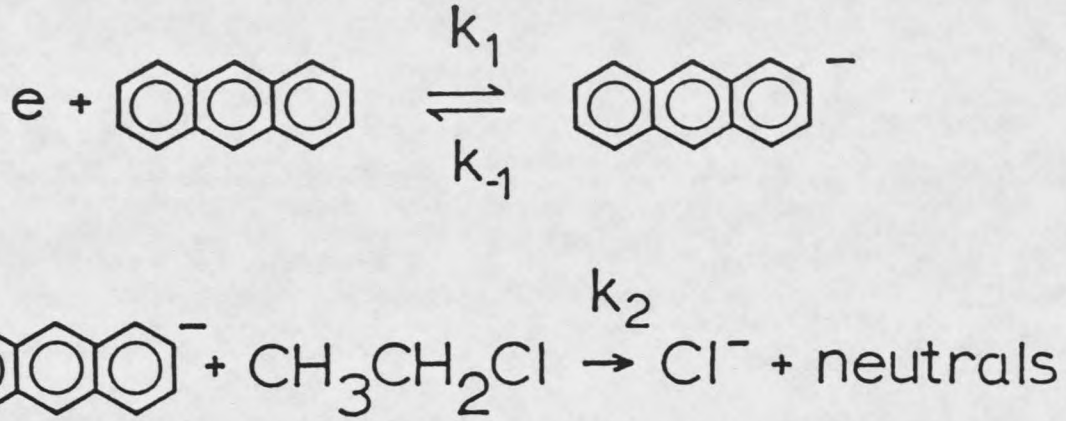

Fig. 19. Proposed mechanism for the ethyl chloride enhanced response of anthracene in the CC-ECD.

sensitized response was observed. This proposed mechanism also suggests some limitations to the alkyl chloride sensitization scheme. When stable negative ions are produced by a dissociative mechanism, or resonance electron capture with a small electron detachment rate, no sensitization would be expected to occur even when the EtCl is reactive to the analyte's negative ion(s).

The advantage of chemical doping for the analysis of anthracene can clearly be seen in Figure 20. In this experiment, calibration curves were produced on the Varian GC-CC-ECD instrument for three detector gas conditions. At the detector temperature of 330° C anthracene gave weak, useless, and even negative responses under clean N_2 detector gas conditions. With EtCl doping a large sensitized response was observed. However, with small concentrations of analyte, where the electron production rate by positive ion chemistry exceeded the loss rate by sensitized electron capture, negative responses were still seen. The addition of TMA to the EtCl doped gas produced a linear calibration curve with a Y-intercept at zero, and showed an even higher molar sensitivity for the anthracene molecule. Because of the limitations of the experimental procedure, a calibration curve was not done with TMA alone in this experiment. Subsequent experiments were done with clean N_2 and TMA doping, and the conditions made to resemble the experiment used to produce Figure 20 as closely as possible. The

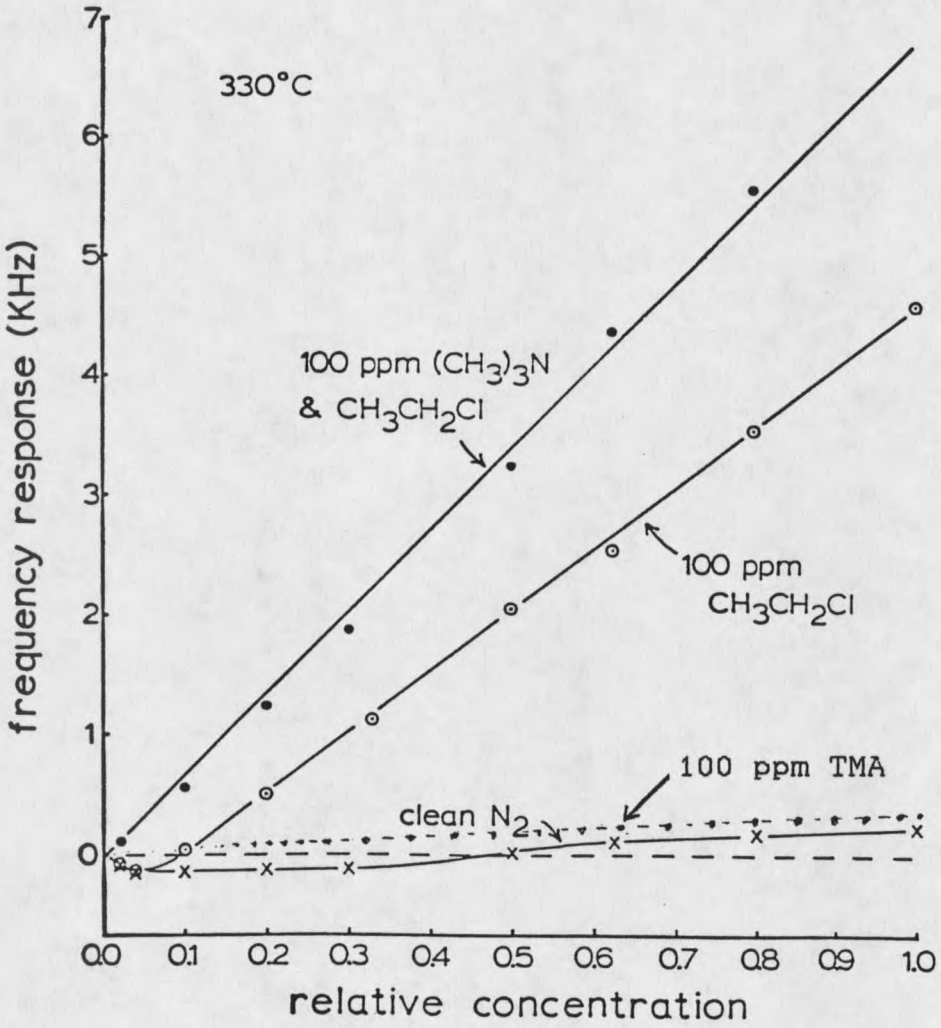

Fig. 20 Calibration graphs for the peak height responses of the Varian GC-CC-ECD to anthracene samples with N_2 as the carrier gas, N_2 carrier doped with CH_3CH_2Cl , N_2 carrier doped with $(CH_3)_3N$ (dotted line) and N_2 carrier doped with $(CH_3)_3N$ and CH_3CH_2Cl. Detector temperature 250° C.

results obtained from this second experiment with TMA were normalized to the data in Figure 20. The dotted line is the curve expected for TMA doping alone.

Calibration curves for anthracene were developed under the conditions of EtCl doping at various detector temperatures. These results are shown in Figure 21. A relative concentration of one corresponds to a sample size of 150 ng injected into the detector. Calculated EtCl concentrations within the detector were between 300 and 400 ppm for the entire experiment. Detector baseline went from 1.5 to 2.7 kHz for the lower detector temperatures. A linear relationship with higher EtCl concentrations was again noted for detector temperatures exceeding 300° C. The baseline at the 330° C detector temperature was between 4.0 and 4.5 kHz; the frequency increasing with the amount of EtCl dopant levels. An acceptable level of baseline for the Varian detector, when using N_2 carrier gas, is from 1.5 to 4.0 kHz. Thus, even at 330° C, only small losses of baseline were observed and the baseline remained near acceptable values when using up to 400 ppm EtCl dopant. The peak shapes for low levels of anthracene concentrations were normal except at the 330° C detector temperature, where the "W" shaped character became evident. The response value that was assigned to a peak with "W" shaped character was the largest normal response observed relative to the baseline in the chromatogram. The most important characteristic of this

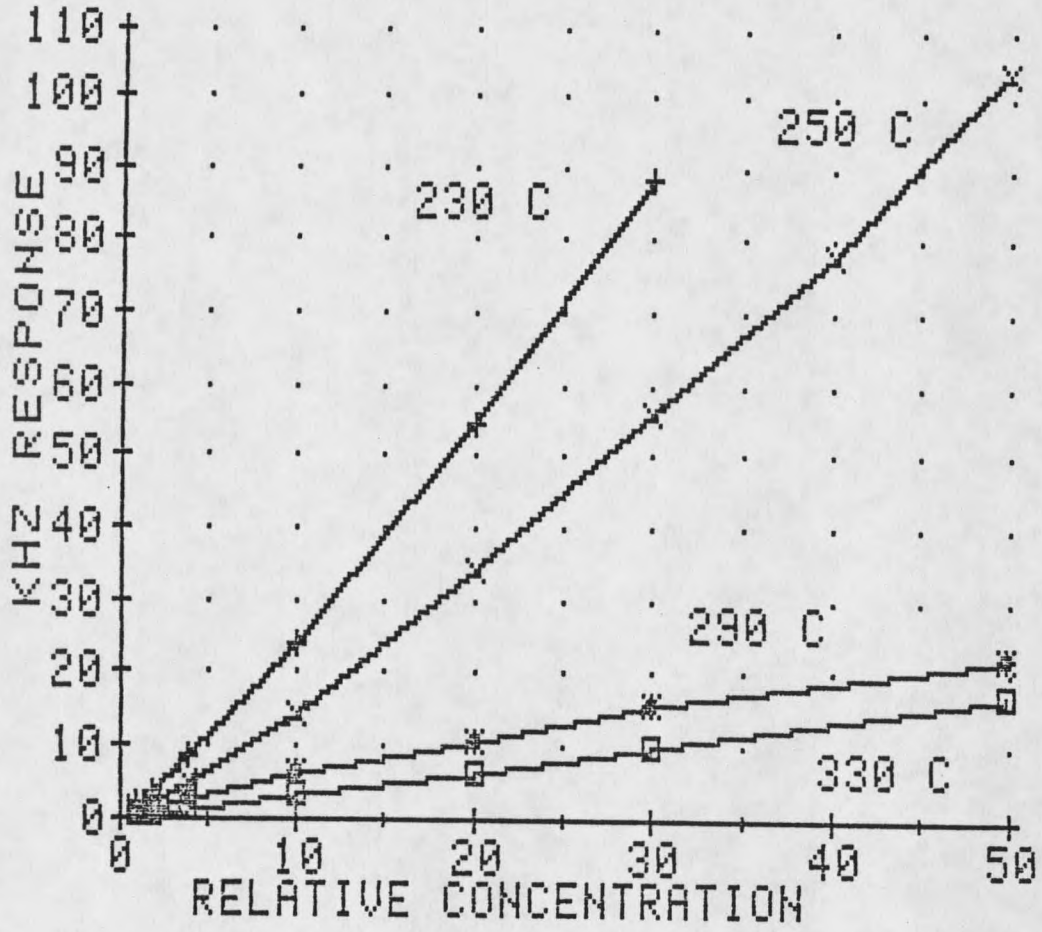

Fig. 21. Calibration graphs for the peak height responses of the Varian GC-CC-ECD to anthracene samples with ethyl chloride doping at various detector temperatures.

experiment was that the level of response for the sensitized condition was favored by the lowest possible detector temperatures.

In another experiment, four different alkyl chlorides were doped into the carrier gas and the sensitized response to anthracene was measured. These results have been previously reported[53]. The four alkyl chlorides, ethyl chloride, 1-chloropropane, 2-chloropropane, and 1-chlorobutane all gave identical sensitization levels for the anthracene molecule. This information gave additional support to the mechanism proposed for EtCl.

A capillary column with a splitless injection port was installed into the Varian GC-ECD system to examine the response of numerous compounds that were potential candidates for sensitization by the mechanism proposed for anthracene. The compounds chosen were low EA molecules known to respond by a resonance electron capture mechanism. Each sample was diluted in benzene or toluene as a pure standard and its retention time was identified by flame ionization detection. ECD detection followed by simply moving the column within the same chromatograph to the appropriate detector housing containing the ECD.

Each compound was tested individually for three conditions of detector gas: clean N_2, TMA doped, and EtCl/TMA doped. The detector temperature chosen for the survey was the lowest possible relative to the minimum

temperature needed for the chromatographic analysis. In Figure 22, the response to a 38-ng benzophenone sample is shown for clean N_2, 100 ppm TMA doped, and TMA with EtCl. The significant improvements in signal to noise as well as the increased signal with EtCl/TMA doping for benzophenone was evident from the results shown. The enhanced values relative to the clean N_2 response for the benzophenone sample were 1.0 : 1.35 : 99.

Calibration curves for benzophenone, shown in Figure 23, include four detector gas conditions and reveal that only in the TMA/EtCl doped condition was a linear response versus concentration observed. Clean N_2 and TMA doped alone responses yielded weakly responding and non-linear calibration curves. With EtCl doping, a near-linear calibration curve was observed, possibly due to the overwhelming sensitivity of the electron capture response relative to the effects caused by the positive ions formed within the ECD.

Numerous other compounds were analyzed for sensitization by alkyl chlorides and the results of these experiments are included in Tables 1, 2, and 3. Some of the compounds were chosen at random, but many of the PAHs studied had been previously characterized by O_2 doping. It was obvious by their mechanism of response that these other PAH's should be included as potential candidates for alkyl chloride sensitization. When a compound showed significant enhancement,

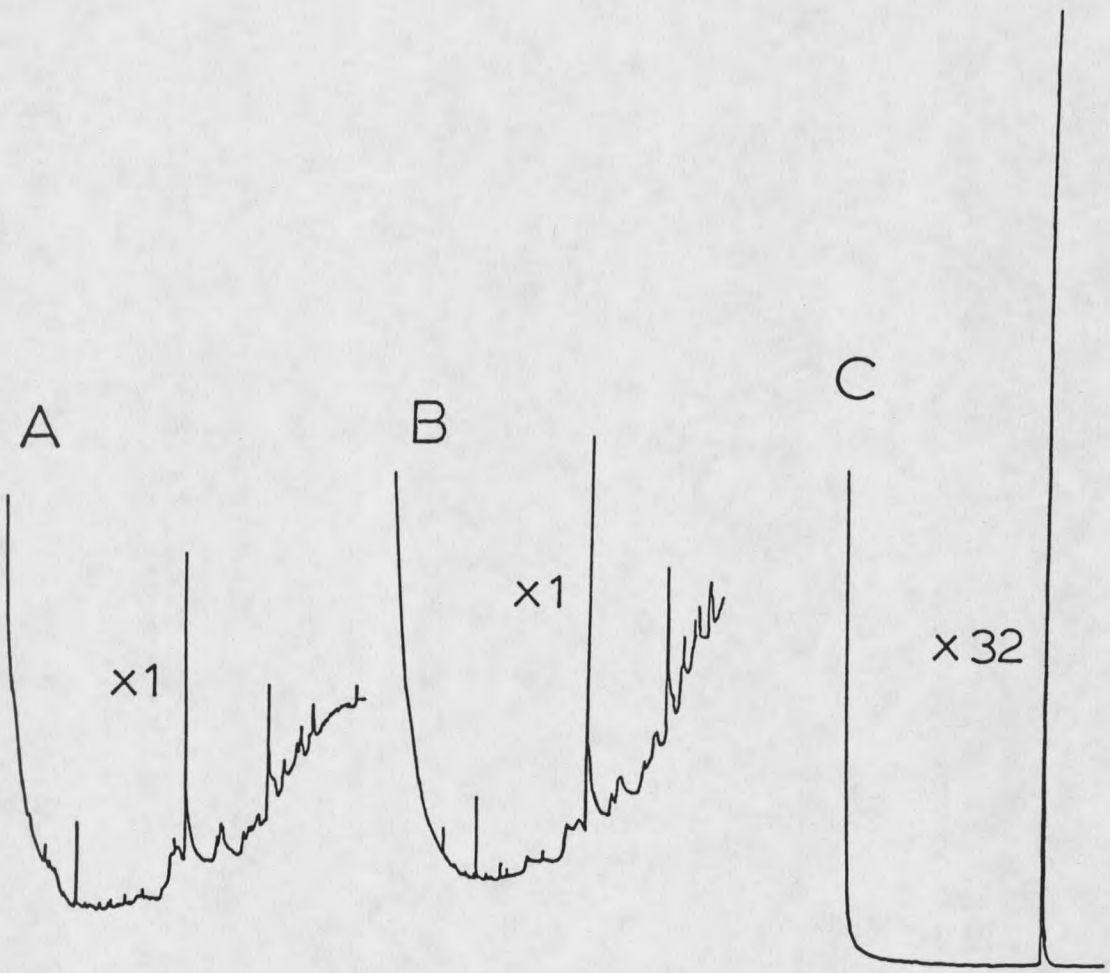

Fig. 22. Repeated capillary analyses on the Varian GC-CC-ECD of sample containing 38 ng benzophenone using the following make-up gases: (A) pure N_2, (B) 100 ppm $(CH_3)_3N$ in N_2, and (C) 100 ppm $(CH_3)_3N$ and 100 ppm CH_3CH_2Cl in N_2. Detector temperature 250° C.

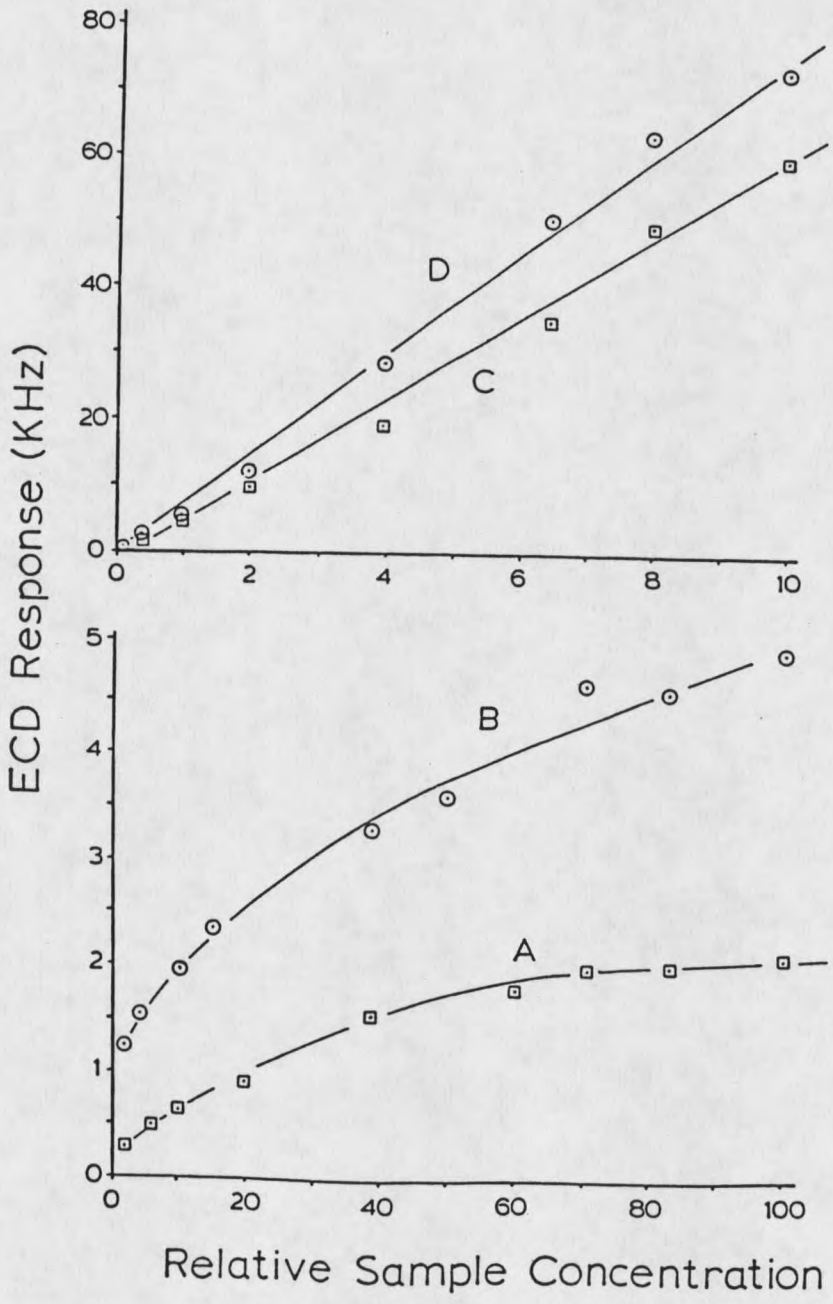

Fig. 23. Varian GC-CC-ECD peak height responses to varied amounts of benzophenone using the detector gases: (A) pure N_2, (B) 100 ppm $(CH_3)_3N$, (C) 100 ppm CH_3CH_2Cl in N_2, and (D) 100 ppm $(CH_3)_3N$ and CH_3CH_2Cl. Amount benzophenone injected equals 0.56 ng per relative concentration unit. Detector temperature is 250° C.

compounds similar in molecular structure were also tested. By no means was this a comprehensive or an exhaustive investigation of sensitization by EtCl to all compounds. It was only conducted to ascertain whether prediction of sensitization was possible by compound type according to the proposed mechanism.

Table 1 contains those compounds which exhibited reproducible enhancements with EtCl doping at 250° C. The standards were analyzed first by FID to measure their retention times. Then, their concentrations were adjusted to obtain signals of approximately 1 kHz under TMA doped conditions in the ECD. Analyses were performed much in the same manner as for the case of benzophenone. The reproducibility of measurements for all three conditions of detector gas were within 10% on a daily basis. To insure that the sensitized response was in the plateau region with a sufficient amount of EtCl doped into the detector, additional quantities of EtCl were added to the diluter and the measurements were repeated.

The enhancement values reported are used only to give a relative idea of the types of enhancement levels to be expected. This was because the enhancement values exhibited significant dependence on the concentration of the analyte used. This was evidenced by the differences in enhancement observed for benzophenone in Figure 22 and Table 1. These chromatograms were developed on the same day, yet the

Table 1. Relative ECD responses to aromatic molecules having positive electron affinities which were enhanced by ethylchloride in the detector gas at 250° C.

Compounds	Rel. ECD Response[a] in N_2	Response Enhancements[b] TMA-Doped	TMA/EtCl-Doped	EA[c] (KCAL-mole^{-1})
Phenanthrene	0.02	2.5	57	7.1
Xanthene	0.2	1.7	4.5	
Chrysene	0.3	1.1	2.0	9.4
Anthracene	1.0	1.9	58	12.9
2-Methylanthracene	2.0	2.6	79	
9-Methylanthracene	1,0	1.7	6.3	
10-methylbenz(a)-anthracene	0.3	1.5	7.7	
9,10-Dimethyl-anthracene	4	1.3	40	
Pyrene	0.5	2.5	87	13.5
Benzo(e)pyrene	4	10	64	
1,2,3,4 Dibenz-anthracene	4.7	1.7	16.5	
Benzophenone	20	3	84	14.7
Acenapthylene	140	1.0	1.9	
Coumarin	40	1.2	14	
Azulene	100	1.0	2.0	15.2
1,2 Benzanthracene	4	2.4	100	15.4
2-Acetylphen-anthrene	115	2.0	8.4	
3-Acetylphen-anthrene	120	1.2	5.0	
9-Acetylphen-anthrene	165	1.6	5.6	
Fluoranthene	460	1.2	3.3	
Acenapthylene	470	0.9	3.5	

a) Peak height per weight analyte injected normalized to the case of anthracene in clean N_2.

b) Response observed with 100 ppm indicated dopants relative to that observed with use of pure N2 detector gas.

c) Electron affinity values taken from ref. [45]. All compounds are listed in order of their estimated or indicated EA value.

responses in Figure 22 for a 38 ng sample are 1.0 : 1.35 : 99 and the values in Table 1 for a 4.6 ng sample are 1.0 : 3.1 : 84. The dependence of relative responses on analyte concentration was due to the fact that the responses, in pure N_2 and with TMA only, were non-linear and in the fully doped condition were linear with concentration. This non-linear behavior has also been noted for many of the other compounds. Therefore, the enhanced values given have thus been set to the arbitrary condition of a 1 kHz TMA doped response. The relative responses between the compounds will also vary for this reason, and the fact that only peak heights were measured and not peak areas. Peak areas were not used because they would be meaningless for those compounds with unusual peak shapes. Day-to-day variations in enhancements were also observed and will be discussed in the section on temperature dependence of the EtCl sensitized responses.

Figure 24 is a multicomponent chromatogram of some of the compounds that have been found to be sensitized by EtCl doping. Peak "f", which is assigned as the response to 1-chloroanthracene, was not enhanced by EtCl and was included only to illustrate the attenuation in recorder sensitivity needed to maintain the enhanced signals on scale. Significant improvements in the signals observed with TMA and TMA/EtCl doping can be seen for the compounds shown. The tabulated results from this multicomponent

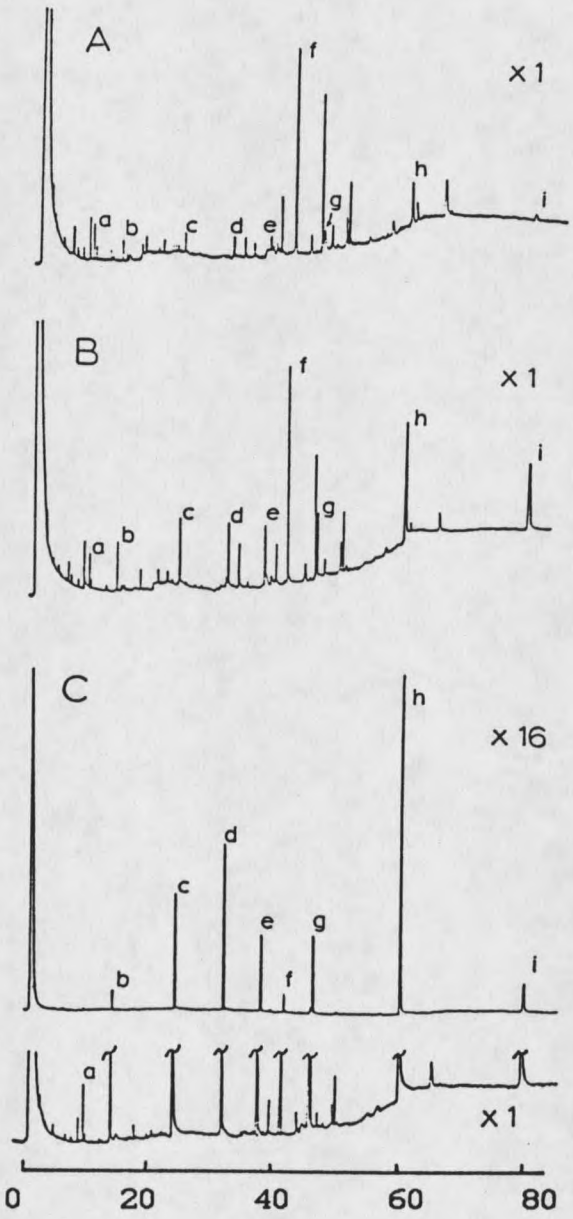

Fig. 24. Repeated capillary analyses on the Varian GC-CC-ECD of a complex mixture using detector gases: (A) pure N_2, (B) 100 ppm $(CH_3)_3N$, (C) 100 ppm CH_3CH_2Cl in N_2, and (D) 100 ppm $(CH_3)_3N$ and CH_3CH_2Cl. Compounds present are: (a) azulene, 0.15 ng; (b) coumarin, 0.8 ng; (c) benzophenone, 4.6 ng; (d) anthracene, 11 ng; (e) 2-methylanthracene, 11 ng; (f) 1-chloro-anthracene, 5 ng; (g) pyrene, 28ng; (h) benz[a]anthracene, 29 ng; (i) benzo[e]pyrene, 16 ng. Detector temperature is 250° C.

sample are reported in Table 1. The various levels of improvement seen with TMA can be explained by the degree of competition between the normal electron capture response in N_2 and the stabilized positive ion chemistry. This effect is dependent on the change in the average recombination rate of the positive ions during the elution of the compound as well as the compound's concentration. As has been previously discussed, this limited production of electrons was not a linear function of sample size, so that with larger samples less improvement was expected with TMA doping. In the chromatograms of Figures 22 and 24, the addition of the TMA and EtCl chemical dopants did not increase the noise level in the baseline of the CC-ECD, and even an improvement for the fully doped condition can be seen. This point is well illustrated as one looks between the eluting compounds "B" and "C" in Figure 24 for each of the three detector gas conditions. It was evident that some peaks, due to impurities, were no longer seen with EtCl/TMA doping. This characteristic noted previously with other samples was a reproducible effect for this sample. An interesting speculation would be that the alkyl chlorides behave as originally proposed. That is, they are removing a sensitizing species from the detector plasma and the impurities within the sample are thus rendered incapable of responding within the detector to these sensitizing species. If this is true then the sensitization seen for anthracene

was an enhanced, accidental discovery. It was fortuitous that anthracene was chosen as the test compound for positive ion characterization.

The increase seen in relative sample size for the later eluting compounds was not due to a decrease in molar sensitivity for the compounds but rather was a result of band broadening from the increased retention times caused by the significant difference in molecular sizes and weights in the compounds represented here. Temperature programming was utilized in the multiponent chromatograms (Figures 24, 25, and 26), up to the 220° C limit, while using a detector temperature of 250° C. The limiting column temperature was set to prevent condensation of sample onto the detector foil. Therefore, long retention times and band broadening were seen in this low detector temperature analysis. Other compounds that enhanced (Table 1), but which had highly responding electron capturing impurities, were not included in multicomponent samples.

In Table 2 are those compounds which were studied that did not enhance with EtCl doping. It can be seen in the relative responses of the compounds that when high molar sensitivities were observed, such as the case for the quinones, halogenated, and nitrated compounds, no enhancements were observed, and assistance by positive ion stabilization was minimal. These results agree with the theories presented for both the positive ion stabilizing

Table 2 Relative ECD responses to aromatic molecules having positive electron affinities for three detector gas compositions at 250° C.

Compounds	Rel. ECD Response[a] in N_2	Response Enhancements[b] TMA-Doped	Response Enhancements[b] TMA/EtCl-Doped
Acridine	41	1.3	1.4
1-Chloranthracene	100	1.0	1.1
9-Chlorphenanthrene	380	1.1	1.1
9-Acetylanthracene	300	1.0	1.1
Napthaquinone	8,000	1.1	1.1
Napthalene	0.1	1.3	1.2
Antraquinone	2,000	1.08	1.1
2,3-Benzo-fluorene	5.5	1.2	NR[c]
1,2 Benzo-fluorene	5.3	1.1	NR
Fluoranthene	68	.8	1.39
Benzanthrone	280	1.0	.8
Anthrone	820	1.0	1.1
2,3 Benzanthracene	0.2	1.1	.9
Perylene	18.7	1.2	1.2
Dibenzofuran	0.5	1.1	1.0
3-Acetylcoumarin	88	1.0	1.0
3-Nitrobenzophenone	8400	1.0	.7
3-Acetylindole	3.8	1.1	.9
5,6-Benzoquinoline	12	1.2	1.8

a) Peak height per weight analyte injected normalized to the case of anthracene in clean N_2.

b) Response observed with 100 ppm indicated dopants relative to that observed with use of pure N2 detector gas.

c) Indicates that no response was observed

amines and the alkyl chloride dopants. The electron attachment rate is quite high for these compounds, hence only a small effect was seen with TMA doping. The alkyl chlorides are not able to assist the response since these molecules with high sensitivity are capable of producing stable molecular and fragment anions and electron transfer to EtCl to produce Cl^- would be of no benefit. For the compounds which exhibited a relative sensitivity less than that of anthracene, the lack of sensitization by the alkyl chlorides can be explained by either of two reasons. With lower sensitivities, k_1 and/or the equilibrium concentration of a negative ion may have been too small to be effective for reaction with the EtCl molecules, if indeed any molecular negative ions existed at all. Secondly, the proposed mechanism required the negative ion be reactive to the EtCl molecule, which for some molecular negative ions is conceivably not occurring at all. These reasons could also be used to explain sensitization differences between similar isomers where the rate of reaction is isomer dependent.

The two compounds in Table 2, 1,2-benzofluorene and 2,3-benzofluorene, gave small responses with very low molar sensitivity for both the clean N_2 gas and the TMA doped condition. However, in the TMA/EtCl doped condition the response was entirely removed. The reactivity seen for these two compounds was quite possibly similar to that which has been discussed for impurities in the baseline of the

multicomponent chromatogram shown in Figure 24. The exact retention time of these weakly responding compounds was ascertained from their relative FID retention time windows and was further verified by their O_2 doped sensitized response.

In Table 3 the responses for compounds which exhibited negative peaks at the 250° C detector temperatures are shown. The enhancement values for the EtCl/TMA doped condition were calculated in a different manner than that used previously in this study. Comparisons to the TMA doped response were used since the negative deflections could not be compared to the normal responses seen for the TMA and TMA/EtCl conditions.

One example in particular, which is listed in Table 3, needs further discussion. These are the amine-substituted PAHs, which gave very poor and unreproducible responses. These characteristics are thought to be due to degradation reactions the compound undergoes within the chromatographic system. Degradation was further identified as the causal mechanism by conducting experiments where injection port temperatures and degree of column insertion were varied. At times significant enhancements were seen for the amine compounds. This effect was not reproducible and may have been due to the formation of a degradation product similar to the unsubstituted parent anthracene molecule.

Table 3 Relative ECD responses for aromatic molecules that exhibited negative peaks in clean N2 carrier gas on the Varian GC-ECD, detector temperature of 250° C.

Compounds	Rel. ECD Response[a] in TMA-N_2	Response Enhancements[b] TMA/EtCl-Doped
Triphenylene	0.04	1.0
7,8-Benzoquinoline	1.8	0.6
Fluorene	1.8	NR[c]
Acenapthene	0.4	0.8
Dibenzothiphene	0.3	1.0
1-Aminoanthracene	0.08	5.0
1-Aminoanthracene[d]	0.6	0.9
2-Aminoanthracene	0.1	0.9
2-Aminoanthracene[d]	0.8	1.8
9-Aminoanthracene	0.6	0.8

a) Peak height per weight analyte injected normalized to the TMA response of anthracene in Table 1.

b) Response observed with 100 ppm indicated dopants in the detector gas relative to the TMA response.

c) Indicates that no response was observed.

d) Data collected from different experimental set.

A second multicomponent sample was also developed for some of the other compounds included in Table 1. The procedural sequence used to develop this multicomponent system differed from the previous experiments which produced the multicomponent chromatograms in Figure 24 and the data shown in Table 1. In this experiment, after the responses with clean N_2 were recorded, EtCl was doped into the system to measure the responses for the EtCl doped condition alone. TMA was later added to produce a chromatogram for the fully doped condition. The results of these experiments are reported in Figures 25 and 26. The most interesting characteristic to be noted within these chromatograms is the striking difference between the clean N_2 and the EtCl doped condition. The compounds which made up the sample show spectacular enhancements for the EtCl doped condition. However, even with the enhanced signals, the peak shapes were non-gaussian and complicated with unusual shoulders, particularly for the systems with large aromatic rings. Other interesting features in Figure 25 are the negative peaks seen with EtCl doping. The negative peaks observed were unique to the EtCl doped system. They are believed to be due to impurities from the standards used, since they do not agree with the retention times of the standards used in the sample.

To produce Figure 26, TMA was introduced into the EtCl doped diluter to further demonstrate the value of positive

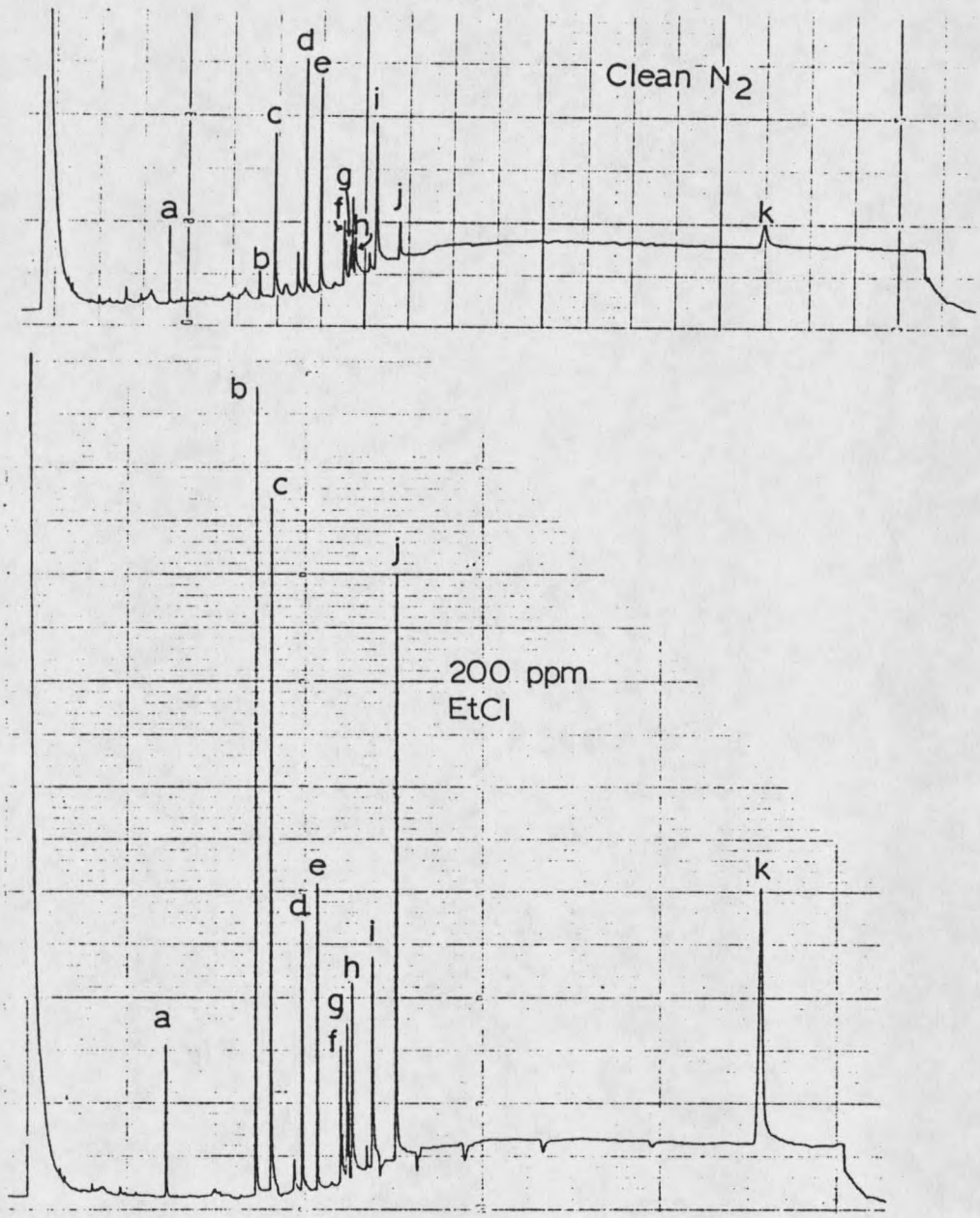

Fig. 25. Repeated capillary analyses on the Varian GC-CC-ECD of a complex mixture using detector gases: (A) pure N_2 and (B) 100 ppm CH_3CH_2Cl in N_2. Compounds present are: (a) acenapthylene, 2.3 ng; (b) anthracene, 8.7 ng; (c) xanthene, 3.3 ng; (d) 9-chlorophenanthrene, 4.0 ng; (e) fluoranthene, 6.8 ng; (f) 9-acetylphenanthrene, 2.2 ng; (g) 3-acetylphenanthrene, 2.3 ng; (h) 2-acetyl-phenanthrene, 2.8 ng; (i) impurity; (j) 1,2-benz-anthracene, 9.0 ng; (k) 1,2,3,4- dibenzanthracene, 24 ng. Detector temperature is 250° C.

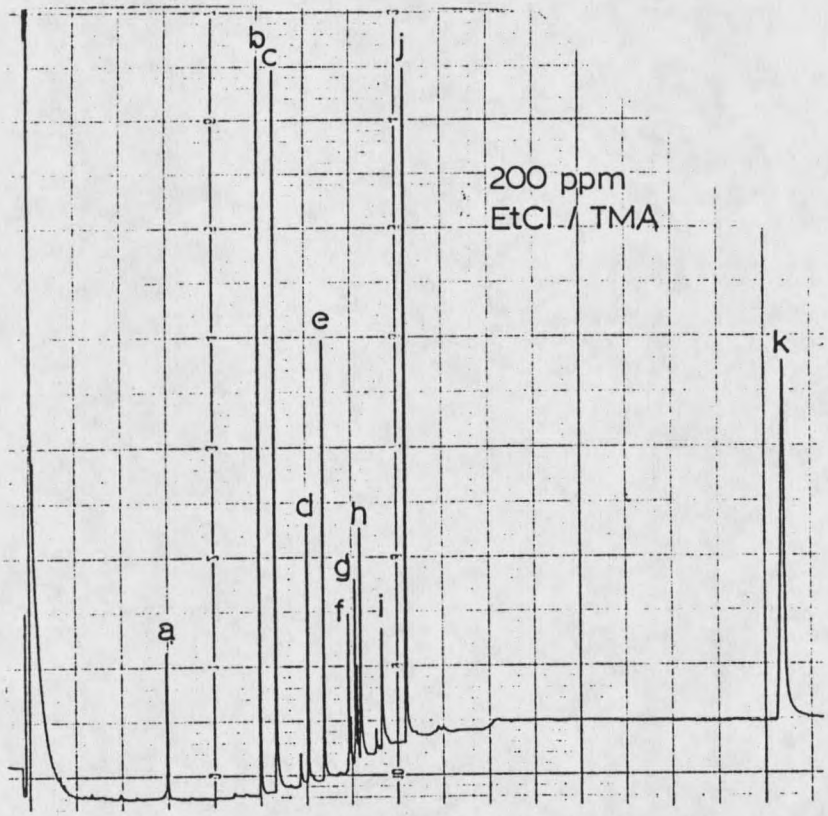

Fig. 26. GC-ECD analysis of the sample in Figure 25 with 100 ppm CH_3CH_2Cl and 100 ppm $(CH_3)_3N$ doped into N_2 detector gas.

ion stabilization when using alkyl chloride sensitization. The unusual shapes to the peak shoulders for the EtCl doped condition were no longer seen, and even further levels of enhancements are obtained. The negative peaks unique to the EtCl doped condition were also eliminated by the addition of TMA to the EtCl doped diluter. For the EtCl doped condition, the sensitized response, limited by impurities, is believed to be eliminated according to the original hypothesis by which the alkyl chlorides were selected. Therefore, there was no loss of electrons to impurities with EtCl doping, which was observed to some degree for the undoped N_2. The negative peaks seen were the result of the impurities (probably large aromatic ringed systems, based on the retention times and the types of standards) producing positive ions which were slower to recombine with electrons. It was believed that this recombinant effect of electron production was the only mechanism of response seen in the EtCl doped condition to the non-electron capturing impurities. In the fully doped condition, the limited, sensitized response to impurities was eliminated by the EtCl, and TMA removed the effects of changes in the rate of positive ion-electron recombinations. The net result was the production of a smoother baseline, removing the unusual responses from non-electron capturing species. At the same time, there was selective electron capture sensitization to those compounds represented in the chromatogram.

In Figure 25 (A), with clean N_2 as the carrier gas, the acetylated phenanthrenes exhibited weak responses and peak assignments were difficult due to inadequate chromatographic resolution. The selective electron capture sensitization by EtCl brought out these peaks from the baseline and allowed for their identification through the increased sensitivity and the magnitude of enhancement. This was similar to isomer identification by O_2 doping, which was found to be an effective technique for assigning responses to compounds with overlapping peaks[37]. The alkyl chloride dopants were also effective for the identification of anthracene methyl isomers, as well as this example, with the acetylated phenanthrenes. The digitized results from this chromatogram are included in Table 4.

In Table 4, the relative ECD responses are reported against the response of anthracene in clean N_2. The enhanced level of responses for EtCl and EtCl/TMA doping are compared to the clean N_2 response of the sample analyzed. The variations in values between this Table and the information reported in Table 1 were due to the changing molar sensitivities for these weakly responding compounds, particularly with the clean N_2 response. The deviations in the responses for these compounds were due to the instrumental variations of flow rate, carrier gas quality, temperature, and chromatographic parameters. Such instrumental variations often lead to significant variations

Table 4 Tabulated Data from the multicomponent sample in Figures 26 and 27.

Compounds	Rel. ECD Response[a] in N_2	Response Enhancements[b] EtCl-Doped	TMA/EtCl-Doped
Anthracene	1.0	36.5	38.0
Acenapthylene	9.8	2.3	2.4
Xanthene	1.5	4.9	6.0
9-Chlorophenanthrene	20.0	1.1	1.2
Fluoranthene	11.0	1.4	2.1
9-Acetylphenanthrene	8.5	2.6	3.2
2-Acetylphenanthrene	4.1	5.7	8.3
3-Acetylphenanthrene	3.9	5.9	8.4
1,2 Benzanthracene	1.3	17.5	27.0
1,2,3,4 Benz-anthracene	0.3	12.2	16.5

a) Peak height per weight analyte injected normalized to the response of anthracene in clean N_2.

b) Response observed with 100 ppm indicated dopants relative to that observed with use of pure N2 detector gas.

in the electron capture coefficients for low sensitivity compounds. The dependence of molar sensitivity on concentration may also be a factor in the changing molar sensitivity seen for these types of compounds.

Computer Modeling

The non-linear calibration curves obtained in the TMA doped responses for benzophenone and anthracene indicated that the existing mathematical models were still unsatisfactory. These mathematical models predicted linear calibration curves, and included the assumption that the positive ion reactions did not affect the measured electron density. The insight brought about by TMA chemical doping suggested that the deviations from the current resonance electron capture theory were not caused solely by positive ion dynamics, since non-linear calibrations were found even with TMA present. Therefore, it was necessary to reexamine the theory of resonance electron capture, beginning with the assumptions used in their development.

To characterize the chemical dynamics, a computer model was developed which was capable of considering the many chemical processes simultaneously occurring in the ECD. With a computer program it would be easy to make changes in each reaction rate and readily determine the effects of these changes. A listing of the program used for these purposes is included in the Appendix. The program was written in Applesoft Basic to be run on an Apple II series personal computer. After the input of appropriate program variables, it was compiled into binary machine language for more rapid operation. A flow chart is included in the

Appendix and describes the operating principles and sequencing of the program. The program produces mathematical results through digital integration by successive approximations.

A major assumption on which the entire resonance electron capture theory rests is whether or not kinetic equilibrium is attained in the time between the pulses of the CC-ECD. An examination of this assumption was necessary since the previously derived models used steady-state approximations of the negative ion density to calculate an electron density. The electron density was then related to the frequency of pulsing for the CC-ECD. The values of k_1 and k_{-1} used in the computer model were taken from the studies of Wojnarovits and Foldiak[30].

Using very small time intervals it was possible to calculate the populations of negative ions and electrons. Their amounts could then be plotted up to the time, T, of the pulse. The pulse period reflecting the simulated detector response. The computer model results showed that equilibrium was easily attained by the time of the pulse and the assumption that negative ions had reached a steady-state was valid. The time at which equilibrium was attained was found to be dependent on the electron attachment and detachment rate values used and, the concentration of the compounds represented in the study. Using the default values listed, linear calibration was obtainable for the

model systems studied. With large sample sizes the constant current detector pulses very fast; up to the defined limit of 100 kHz. At these very fast pulsing frequencies the equilibrium or the steady-state approximation may be unachievable between the pulses, and this was one possible explanation for the non-linear experimental calibration curves observed. Azulene, anthracene, and phenanthrene were studied by the computer model and all of these compounds gave linear to near-linear calibration curves by computer modeling.

The conclusions derived from this study indicated that steady-state concentration was obtained, and fast pulsing in the CC-ECD could not explain the experimental results observed with TMA doping. The results just discussed in the preceeding paragraph were done with the default parameters shown in the Appendix, with the exception of the interval of time measurements, which were varied according to the sample size, and the forward and reverse rate constants. The selection of differing time intervals was done to make the program function efficiently and within a reasonable amount of time. The default values listed in the program were chosen to closely approximate the existing conditions for the Varian GC-ECD system. Theoretically calculated frequency responses were within an order of magnitude (approximately 3x-4x larger) to the calculated sample concentration within the detector at a similar peak height.

Non-linear results were obtained when the values of XRECOMB and WRECOMB (see Appendix) were changed relative to each other. XRECOMB was the variable assigned to the recombination rate of negative ions with positive ions and WRECOMB was the variable assigned to the recombination rate of electrons with positive ions. The default values were representative of the assumptions made in previous models for resonance electron capture processes, where the recombination of negative ions with positive ions was assumed to be of equal value to that of the recombination of electrons with positive ions. However, Smith and Adams[54] report that these values are different due to the significant variations in the sizes of the negatively charged species. Using values similar in magnitude to those reported by Smith and Adams, results obtained for benzophenone and anthracene under TMA doped conditions could be explained by the differences in the recombination rates represented by XRECOMB and WRECOMB. This effect is probably the reason why non-linear response versus concentration in the TMA doped detector was observed for these weakly responding compounds. Other factors, such as limited quantities of sensitizing impurities, could also explain the higher molar sensitivity seen with lower concentrations of sample, or possibly a combination of all of these factors just mentioned. For strongly responding compounds the importance of these effects is lessened by a faster electron

capture rate, and linear calibration curves were subsequently obtained.

The effect of temperature on the variation in rate constants was also examined with the computer model. The theoretical results were obtained using the values determined by Wojnarovits and Foldiak[30] from their temperature dependency studies of resonance electron capturing compounds. The theoretical results of these studies will be included in the next section on temperature dependence.

Temperature Dependence

In order to assess the mechanism of sensitized response, the temperature dependence to those compounds which enhanced with the alkyl chlorides was tested according to existing theories of resonance electron capture reactions in the ECD. A detector of conventional geometry (concentric coaxial electrode) was used for these experiments, since this type of detector has been well characterized in terms of the physical properties involved in the response. For the measurements of temperature dependent reactions, a commercial Hewlett Packard 5890A, fitted with an ECD of conventional geometry was chosen. Studies on a Varian ECD with its displaced coaxial anode were also done as a comparison to determine whether data provided by this detector were consistent with the HP 5890A. The general

effect of temperature was in agreement between the two detectors.

With the Hewlett Packard system the importance of temperature on the sensitized response is demonstrated in Figure 27. The response of anthracene at two detector temperatures is plotted against varying amounts of EtCl in the detector gas. In this Figure it can be seen that, as the detector temperature was lowered, a larger maximum frequency of sensitized response was obtained. Also a greater concentration of EtCl was needed to achieve the plateau region of the sensitized response. This point is also illustrated in Figure 17, where the larger sample size required a greater concentration of EtCl to reach the maximum sensitized response. In both cases, a higher response was attributed to a larger equilibrium concentration of anthracene negative ions which required a proportionate increase in EtCl to reach the limiting sensitized response. The requirement that an increased level of EtCl dopant was needed is consistent with, and gives further support to, the proposed mechanism by which EtCl is thought to sensitize the response. In the HP-GC-ECD system the sensitized response required higher levels of EtCl dopant to achieve the plateau region of the curve than for the same level of kHz response reported in Figure 17 for the Varian GC-ECD system. This difference was reproducible between the two detectors and is attributed to the significant variations in the EC cell

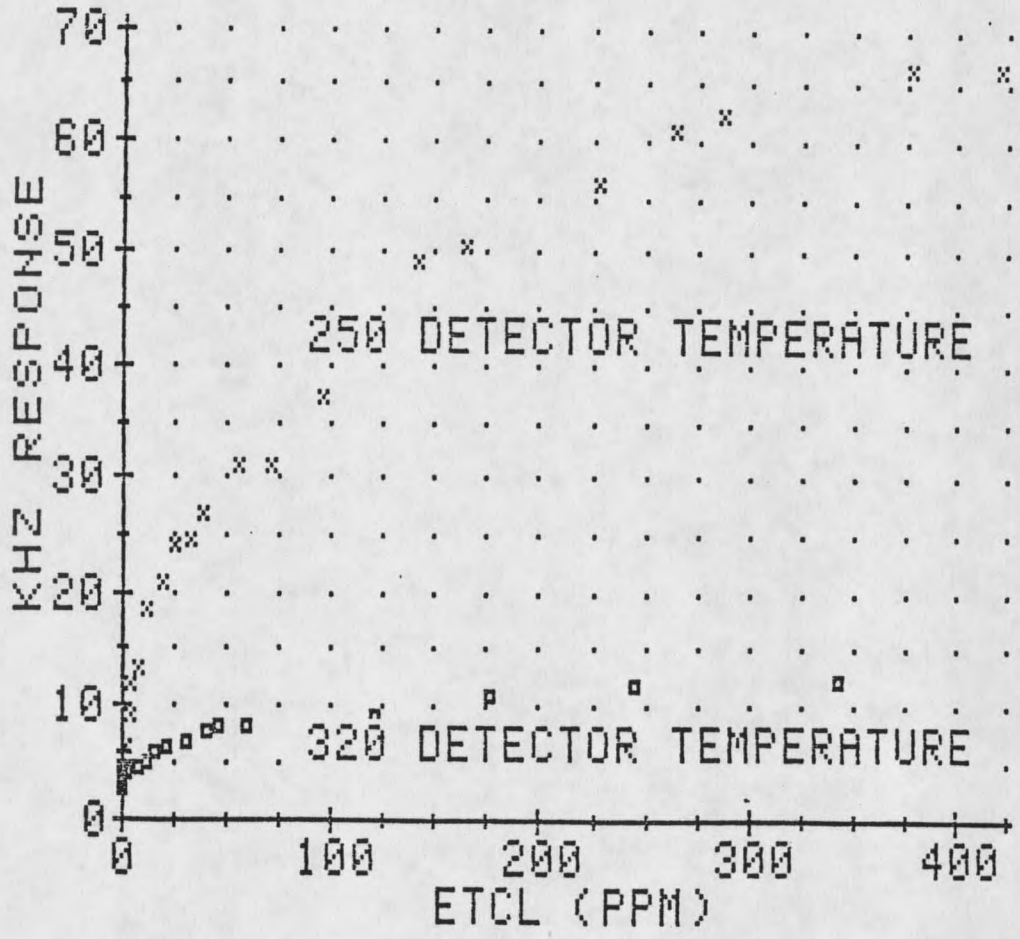

Fig. 27. Hewlett Packard GC-CC-ECD sensitized responses of anthracene to differing CH_3CH_2Cl concentrations at two detector temperatures.

designs and volumes. These experiments in Figures 17 and 27 emphasize the need to chemically dope the detector with sufficient levels of EtCl to ensure that the plateau region is in effect for the highest level of response expected. If this requirement is met, then linear calibration curves should be achieved for the TMA/EtCl doped condition with compounds that sensitize.

The temperature dependent results obtained for the TMA and TMA/EtCl doped conditions tested on three compounds which showed enhancements with the alkyl chloride dopants are shown in Figure 28. The TMA doped condition is thought to represent true resonance electron capture, since the response would not be complicated by the protonation of analyte molecules. In all three cases represented in Figure 28, the response increased with lower detector temperatures, both for the normal resonance EC response and the alkyl chloride sensitized condition. With anthracene [Figure 28 (A)] and azulene [Figure 28 (B)] the response for both conditions was either reached, or was approaching a limiting response with the lowest temperatures. According to the existing theory of resonance electron capture reactions in the ECD, this limiting response was caused by a decrease in the electron detachment rate to a value no longer significant, relative to the rate of reaction of the negative ions with the positive ions and/or the alkyl chlorides. The maximum limiting response expected at low

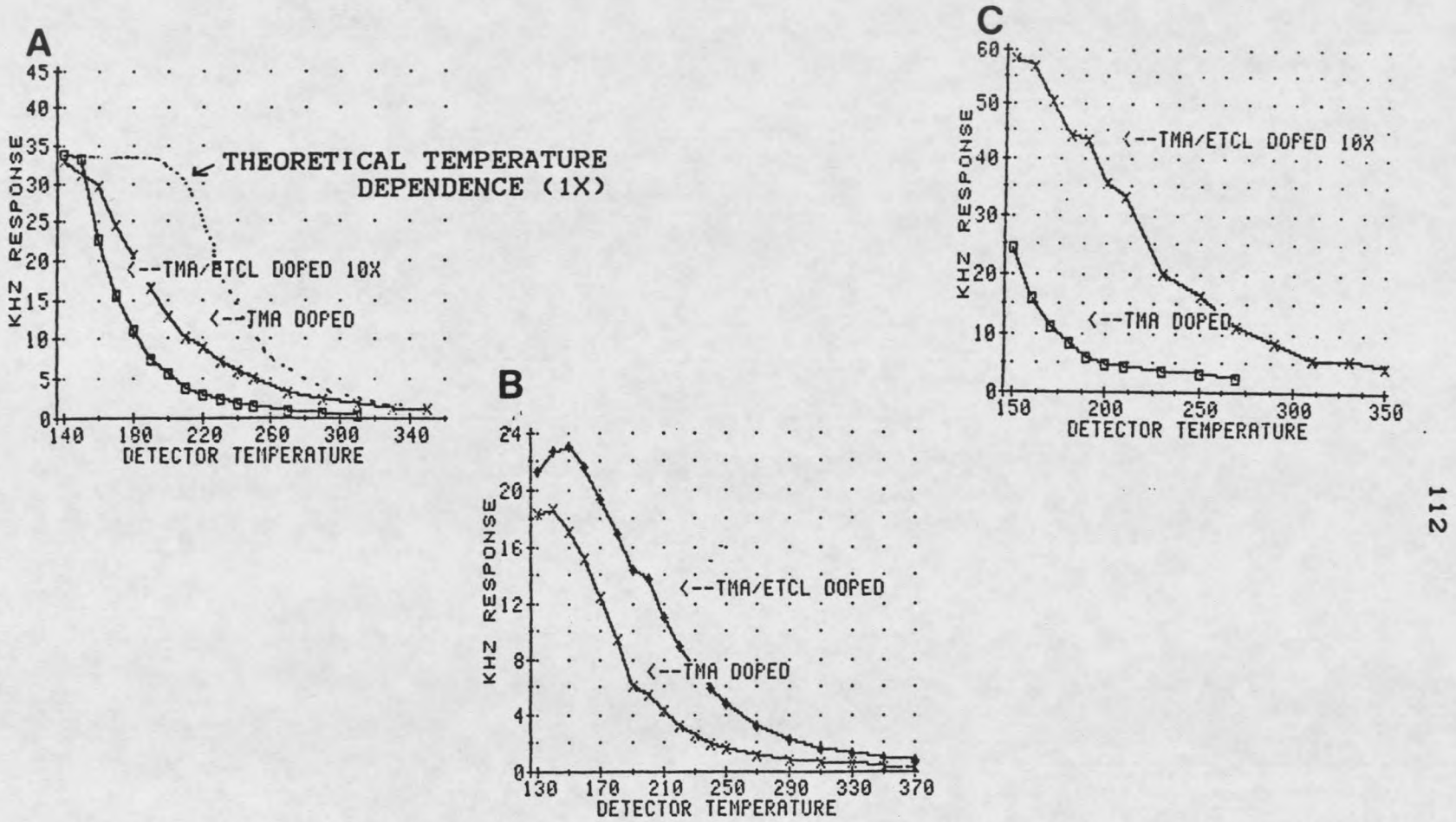

Fig. 28. Hewlett Packard GC-ECD analyses of the temperature dependent molar peak area responses of: (A) anthracene (B) azulene, and (C) benzophenone for the detector gas conditions of: (a) pure N_2 carrier gas, and (b) N_2 carrier gas doped with 400 ppm $(CH_3)_3N$ and CH_3CH_2Cl.

temperatures is then due only to k_1, the electron attachment rate. The theory of resonance electron capture used will also have incorporated into it the mechanism of response for alkyl chloride sensitization. With this it would be predicted that both analyses conditions should achieve the same level of limiting response, with the alkyl chloride doped system reaching the limiting response at higher detector temperatures. To illustrate this statement a theoretical plot represented by a dashed line, is shown in Figure 28 (A). Such a response would be expected with EtCl doped analysis of anthracene according to these kinetic and mechanistic theories.

The temperature dependence of azulene appears to demonstrate the theoretical temperature dependence. The enhancements observed with azulene were very small and were only approximately doubled under the optimum detector temperatures, so conclusions based on this one model system may not be valid. Also, APIMS studies of the negative ions formed with azulene for the EtCl doped conditions showed that the trapping of the azulene negative ion was not 100% effective when doped with an alkyl chloride. In the APIMS analysis, when the EtCl doped results was compared to the undoped system a decrease in the amount of azulene molecular negative ion was about half the signal intensity of the undoped condition. The production of Cl^- was indicated as azulene passed through the detector.

APIMS analysis of benzophenone at 250° C showed that the observance of the molecular negative ion was completely eliminated by EtCl doping. The significant production of Cl^- as benzophenone passed through the detector was also noted. Benzophenone in Figure 28 (C) did not reach a limiting response because of chromatographic limitations. Lower detector temperatures could not be attained to accommodate the production of a stable negative ion; that is, the electron detachment rate for benzophenone was still important relative to the loss rate of negative ions by recombination with positive ions at the lowest possible detector temperature used.

To obtain linear graphs of response to detector temperatures for these resonance electron capturing compounds, a return to the theory presented in the introduction is necessary. The mathematical values in the results to be discussed are not considered valid since the assumptions of the existing theories state that the temperature dependence of the response is solely based on the electron detachment rate, and all of the other reaction processes are temperature independent. The temperature dependence of k_1, the forward electron attachment rate, has been shown in some cases to be extremely dependent on temperature[55]. Normally, with resonance electron capturing compounds the energy of activation is quite small and a reasonable expectation is that k_1 is relatively temperature independent for the

compounds represented here. The recombination rates are assumed to be only slightly affected by changes in temperature. The previous theories also did not consider the changes in flow rate caused by temperature, which are known to affect the responses by diluting or concentrating the sample in the detector. Instead, the theory will be used only as a guide to distinguish the mechanism of response in the same manner as done by Zlatkis et al.[20]. The plots should then give a relative idea of the mechanism of response by the slopes of the "lines" created and the Y-intercepts that are obtained.

Plots of ln $RT^{3/2}$ are plotted against 1/T x 1000 for the data given in Figure 28 and the results are shown in Figure 29. In this example, R is the molar area response in volt-minutes (1 volt = 10 kHz frequency response), and T is the temperature of the detector in degrees Kelvin. The results seen in Figure 29A and B indicate that the TMA doped condition gave results consistent to those predicted by the computer modeling of the Wojnarovits and Foldiak data. The data also showed that the EtCl response produced a similar response slope with a higher Y-intercept. These results can be interpreted by the equations developed which produced the ln $RT^{3/2}$ versus 1/T axes the data are plotted by. These differential equations represent the electron production and loss processes for the EtCl doped condition.

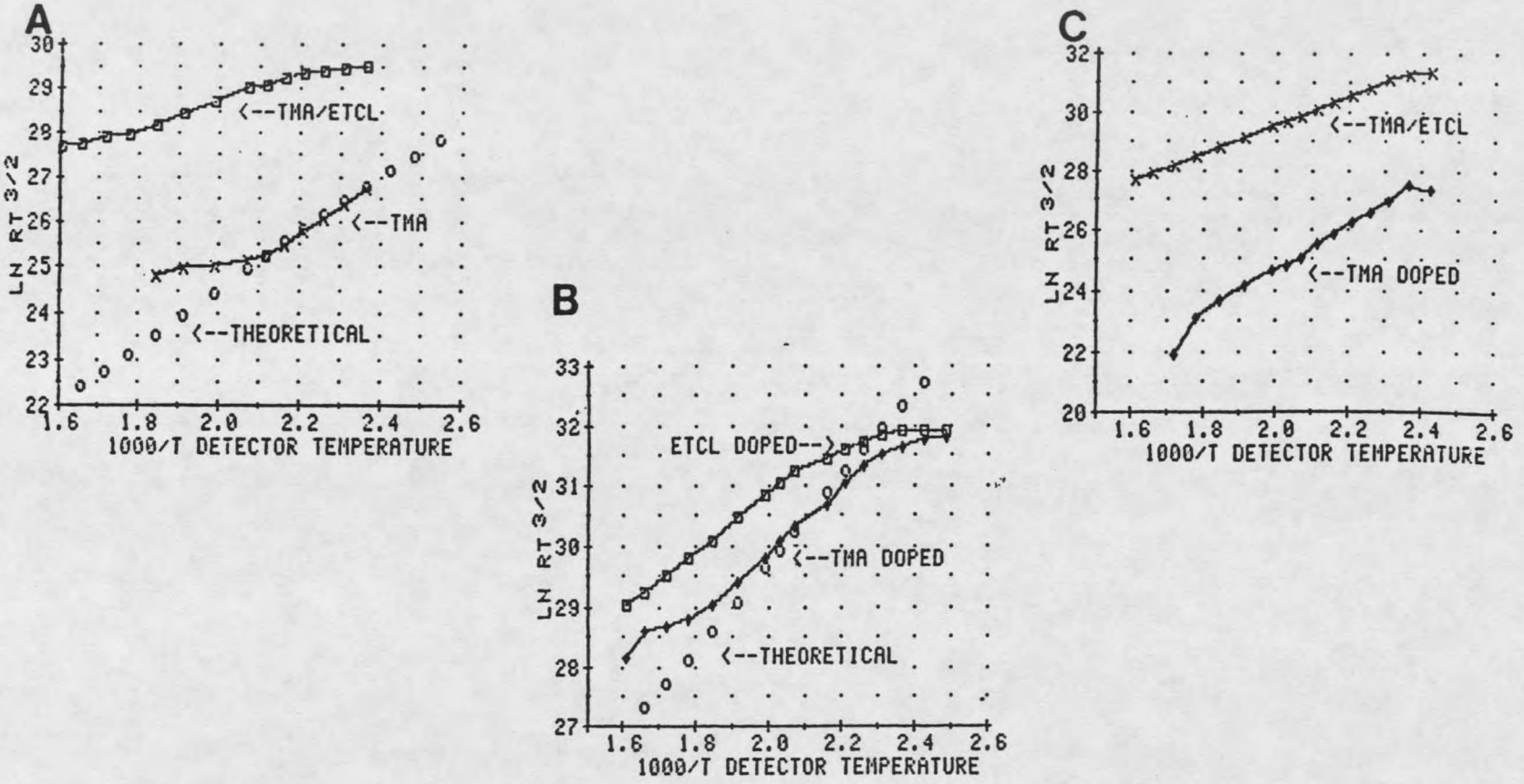

Fig. 29. ln [Molar Response (R) x Temperature(T)]$^{3/2}$ versus 1/T x 1000 plots of the temperature dependent molar peak area responses of: (A) anthracene, (B) azulene, and (C) benzophenone for the detector gas conditions of: (a) pure N_2 carrier gas, and (b) N_2 carrier gas doped with 400 ppm $(CH_3)_3N$ and CH_3CH_2Cl (data taken from Figure 28).

$$dN_{e-}/dt = S + k_{-1}N_{A-} - (k_1 n_A + R_3 n_{p+} + R_4 n_B)N_{e-} \qquad (15)$$

$$dN_{A-}/dt = k_1 n_A N_{e-} - (k_{-1} + R_1 n_{p+}\ R_2 n_{Rad} + k_d + k_2 EtCl)N_{A-} \qquad (16)$$

When a mathematical derivation was applied to these differential equations for the condition where k_{-1} was greater than any other negative ion loss process, equation (17) could been used to describe the temperature dependence of the molar response:

$$\ln RT^{3/2} = \ln\frac{K_{AL}}{K_{EL}} + \ln A + \frac{EA}{K_b \times T} \qquad (17)$$

This equation was derived according to the standard procedures and assumptions that other scientists have used to describe the temperature dependence of resonance electron capturing compounds in the CC-ECD[7,20,30]. K_{AL} denotes a fixed value for the constant loss processes expected for the negative ions. These are the temperature independent values for the recombination with positive ions and also the reactions with radicals. If EtCl was present, its rate of reaction would also be included with this term. The term K_{EL} represents the constant loss processes for electrons in the condition without sample. These include diffusion to the walls, recombination with positive ions, and reactions with column bleed and other impurities in the detector

system. The value A, denotes a fundamental detector constant, including all of the physical parameters affecting the sensitivity of the detector. K_b is the Boltzman constant necessary to consider the statistical mechanical physics of the reactions. The limitations with this type of model have been described earlier.

The slope of the line produced from equation (17) is related to the EA of the molecule and the Boltzman constant. The Y-intercept is a function of the fundamental detector constant, the loss rate of negative ions by recombination, and the non-analyte loss rates of electrons. The limitations in equation (17) can be clearly seen if the data points are projected out to the point where the X-axis equals zero. Due to detector temperature limitations, the temperature dependent data would then represent only a small fraction of the X-axis scale, with a significant proportion of the scale being interpolated to obtain a Y-intercept. However, Zlatkis et al.[20] used these types of models only to characterize the response mechanism operating as is also the purpose here. To visually determine any slight deviations in linearity, the data is plotted only over the range of X-axis values where temperature dependent data were taken.

The temperature dependent responses of azulene (Figure 28B) demonstrate all of the characteristics considered in an ideal model of resonance electron capture. At lower detector temperatures (far right on the X-axis) the "Beta"

region was in effect. In this region, the response was dependent on only k_1, since the negative ion was considered stable to electron detachment relative to its loss rate with positive ions. The curvature in the region between the positive slope and the slight negative slope, is the region where the rate constant for the loss of negative ions by the recombination process, and/or the negative ion trapping by EtCl, was in competition with the loss rates by electron detachment. The "alpha" region, denoted by the straight-lined positive slope, is attributed predominately to the temperature dependence of k_{-1}.

The temperature dependent results for anthracene are also plotted by the same log scale and the results are included in Figure 29 (A). Anthracene exhibited a temperature dependence characteristic of resonance electron capture. At the lowest possible detector temperature there is a slight indication that the "Beta" region is being approached in the EtCl doped analysis. The slope of the line in the TMA doped response closely parallels the results that were obtained with Wojnarovits and Foldiak values used in the computer model. The deviations from linearity at the higher temperatures was caused by a further increase in molar sensitivity due to an increase in the proportion of a dissociative capture mechanism.

Temperature dependent responses of benzophenone, which exhibited one of the most highly sensitized responses with

the alkyl chloride dopants, is shown on the ln $RT^{3/2}$ versus 1/T plot in Figure 29 (C). The data for TMA and the TMA/EtCl doped systems show a similar slope, but with very large differences in the Y-intercept. The larger variations in linearity seen with the TMA doped system were attributed to the decrease in the signal-to-noise ratio caused by a less sensitive response with TMA doping. In the EtCl doped results the low temperature region began to exhibit a slight deviation from linearity with a less significant slope. Unfortunately, instrumental limitations did not allow for lower detector temperatures to be used. The results do suggest, for the EtCl doped system, that a "Beta" region is beginning to be observed and that this was at a higher temperature than for the TMA doped resonance electron capture process.

For all three compounds studied, any deviations in the alpha region slope of the EtCl response, as compared to the TMA doped system, should reflect a temperature dependence of the EtCl molecules reaction rate with the analyte negative ion.

In Figures 30 (A) and 30 (B), the effects of using the argon/10% methane mixture as the detector gas relative to N_2 detector gas is shown. The degree of enhancement with the Ar/Me experiments was less than what was observed with the N_2 system. Instrumental conditions were kept the same except for the changes in carrier and detector gases, and

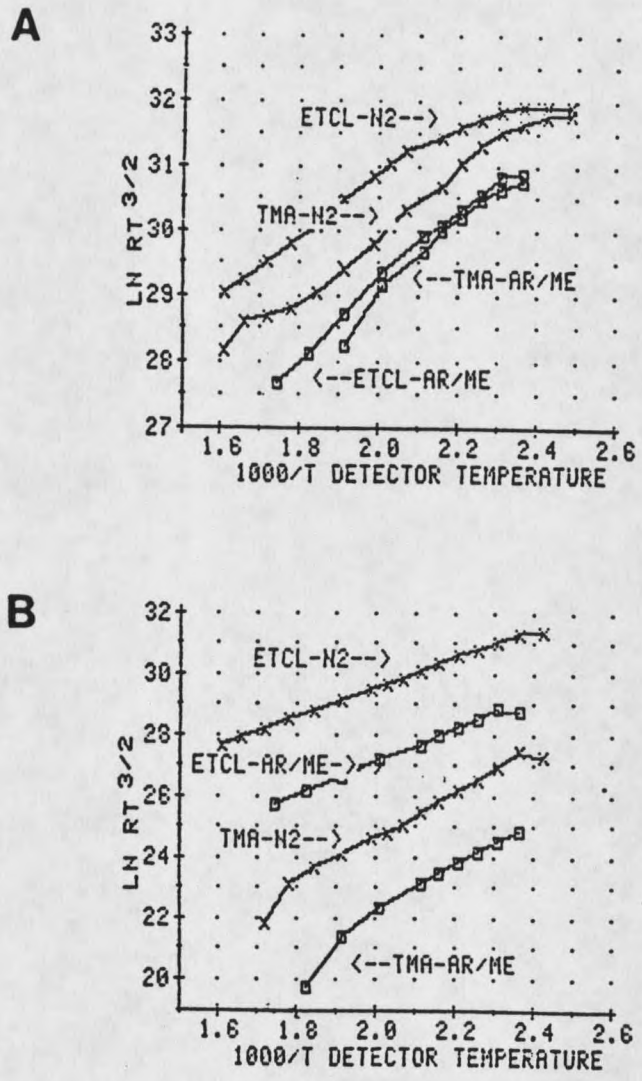

Fig. 30. ln [Molar Response (R) x Temperature(T)]$^{3/2}$ versus 1/T x 1000 plots of the temperature dependent molar peak area responses of: (A) azulene, and (B) benzophenone for the detector gas conditions of: (a) pure N_2 carrier gas; (b) N_2 carrier gas doped with 400 ppm $(CH_3)_3N$ and CH_3CH_2Cl; (c) clean argon/10% methane detector gas; (d) argon/10% methane doped with 400 ppm $(CH_3)_3N$ and CH_3CH_2Cl.

the adjustment of the HP-GC electrometer to accommodate the argon/methane mixture. The results show that the selection of the more inexpensive N_2 carrier gas provided better results, through larger enhancements and sensitivity for these low EA molecules. If the slope of the line reflects the EA, and the EA is a function of the equilibrium between electron attachment and detachment, then the equilibrium is being maintained, regardless of the change in the electron capture cross section of the molecule when using different detector gases.

The kinetic model, as applied to the temperature dependent studies, has allowed for an improved understanding of the alkyl chloride sensitization reaction mechanism. The temperature dependence of the sensitized conditions remained because electron detachment continued to be a significant factor in the analyte negative ion loss rate. The observance of a beta region beginning at slightly higher detector temperatures than for the TMA doped condition also supports the idea that a loss rate of negative ions in addition to the already existing recombinations with positive ions was the cause of the enhancements.

The non-linear calibration curves obtained with TMA doping have helped explain the concentration dependence of the enhancements. Yet, this effect alone does not explain the lack of reproducibility for the same sample on a day-to-day basis. Nor does it explain the variations in

observed enhancement levels when other instruments were utilized. When the conditions of flow rate, detector temperature, and sample size were controlled, variations in the detector's response were still observed. This observation is similar to the results presented in Figure 30, where only the detector make-up gas was changed. In the TMA doped responses of Figure 30, the electron capture cross section of the molecule was changed by the different detector gases, yet a kinetic equilibrium continued to exist between the negative ions and the analyte neutrals. In this example, the change was most probably due to second order electron attachment reactions, where an increase in k_1 was balanced by a proportionate increase in the rate of negative ion loss by k_{-1}.

The level of enhancement and maintenance of equilibrium are graphically illustrated by use of the ln $RT^{3/2}$ versus 1/T plots. These levels are manifested by the degree of difference in the measurement of the Y-intercept, and the occurence of a constant slope. Detector gas conditions which can influence the electron capture cross section include detector cleanliness, carrier gas purity, and the amount of column bleed. Each of these conditions having a varying degree of effect. Variations in these factors will occur even while attempting to retain identical GC-ECD operating conditions.

An oversimplification of the variations in detector enhancements can be explained by the following two schemes. In the first scheme, the EtCl doped condition represents the maximum level of Y-intercept, which is always attained with sensitization. Changes in the enhancement levels will then be caused by variations in the Y-intercept for the normal resonance electron capture process, which is representing the fundamental detector constant, negative ion loss processes, and non-analyte electron losses. This particular scheme is supported by the observation that slight changes in the detector gas conditions often can give large differences in the undoped response. Column bleed and chromatographic system gas leaks often producing this effect. A second scheme which is a variation on the first, is that the Y-intercept with EtCl doping is also affected by slight changes in the detector gas conditions. Possibly by preventing the reaction of EtCl with the analyte negative ion. One of these two schemes, or a combination of the two, is one way in which the variations in EtCl enhancements of the same sample can be interpreted. A similar effect observed with O_2 doping has also been previously noted[35], where maximum enhancement levels were seen only with the optimum conditions of detector and chromatographic cleanliness.

Ion-Ion Recombination Reactions

Tandem ECD Cell analysis, using two EC detectors hooked in series, has been shown to be reasonably effective in performing coulometry for some compounds[26,27]. Coulometry by this technique is based on the diminution of response in the second detector due to the destruction of the analyte molecule by dissociative electron capture in the first EC cell. This describes the efficiency of the electron capture reaction to an analyte molecule. With a fixed frequency (FF) pulser, the area response in the first cell is converted from the current-time units to the number of electrons involved in the response. By knowing the efficiency of reaction, the amount of electrons involved in the response, and having a well characterized detector, mathematical derivations can be applied to determine the amount of analyte injected into the cell without the preparation of ppm to ppt standards. Accurate results within a particular FF pulsing range were obtained for some multihalogenated compounds that underwent dissociative electron capture to produced Cl^- and Br^- [26,27].

One of the limitations of this technique was that only those compounds with a very fast electron attachment rate could be studied. The system required a significant proportion of analyte destruction in the first cell to accurately determine the efficiency of reaction, since the degree of

sample destruction in the first cell was reflected by the difference of the signals between the two cells. Only those compounds with high EA and high molar sensitivity have the ability to produce large enough efficiencies of reaction for coulometric determinations in the tandem cells represented in Figure 3. This is based on standard statistical evaluations where the error in the measurement of EC efficiency increased as the difference became small. This point will be addressed later in the discussion of this study.

In the model described above for coulometry, a number of criteria were established. Only those compounds which exhibited a direct relationship between electron attachment rate and detector response were chosen for evaluation. This required choosing compounds that produced stable negative ions, which upon recombination with positive ions would form neutrals that do not undergo further electron attachment. The neutral radical from the dissociative portion of the reaction must also not undergo electron attachment.

For those compounds responding by a stable resonance electron capture mechanism, a more complete description of the reaction dynamics is required to explain the responses obtained within the two detectors. Stable resonance electron capture denotes those compounds in which the negative ion produced is the molecular anion. Lower detector temperatures help favor this type of mechanism. The molar sensitivity of the ECD to these types of compounds

has been previously stated as being dependent upon the molecule's ability to attach an electron and the stability of the negative ion to electron detachment. Subsequent reactions of the negative ions by recombination with positive ions to produce neutrals can also be very important to the detector's molar sensitivity, and is the basis for the experiments to be described here. The reactions modeled below illustrate two recombination possibilities for the stable resonance electron capture process.

$$A + e^- \xrightarrow{k_1} A^- \qquad (18)$$

$$A^- + P^+ \rightarrow A + \text{Neutrals} \qquad (19a)$$

$$A^- + P^+ \rightarrow B + \text{Neutrals} \qquad (19b)$$

Reaction (18) is the electron attachment of molecule A with a rate of k_1. The experimentally determined value for k_1 will be assigned as ϕ throughout the remainder of this discussion. Reaction (19a) depicts the regeneration of molecule A through a recombination with a positive ion. Reaction (19b) is a competitive recombination reaction with (19a) and denotes the formation of altered neutrals, B, from which A cannot be regenerated. Currently, very little is known of these gas phase ion-ion molecule reactions and the neutrals formed.

This study was done to assess the production of neutrals which may be involved in a further electron capture/neutralization sequence, and to estimate the amount of molecular loss by electron capture in a gaseous mixture when there is an excess of electron density.

The experiments with the tandem ECD cells were performed by monitoring the diminution of molecular species, A, in a reaction vessel in which the electron population was maintained at a relatively constant and known level. This measurement was therefore sensitive to both the consumption of A by reaction (18) and the regeneration of A by reaction (19a), if the latter occurred.

Previous measurements of electron attachment rates have been performed by various methods. The method believed to be the most accurate is that where molecule A is in excess, and changes in electron density, with accompanying alterations in the concentration of A, have then been measured. Such measurements are expected to provide reliable determinations of the rate coefficient, k_1, for reaction (18), but are relatively insensitive to the detailed nature of the subsequent recombination processes, (19a) or (19b). This study will show that the ratio of responses between cell one and cell two give a value θ, which reflects the sum of the electron capture rate and the extent of regeneration by ion-ion recombination. If the combined rate constant θ, is then compared to previous measurements of k_1 or ϕ for the

same chemical systems a quantitative assessment of the relative importance of reactions (19a) and or (19b) can then be deduced.

Knowledge concerning the effects of ion/ion recombination reactions can then be applied to the determination of a compound's overall molar sensitivity, and to the prediction of the validity of a coulometric determination by tandem ECD's. Information in this area is also desired for the proper operation and design of analytical instruments in which the basis of response also involves electrons reacting with molecules, particularly, in the recently developed area of high pressure electron capture mass spectrometry [(HPECMS)(1 - 10 torr pressure)].

Using a number of different chemical systems, data from the tandem cell technique will be presented. Compounds that are known to respond by a dissociative as well as a stable resonance electron capture mechanism will be included in this portion of the investigation. Those compounds that respond by a resonance electron capture are believed to be reactive, at least, in part, by mechanism (19a). Compounds that have given satisfactory coulometric results are predicted to be described by mechanism (19b).

A typical tandem cell analysis is illustrated in Figure 31, where the analyses of C_7F_{14} and SF_6 are shown. The following detector and operating conditions were employed for each analysis: a detector temperature of 150° C, a pulse

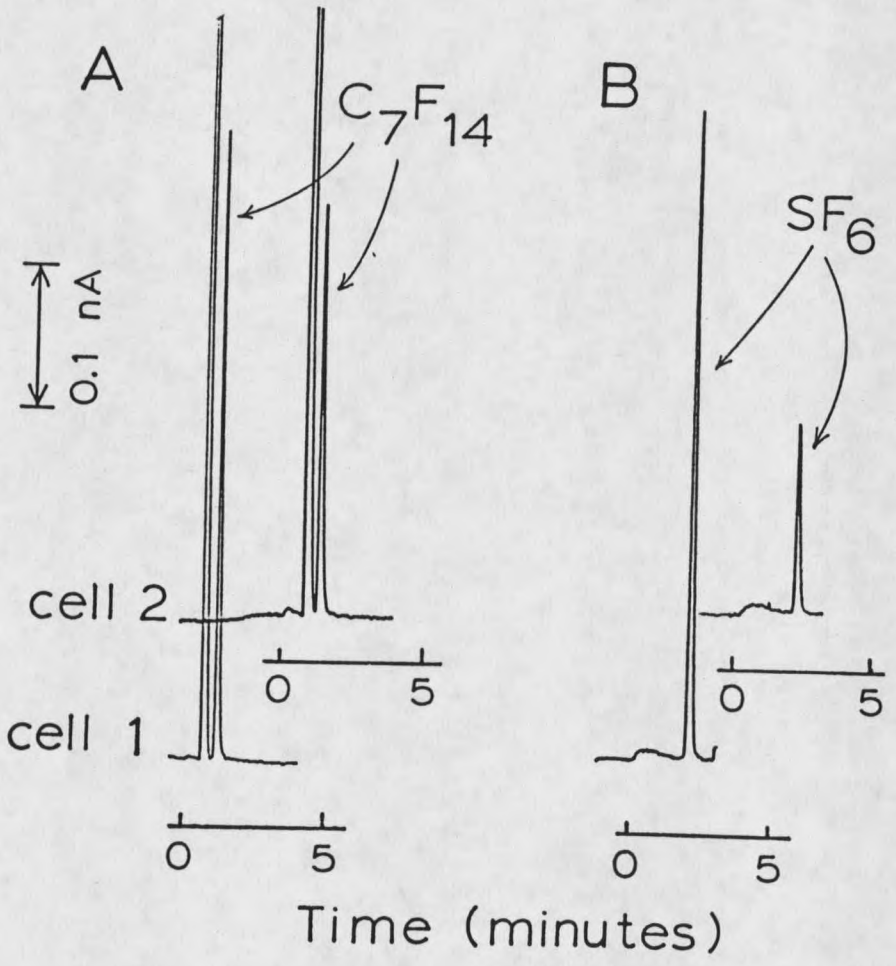

Fig. 31. Typical chromatograms of the tandem detectors to C_7F_{14} and SF_6. (A) is done with a 6 ft. SF-96 chromatographic column, and (B) is using a 6 ft. column packed with 5A molecular sieve. 10% methane in argon carrier gas flow rate is 1.0 ml/sec, detector temperature is 150° C, column temperature is 25° C and detector pulse period is 200 μsec.

period of 200 usec, and a flow rate set to 1.0 cm^3 sec^{-1}. In chromatogram A of Figure 31, C_7F_{14} eluted from the column about 1.3 minutes after the sample introduction. In chromatogram B, the elution of SF_6 occured about 2.0 minutes after sample introduction onto the column. The disturbance of signal prior to elution of C_7F_{14} in chromatogram A was due to the passage of nitrogen and small quantities of oxygen through the detectors. In chromatographic system B, oxygen and nitrogen were retained beyond the time scale shown, so that SF_6 was the first sample component detected.

Theory of Tandem Cell Analysis

Electron population measurements

The kinetic measurements described here require that the average electron population in each ionization cell be continuously maintained at a relatively constant and known magnitude. This requirement is assured by continuous measurement of the steady-state, time-averaged current obtained from cells one and two, while pulses of a known frequency are applied to the detector electrode. Typical measurements of this type are shown in Figure 32. The relationship between the magnitude of the current observed with a pulsed electron capture detector and the electron population existing in the cell has been previously studied in this laboratory[15,56,57]. A more complete description of the chemical and physical relationships of these tandem EC

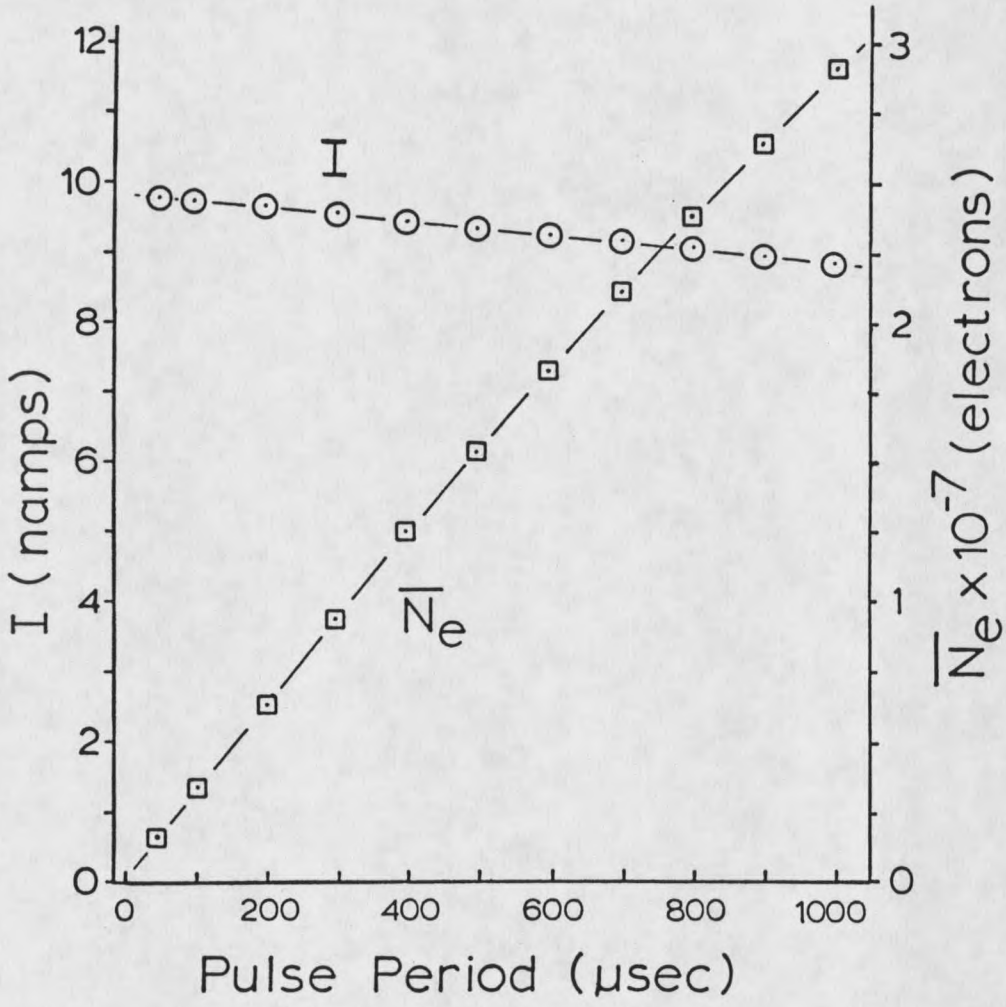

Fig. 32. Typical measurement of standing current, I, measured with cell one or cell two as a function of the pulse period, $\overline{T_P}$, used. The average electron density, $\overline{N_e}$ at each value of T is determined from I by equation (21).

detectors is found in publications by Grimsrud et al.[56,57]. An expression for the measured current, I, of a pulsed ECD is given by equation (20).

$$I = \frac{N_e{}^T}{T} (1 - \lambda) \qquad (20)$$

$N_e{}^T$ is the population of electrons existing in the cell at the instant in time just prior to an electron-collecting pulse that occurs at time = T, and λ is the fraction of space-charge driven positive ions which are transported to and measured by the central anode pin. For the cells shown in Figure 3, the value of λ has been determined to be relatively small, 0.05, and constant for all values of T. It is seen in Figure 32 that the magnitude of measured current decreased only slightly (less than 10%) as the pulse periods were increased over the range shown here. This slight decrease is attributed to the second order loss rates of electrons with positive ions and to impurities in the chromatographic system. In terms of equation (20), the constancy of I indicates that over the range of pulse periods, T = 20 to 1000 μsec, the ratio, $N_e{}^T/T$, remains relatively constant. This, in turn, indicates that for pulse periods up to 1000 μsec, the instantaneous electron population in each cell increases in a near-linear manner with time from $N_e = 0$ just after a pulse, to $N_e{}^T$ just prior to the next pulse. Therefore, the

average electron population, $\overline{N_e}$, will be given by $\overline{N_e} = 0.5 \times N_e^T$. From this relationship and equation (20), the following expression provides estimates of $\overline{N_e}$ at any T for the cells shown in Figure 3.

$$\overline{N_e}(\text{electrons}) = \frac{0.5}{(1 - 0.05)} (IxT) = 3.28 \times 10^3 \times I \times T \quad (21)$$

In this equation, I represents a current measurement in nanoamps, and T, the pulse period in microseconds. The average electron population, calculated by equation (21) for each current measurement, is also shown in Figure 32. It is seen that over the range of pulse periods used here, N_e can be varied from near zero to about 3×10^7 electrons. To ensure the maintenance of a nearly constant average electron density, the amount of compound used never exceeded that which would cause more than a 10% reduction of the total standing current.

Theoretical Modeling of the Relationships Between Peak Areas and System Dynamics

For the general reaction sequence described by reactions (18), (19a), and (19b), three distinctly different cases will be considered. The fate of the negative ion, once it is formed by resonance electron capture, will be discussed in terms of the various molecular responses possible.

Case I: In this analysis, the mechanism described by reactions (18) and (19b), will be considered where the negative ion species A^-, formed by resonance electron capture, recombines with positive ions to form neutrals, including species B. The neutrals formed in this model do not undergo further electron attachment. The recombination reaction (19a) does not occur. Since diffusion of the neutral species within the cells will be fast relative to their rate of transport through the cell by simple ventilation, the cells can be considered to be well mixed with respect to the concentration of A. Therefore, the following conservation equation can be written to equate the production and losses of A occurring in cell one.

$$\frac{F}{V}[A]_o = \frac{\overline{\phi N_e}}{V}[A] + \frac{F}{V}[A] \qquad (22)$$

$[A]_o$ is the concentration of A in the carrier gas which is entering cell one, [A] is the steady-state concentration of A in cell one and is also the concentration of A in the gas which is entering cell two, F is the temperature-corrected carrier gas flow rate through the detector, V is the volume of the cell, and ϕ is the second-order rate constant for the electron attachment reaction (18).

From equation (22) an expression for the ratio of $[A]/[A]_o$, can be written. Since the peak area responses Q_1 and Q_2, of the two detectors will be directly related to the

amount of A introduced into each cell, the measured ratio, Q_2/Q_1, is also equal to the ratio, $[A]/[A]_o$. Therefore, the following equation predicts the measured ratio of Q_2/Q_1.

$$Q_2/Q_1 = \frac{F}{\overline{\phi N_e} + F} \qquad (23)$$

Rearrangement of equation (23) allows for the determination of ϕ for Case I measurements from the ratio of responses, Q_2/Q_1, in the two detectors and is shown in this equation:

$$\phi = \frac{F}{\overline{N_e}} (Q_2/Q_1 - 1) \qquad (24)$$

To examine the relationship of theory to the experimental results, predictions of Q_1 and Q_2 are derived by the integration of the sum of all the A molecules lost to electron capture in cell one over the time of the chromatographic peak. This is shown by equation (25).

$$Q_1 = V \int ([A]_o - [A])\, dt \qquad (25)$$

By combining equations (22) and (25) to the term [A], the following expressions for Q_1 are obtained:

$$Q_1 = \frac{\overline{\phi N_e}}{(\overline{\phi N_e} + F)} \times V\ [A]_o\, dt = \frac{\overline{\phi N_e}}{(\overline{\phi N_e} + F)} \times Q_A \qquad (26)$$

Q_A is the total number of A molecules introduced to cell one over the time of the chromatographic peak. By combining

equation (23) and (26), the Case I expression for Q_2 is also obtained.

$$Q_2 = \frac{F\phi\overline{N_e}}{(\phi\overline{N_e} + F)^2} \times Q_A \qquad (27)$$

Prediction of peak area response and the ratio of response can now be made for model systems by use of equations (23), (26), and (27). Examples for Case I are shown in Figure 33 for four selected values of ϕ ranging from 1.0×10^{-8} to 3.0×10^{-7} cm^3 sec^{-1}. In these calculations, the magnitude of F and of $\overline{N_e}$ used for each pulse period, T, are similar to those commonly observed in experiments, so that these model predictions can be meaningfully compared to experimental results. The curves shown for Q_1 and Q_2 in Figure 33 are the predicted peak areas relative to the largest peak area predicted for cell one with T = 1000 μsec. It is seen that the family of curves predicted for Q_1, Q_2, and Q_2/Q_1 in Case I, are a sensitive function of the magnitude of ϕ used.

Case II: In this example, both of the recombination pathways, (19a) and (19b), are considered to be occurring. The system then becomes more complex because the molecule, A, is at least partially regenerated by the recombination reaction. For this case, the conservation equation for compound A in cell one is given by the following expression:

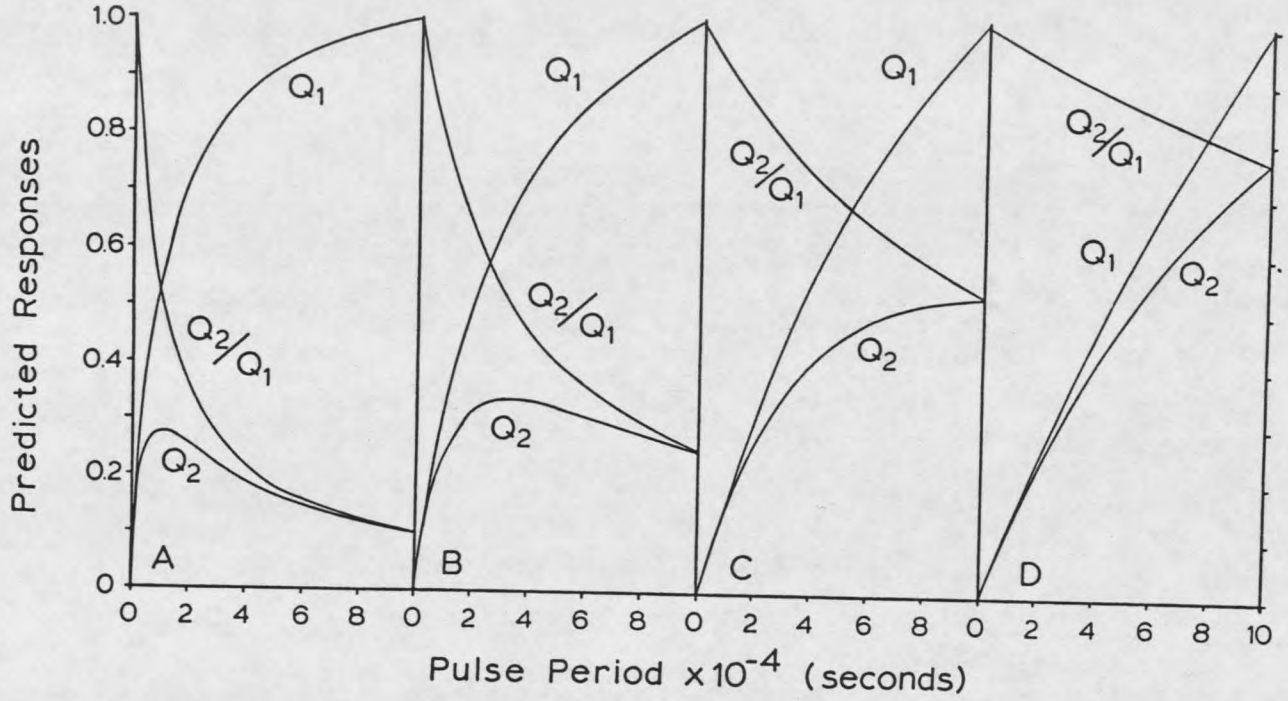

Fig. 33. Prediction of Q_1, Q_2 and Q_2/Q_1 responses of tandem cells as a function of pulse period to chemical substances which behave in accordance with Case I. The four examples shown have been calculated by equations (23), (26), and (27). with $N_e = 3.0 \times 10^4 \times T$ (μsec) and F = 1.0 ml/sec. values represented are (A) 3.0×10^{-7}, (B) 1.0×10^{-7}, (C) 3.0×10^{-8}, and (D) 1.0×10^{-8} cm3 sec-1.

$$\frac{F}{V}[A]_o + \delta R\frac{N_p^+}{V}\frac{N_A^-}{V} = \frac{\overline{\phi N_e}}{V}[A] + \frac{F}{V}[A] \qquad (28)$$

This equation differs from equation (22) in that an additional term is required to describe the regeneration of A by reaction (19a). This new collective term includes expressions for the average populations of positive ions and negative ions. This term also includes, R, the positive ion to negative ion recombination rate coefficient, which is given a magnitude of 1×10^{-6} cm^3 sec^{-1} at atmospheric pressure[54], and δ, the fraction of recombination events which proceed by way of reaction (19a). For the evaluation of Case II, the conservation equation for the production and loss of the negative ion, A^-, is also required and this is given by:

$$\frac{\overline{\phi N_e}}{V}[A] = R\frac{N_p^+}{V}\frac{N_A^-}{V} \qquad (29)$$

In this equation the production of A^- is by electron attachment to A and the loss of A^- is described entirely by the ion-ion recombination reaction. Other potential means of A^- loss such as diffusion to the walls or ventilation out of the cell are prevented, just as they are for electrons, by the continuous maintenance of the positive space-charge potential within the ionized gas[16]. The reaction of A^- with radicals is not considered in this model, and will be considered small relative to the ion-ion recombination rate.

Substitution of equation (29) into equation (28), and again by acknowledging that $[A]/[A]_o = Q_2/Q_1$, equation (30) and (31) for Case II are obtained.

$$Q_2/Q_1 = \frac{F}{(1-\delta)\overline{\phi N_e} + F} \qquad (30)$$

$$(1-\delta)\phi = \frac{F}{\overline{N_e}}(Q_1/Q_2 - 1) \qquad (31)$$

These expressions, and also those that could individually be derived for Q_1 and Q_2 in the Case II mechanism, are very similar to those previously derived for Case I, with the exception that ϕ is represented by the term $(1-\delta)\phi$ for Case II. Thus, the predictions of the results shown in Figure 33 for Case I examples in which four different ϕ values have been assumed will also serve as models for Case II, given that the rate coefficient is redefined to represent the collective term, $(1-\delta)\phi$. For that reason, molecules which are regenerated by the pathway (19b), a decrease in the rate constant as measured by the Q_2/Q_1 ratio is expected, as well as an increase in molar sensitivity for the Q_1 response relative to k_1 in reaction (18).

Case III: If the neutral species B, formed by ion recom- bination in reaction (19b), is also capable of attaching electrons rapidly, the peak area response

equations developed for Cases I and II would not be applicable. This is due to the unknown rate of electron attachment the neutral species B would have with the electrons and its concentration within the cell. However, if a system behaves in the manner of Case III, this would be determined in the electron attachment mass spectrum of substance A, by the appearance of a characteristic negative ion, C^-, formed from the reaction, $e^- + B \text{ ---> } C^-$.

Degree of Accuracy Expected for the Q_2/Q_1 Ratio

The response ratio between the two detectors is dependent on a variety of experimental parameters, as well as the compound being examined. The experimental parameters of electron density, controlled by the pulse period, and the residence time of the compound within the detector, controlled by the flow rate, each have a significant effect on the measured Q_2/Q_1 ratio. To optimize the accuracy of the rate constant determined by the Q_2/Q_1 ratio a statistical analysis was performed to characterize those ratios which would be expected to give the most accurate results. Then, with appropriate selection of experimental parameters, the most accurate determination of the rate constant, ϕ, can be calculated.

The accuracy of the rate measurements are dependent on the accuracy of the individual peak area measurements, Q_1 and Q_2. Equation (32) expresses the relative uncertainty of

determinations, σ_{ϕ}/ϕ, for Case I as a function of the peak area measurements and their uncertainties, $\sigma_Q = \sigma_{Q1} = \sigma_{Q2}$.

$$\frac{\sigma_{\phi}}{\phi} = \frac{(Q_1^2 + Q_2^2)^{1/2}}{Q_2^2\,(Q_1/Q_2 - 1)} \times \sigma_Q \qquad (32)$$

This equation was obtained by applying normal statistical procedures for the determination of propagation of errors to equation (24). It describes the intuitive expectation that determinations of ϕ by equation (24) for Case I systems, or of $(1 - \delta)\phi$ by equation (28) for Case II systems, will be subject to increasing uncertainty as Q_1/Q_2 ratios approach unity or as Q_2 becomes small. The most reliable determinations of rate coefficients determined by equation (32) are those where experimental conditions allowed the ratio, Q_1/Q_2 to fall between the range of about 1.5 to 5.

Electron Capture Mass Spectra

To insure that the resonance electron capturing compounds studied would not be responding by a Case III mechanism, APIMS analysis was performed to discern the possibility of additional electron capture processes that might involve neutral species which had originated from the parent molecule by dissociative electron capture or positive-negative ion recombinations. Only those compounds were chosen that exhibited either Case I or Case II

characteristics of analysis. The compounds that were chosen for the initial analysis were based on the APIMS observations of the following well behaved compounds; SF_6, $CFCl_3$ (freon-11), C_7F_{14} (perfluoromethycyclohexane), and CCl_4.

In Figure 34, the APIMS spectra of C_7F_{14} and SF_6 are shown under conditions similar to those with which the data were aquired using the tandem cells. The spectra indicates that there was a predominance of the A^- ion for both of these compounds. Ions of lower abundance, corresponding to the $[A - F]^-$ ion, were also observed for both of these cases. The intensity of both of these ions at 150° C is about 9% of the total molecular anion. In the APIMS studies, the dissociative fragment ion was seen to increase with detector temperatures above 150° C. This observation is consistent with known ECD temperature dependencies. The cause of the weak $C_7F_{13}^-$ signal in the spectrum of C_7F_{14} is attributed to a dissociative mechanism and has also been observed with similar intensity at 150° C within an ion source of much lower pressure and much lower ion density[58]. Octofluorotoluene (C_7F_8) is considered to undergo stable resonance electron capture with a production of molecular anion as indicated by similar observations with the HPECMS[59].

The mechanisms of response for $CFCl_3$ and CCl_4 have previously been considered[27], and the negative ion products from their dissociative electron capture reactions having

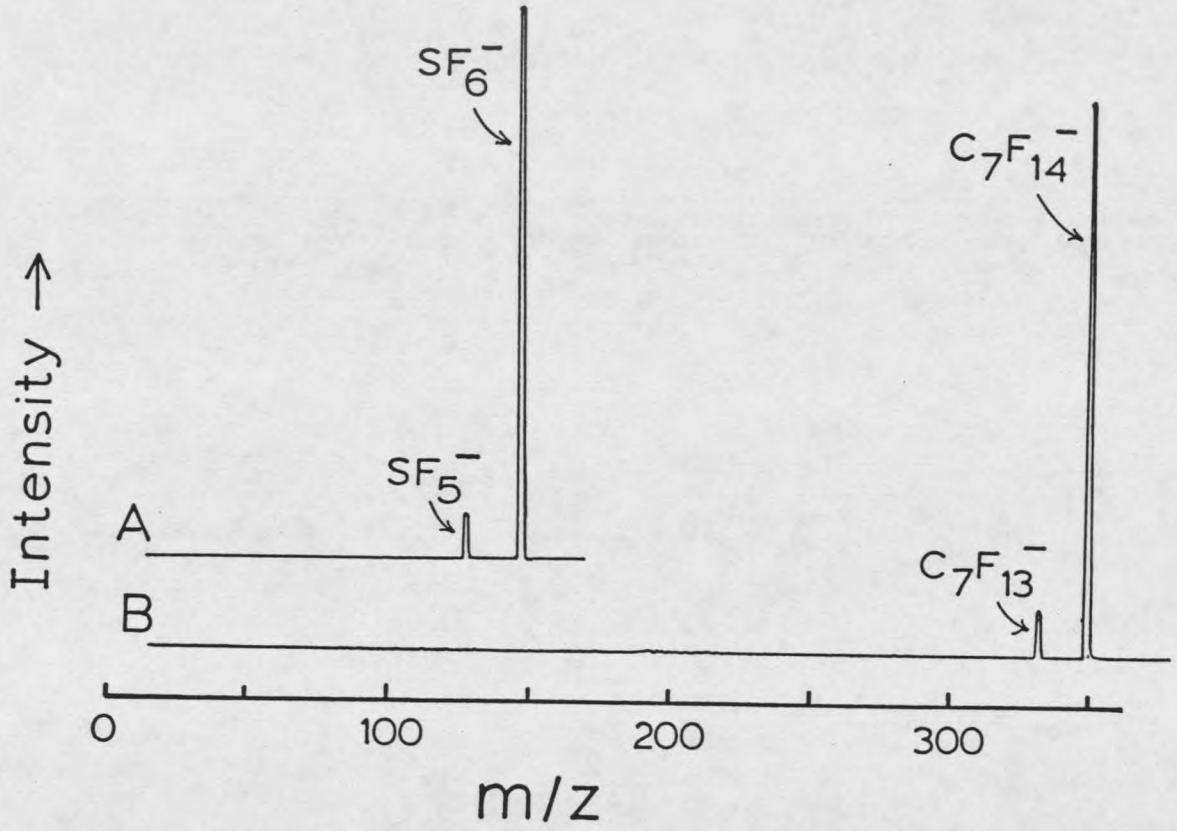

Fig. 34. APIMS electron capture mass spectra of SF_6 and C_7F_{14}. Carrier gas is 10% methane-in-argon, ion source temperature is 150° C.

been analyzed by APIMS. CCl_4 produces a Cl^- ion and the remaining neutral CCl_3 is not considered to be reactive to electron capture. No indication of CCl_4^- ion was observed by APIMS at detector temperatures as low as 100° C. $CFCl_3$ also responds by a similar dissociative mechanism with the production of Cl^-. The remaining neutral CCl_2F is believed to be unreactive to further electron attachment. The expected product of recombination between the positive and negative ions HCl, has been investigated[21], and is not considered to be reactive to electrons. Because molecule A would be destroyed by the dissociative process, the Case I model should be effective in describing the results of these two compounds, provided that the neutrals formed do not further react with electrons.

Kinetic Measurements

Shown in Figure 35 are the results obtained by the repeated analysis at different pulse periods of the five compounds selected for study in the tandem cells. Peak area measurements, Q_1 and Q_2, relative to the largest Q_1 value measured at T = 1000 μsec, and the ratios, Q_2/Q_1, are shown for numerous experiments using pulse periods ranging from T = 20 to 1000 μsec. The conditions of flow rate and average electron population existing during these determinations were made similar to those used for the creation of model behavior in Figure 33, so that a visual comparison of

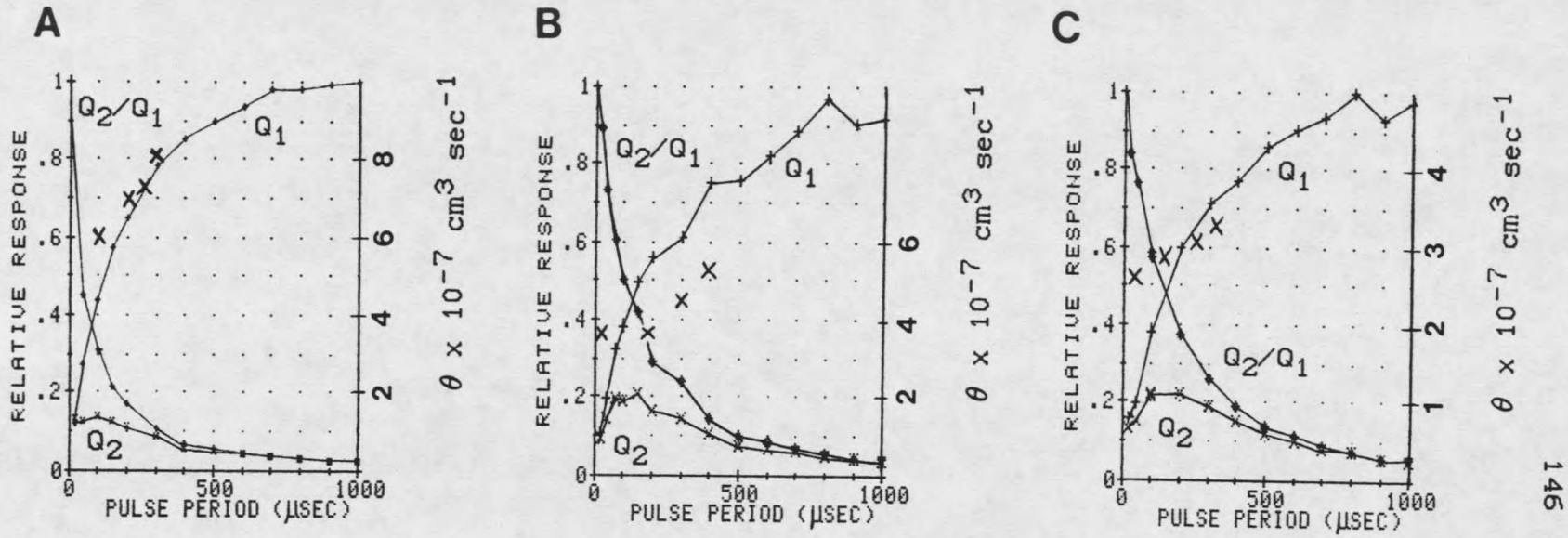

Fig. 35. Experimentally determined Q_1, Q_2, and Q_2/Q_1 responses of the tandem detectors by the repeated analyses at different pulse periods of these compounds: (A) CCl_4 (B) $CFCl_3$, (C) SF_6 (D) C_7F_{14}, and (E) C_7F_8. Also shown (X's) is the calculation of θ by equation 19 to measured values of Q_1/Q_2 and I. Flowrate is 1.0 ml/sec, detector temperature is 150° C.

D

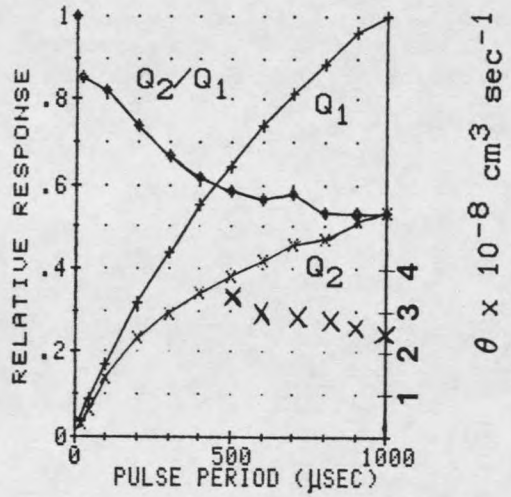

E

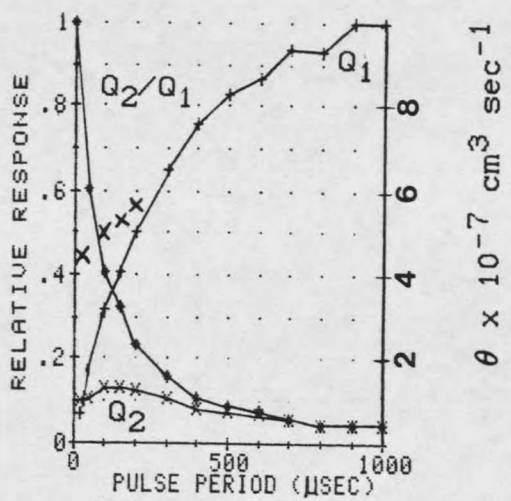

Fig. 35 - Continued

the experimental results in Figure 35 with the predictions in Figure 33 are valid. Because the results of these experiments have not yet been assigned as Case I or Case II possibilities, in which the rate constant measured may represent ϕ or $(1 - \delta)\phi$, a new term θ, is defined to describe the experimentally determined rate coefficient. Also included in Figure 35, and labeled on the right hand Y-axis of each chart, are the values of θ calculated from the Q_2/Q_1 ratios according to equation (33).

$$\theta = \frac{F}{\overline{N_e}} (Q_1/Q_2 - 1) \qquad (33)$$

The magnitude of $\overline{N_e}$ at each T was determined from the measured detector current in accordance with equation (18). For the determinations shown, only data collected at T values for which the greatest accuracy is expected have been used. In accordance with equation (32), these generally occurred when the measured ratio, Q_1/Q_2, fell between the range 1.5 to 5. For a given set of experimental conditions the reproducibility of the method was quite high.

To ensure the validity of the method and the conformity between theory and experiment, the experimental parameters of sample size, flow rate, and detector temperature were also examined to assess their effects on the analysis. Changes in detector temperature may shift the mechanism of response from stable resonance electron capture to

dissociative capture or vice versa and temperature studies were conducted to ensure that the proper mechanism was known for the compound being studied.

In Figure 36 the effects of varied sample sizes on measured Q_2/Q_1 ratios are shown at three different pulse periods for two of the compounds studied. As clearly indicated in this figure, the measured Q_2/Q_1 ratios, from which the rate coefficients, θ , were obtained, were not dependent on the choice of sample size, provided the maximum current response did not exceed 10% of the standing current. This result was expected and reaffirms the constancy of average electron density, $\overline{N_e}$, in both cells. Similar results were also obtained for SF_6 and C_7F_8.

Experimental determinations of θ (Equation 33) with varying flow rates are shown in Figures 37 and 38 for four of the compounds examined. The flow rates were adjusted by changing the amount of make-up gas entering the detector so that the chromatographic pulse of the compound into the detector would remain constant. Flow rates were selected from within the range of flow rates these detectors are known to produce successful coulometric results, whereby a well mixed reactor could still be assumed. The ratio of Q_2/Q_1 is known to change with flow rate. For example, with slower flow rates, the residence time of the sample within the detector is increased, and a larger efficiency of reaction with electrons is expected. This is seen as an

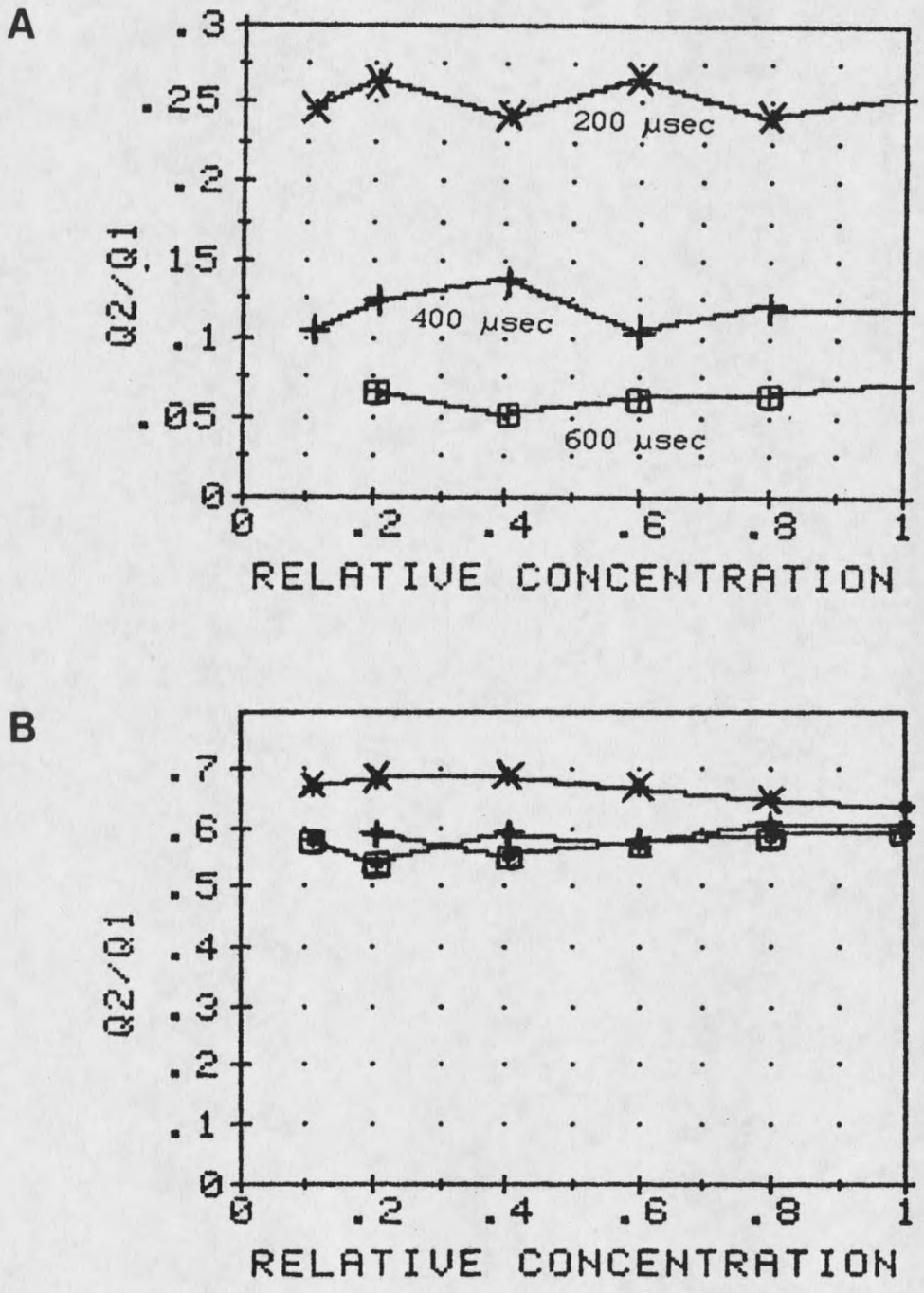

Fig. 36. Effect of varied sample size on measured peak ratios, Q_1/Q_2 for (A) C_7F_8 and (B) C_7F_{14}, at 3 different pulse periods; (×) = 200 µsec, (+) = 400 µsec, and (□) = 600 µsec. Detector temperature is 150° C. Flowrate is 1.0 ml/sec.

increase in the Q_1 response and concurrent decrease in the Q_2 signal.

For a proposed Case I example, such as CCl_4, the most accurate results are expected at higher flow rates. A larger range of pulse periods are capable of being used for the determination, within the limitation of the 1.5 to 5 Q_1/Q_2 ratio scope. From the data in Figure 31, supposing that C_7F_{14} is responding in a Case I manner also, the most accurate θ determinations would be favored by lower flow rates, thereby increasing the efficiency of reaction and allowing the possibility of larger differences between the Q_1 and Q_2 response. The magnitude of the variations in θ with F, shown in Figures 37 and 38, are of the same order of magnitude as the estimated uncertainty of the method at a given flow rate, about $\pm$30%. Therefore, it is concluded that this test of flow rate variation is also consistent with expectations.

General trends in the θ values measured for the compounds are included in Table 5 and are compared to the experimental conditions of pulse period, flow rate and detector temperature. Because these general trends in θ values were noted with varying with flow rate and $\overline{N_e}$, it is apparent that equation (33) does not completely describe θ and some systematic error is present in the equation. There is no reasonable explanation for the variations in the pulse periods observed, particularly since this affect appears to

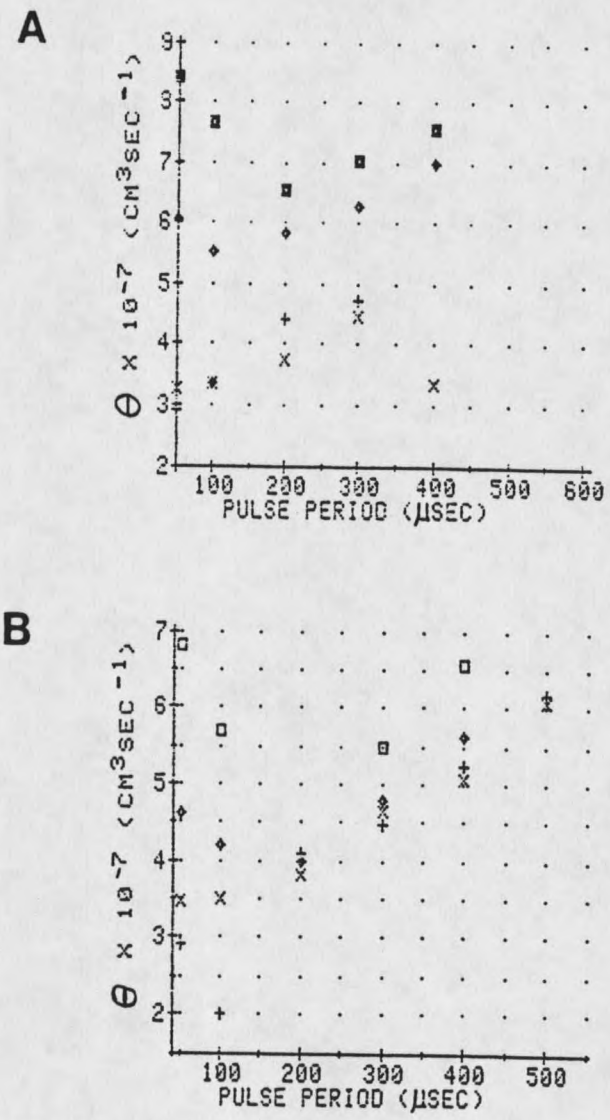

Fig. 37. Measurements of of rate coefficient, θ , for (A) C_7F_8 and (B) $CFCl_3$ using several different carrier gas flowrates. Flowrates are 1.0 (×), 1.2 (+), 1.5 (◇), and 1.9 (□) ml/sec. Detector temperature is 150° C.

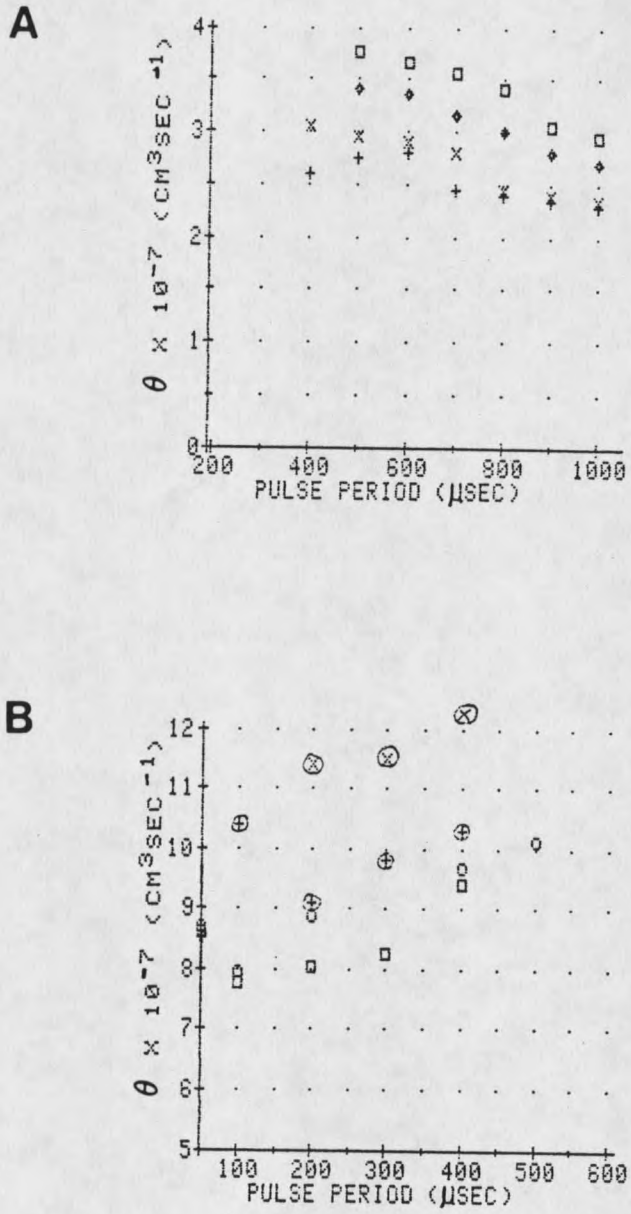

Fig. 38. Measurements of of rate coefficient, θ , for (A) C_7F_{14} and (B) CCl_4 using several different carrier gas flowrates. Flowrates are 0.25 (+), 0.5 (×), 0.75 (◇), 1.0 (□), 1.2 (○), 1.5 (⊕), and 1.9 (⊗) ml/sec. Detector temperature is 150° C.

Table 5 General trends of calculated θ variations to experimental parameters[a].

Molecule	Pulse Period	Flow Rate	Detector Temperature
C_7F_{14}	-	+	-
CCl_4	+	+	-
C_7F_8	+	+	-
$CFCl_3$	+	+	-
SF_6	+	+	-

[a] (+) indicates an increase in θ with the increasing experimental parameters, and a (-) indicates an inverse relationship.

be compound specific. Therefore, all the pulse period data falling within the 1.5 to 5.0 Q_1/Q_2 ratio limitation is included in the overall result(s), with the error range shown.

With higher flow rates there appeared to be a smaller range of differences in θ measured over the range of pulse periods used. A possible explanation for the observations at low flow rates is that the detector cannot be considered to be a well-mixed reactor. This effect is aggravated by the use of small pulse periods, which cause a decrease in the size of the region where negatively charged species reside, according to the space charge model previously discussed. The tendency of the calculated θ to get larger with increases in flow rates could also be the result of a

systematic error in calculating the temperature corrected flow rate for these studies. Our detector oven is Variac controlled and does not include a fan, resulting in temperature gradients of as much as 10 degrees within the detector housing. Thus, the temperature that is measured could possibly be in error relative to the actual detector temperature. This error would alter the temperature corrected flow rate used in equation (33).

Decreases in the calculated θ value with increases in detector temperature can be attributed, at least, in part, to the sum of these variables: changes in k_1 (the electron attachment rate), changes in the recombination rate between positive and negative ions, electron detachment occurring at the higher detector temperatures, or a change in the degree of dissociative electron capture compared to resonance electron capture. Individually, none of these effects are capable of explaining the magnitude of change in θ seen with the different detector temperatures studied, so a cumulative effect may be responsible.

It is easily seen in equation (33) that a faster rate constant was obtained by an increase in the Q_1/Q_2 ratio. One explanation proposed for a faster θ measured at the low temperature (100^{o} C) can be inferred from the previous discussion on sensitization. After the use of carrier gas scrubbers, the concentration of oxygen present in the system was reduced to a concentration of approximately 1 ppm or

less. It is known that the degree to which O_2 sensitization occurs is often favored by lower detector temperatures which provide a larger equilibrium concentration of the O_2^- reagent ion. Therefore the possibility exists, and it seem reasonable, that O_2 is sensitizing the response in the first cell to some extent. In the second cell, the same degree of sensitization would not be achieved because the sensitizing species, O_2, was destroyed in the first cell. This would result then, in a higher Q_1/Q_2 ratio and subsequently the determination of a higher calculated θ value. Many scenarios can be envisioned for other sensitizing species similar to the one just described for O_2.

The potential that a systematic error was induced by positive ion-molecule reactions was also considered, since an additional loss term for molecule A could be described, based on the results of positive ion formation acquired in this investigation. This possibility was tested for by measuring the Q_2/Q_1 ratio with 100 ppm triethylamine (TEA) doped into the detector gas. With TEA present in the detector gas, no significant differences were noted in the Q_2/Q_1 ratios over the pulse period range between 20 and 1000 μsec, relative to the undoped condition. Theoretically, this was a possibility with up to 20% deviations at small pulse periods. The use of small concentrations of analyte and the low PA of the molecules examined probably caused this effect to become unimportant. The moderate proton

affinity of CH_4 to produce the CH_5^+ ion, and its concentration at 10% within the argon detector gas, probably insured the positive ionization of solute to be minimal and, therefore, no effect was observed.

Extent of Regeneration by Ion-Ion Recombination

By comparing the rate coefficient, θ, measured by the Q_2/Q_1 ratios, with a prior determination of ϕ for each compound, it is possible to determine the magnitude of, δ, the regeneration of A by recombination. Through inspection of equations (24), (31), and (33), it is apparent that the equation, $\theta = (1 - \delta)\phi$, describes both Case I analysis (where $\delta = 0$) and the Case II analysis. This equation, upon rearrangement, yields equation (34), describing the extent of regeneration.

$$\delta = 1 - \theta/\phi \qquad (34)$$

The uncertainty of δ will be dependent on the accuracy of the determinations of θ and ϕ and is represented in equation (35).

$$\sigma_\delta = \phi^{-1} [\sigma_\theta^2 + (\theta/\phi)^2 \sigma_\phi^2]^{1/2} \qquad (35)$$

The values σ_θ and σ_ϕ represent the uncertainties in θ and ϕ. The accuracy of the results in θ, determined by the Q_2/Q_1 ratios is taken as twice the standard deviation of the

results obtained. This is relative to the mean from the data points determined when the ratios were within the Q_1/Q_2 limitations.

The overall results for the five compounds studied is included in Table 6. In this Table are the determinations of θ by the tandem cell method and their expected accuracy. Prior determinations of k_1 or ϕ using different instrumentation is also shown. The method of ϕ determinations with the Flowing-Afterglow/Langmuir Probe (FALP) used by Smith et al.[28,29], is considered to encompass the most accurate procedure. This is related to the facts that the procedure is relatively free from systematic error, the electron population is well thermalized, and ϕ values are reported at several temperatures. For C_7F_8, the data were taken from the work of Christophorou[60]. For the remainder of compounds, data were taken from the pulsed HPECMS techniques of Grimsrud, Chowdhury and Kebarle[58]. The pulsed HPECMS technique is also expected to give reasonable values for the determination of a relative ϕ, since the technique gave results compatible to the FALP procedure when determinations were made for the same compound. Also included in Table 6 are the determinations of δ, which describe the extent of regeneration calculated for each of these compounds.

The results obtained for those compounds known to respond by a dissociative mechanism are supported by the information at 150° C given in Table 6. Compounds that

Table 6 Summary of results for the determination of θ and δ by tandem cell analysis.

Molecule	$\theta \times 10^{-7}$ (cm^3 sec^{-1})[a]	$\phi \times 10^{-7}$ (cm^3 sec^{-1})[b]	δ[c]
C_7F_{14}			
150° C[d]	0.36 ± .13	1.2 ± 0.2	0.70 ± .12
100° C	0.43 ± .12	1.0 ± 0.2	0.57 ± .15
150° C	0.40 ± .07	1.2 ± 0.2	0.67 ± .10
200° C	0.31 ± .06	1.4 ± 0.3	0.78 ± .10
CCl_4			
150° C[d]	9.6 ± 1.9	3.8 ± 0.8	0.00
100° C	12.0 ± 3.0	4.0 ± 0.8	0.00
150° C	7.0 ± 1.7	3.8 ± 0.7	0.00
200° C	7.4 ± 0.6	3.6 ± 0.7	0.00
C_7F_8			
150° C[d]	5.4 ± 1.6	3.0 ± 1.5	0.00
100° C	8.1 ± 2.0		0.00
150° C	3.7 ± 0.5	3.0 ± 1.5	0.00
200° C	3.4 ± 0.5		0.00
$CFCl_3$			
150° C[d]	4.7 ± 1.2	3.4 ± 0.7	0.00 ± .24
100° C	6.5 ± 0.7	3.1 ± 0.7	0.00
150° C	4.4 ± 1.0	3.4 ± 0.7	0.00
200° C	3.7 ± 0.5	3.6 ± 0.3	0.00
SF_6			
150° C[d]	4.1 ± 0.7	4.2 ± 0.8	0.02 ± 0.3
100° C	5.0 ± 1.7	3.7 ± 0.7	0.00 ± 0.4
150° C	3.7 ± 0.5	4.2 ± 0.8	0.10 ± 0.2
200° C	2.7 ± 0.5	4.4 ± 0.9	0.38 ± 0.2

[a]composite rate coefficent determined by tandem cells.

[b]best literature value for electron attachment coefficient

[c]efficiency of molecular regeneration by ion-ion recombination

[d]average of values determined at 150° C with varying flow rates

respond by dissociative capture should be characterized by the Case I model, where regeneration of a molecular anion is not possible. The data given for $CFCl_3$ agrees quite well with theory, and the measured rate constants are within the experimental error of the data presented by Smith et al[29]. No indication of regeneration was calculated for $CFCl_3$.

Data presented for CCl_4 also indicate that regeneration was not occurring. However, the rate constants measured here are significantly faster than the electron capture rate constant measured by Smith et al.[29]. These "high" rate constants are calculated when the ratio Q_1/Q_2 is larger than what is predicted by theory. Some possible explanations for this have been given in the discussion on the trends of θ variations with experimental parameters. $CFCl_3$ and CCl_4 both have similar EC attachment rates. One very significant difference involved in their mechanism of response was their neutral radicals remaining after the dissociative electron capture reaction. $CFCl_3$ dissociates to produce a $\cdot CFCl_2$ radical and CCl_4 dissociates with the capture of an electron to produce the $\cdot CCl_3$ radical. Subsequent indirect or direct electron capture reactions with the parent molecule, or these newly formed neutrals, may be one possible reason for the differences in the calculated θ values.

For those compounds responding by a resonance electron capture mechanism, a Case II model should best describe the response, where the molecular anion is regenerated through

an electron transfer to a positive ion. The results of experiments with C_7F_{14} indicate a statistically significant degree of regeneration. The value of regeneration at 0.70 ± 0.15 allows for δ to fall in the range 0.55 to 0.85. The APIMS mass spectrum of C_7F_{14}, shown previously in Figure 34, indicated that the dissociative electron capture product, $C_7F_{13}^-$, constituted about 9% of the total negative ion production by electron attachment to C_7F_{14} at 150° C. Since positive ion recombination of the $C_7F_{13}^-$ ion could not lead to regeneration of C_7F_{14}, the maximum possible value of an experimentally determined δ value is 0.91. The uncertainty assigned to the measured value of δ, therefore, allows the conclusion that from about 60 to 93% of the molecular anion, $C_7F_{14}^-$, is converted to the C_7F_{14} molecule upon recombination with positive ions.

C_7F_8 is also assigned as a stable resonance electron capture response. The results from our experiments conclude that regeneration is only slightly occurring for this compound. Unfortunately, no APIMS data was collected for this compound, and the maximum possible value of regeneration could not been determined. The electron attachment rate has only been reported at 300° K[61], and a large approximation was necessary to describe a ϕ value for 423° K. From the data presented in Table 6, a maximum value for δ of 0.3 was within the uncertainty of the experimental results. Either a dissociative product, much like the

mechanism of response for $CFCl_3$ is effective, or the molecular anion is simply incapable of significant regeneration. Further studies with this particular compound are needed to give an accurate evaluation of these results.

APIMS mass spectral data at 150° C (Figure 34) indicate that SF_6 was responding predominately by a stable resonance electron capture mechanism. The maximum extent of regeneration due to a small amount of dissociative capture was again, .91, the same as C_7F_{14}. However, the results at 150° C suggested that only 0.02 ± 0.26 of the molecular anion was being regenerated. Therefore, the values of θ and ϕ listed for SF_6 in Table 6 appear to be essentially equal, and the total electron capture/recombination mechanism of SF_6 appears to be best described by Case I, in which the molecular species, SF_6 is not regenerated with high efficiency by the recombination reaction.

The electron affinities for SF_6 and C_7F_{14} have recently been shown to be almost identical, 1.05 ± 0.1 eV and 1.06 ± 0.15 eV, respectively[58]. This property, the similarity of ϕ values listed in Table 6, and the fact that both are believed to respond by stable resonance electron capture, suggest that differing fates of the SF_6^- ion and $C_7F_{14}^-$ ion upon recombination with positive ions are causing the differences in δ calculated for these two compounds with the tandem cell technique. In the determination of the EA values, an unusually high entropy change was shown to be

associated with the negative ionization of SF_6. For the process, SF_6 ----> SF_6^-, an entropy increase of about S^o = 11 e.u. was deduced from numerous measurements of electron transfer reactions[58]. The corresponding entropy measurements for the change, C_7F_{14} ----> $C_7F_{14}^-$, revealed S^o = 0 e.u.

Large changes in entropy values are believed to be indicative of intramolecular geometric changes accompanying the negative ionization of the molecule. SF_6^- would then differ considerably in geometry from that of SF_6. Photodetachment studies by Drazic and Brauman[62] also found a large entropy change with electron attachment to SF_6, and a low symmetry ion, of the type $SF_5{:}F^-$, was proposed. This ion would differ greatly from the octahedral structure of molecular SF_6. If this were the case, the failure of SF_6^- to form SF_6 upon recombination is easily theorized. Another possible explanation for the failure of SF_6^- to recombine with positive ions can be envisioned by the processes involved in the recombinant event. The electron transfer process occurs at some point in time as the oppositely charged ions are accelerated towards each other by the coulombic force. Immediately following the instant of the electron transfer, the two participants, which are now neutrals, will momentarily possess excess internal energy from the electron transfer reaction and excess kinetic energy from the coulombic attraction. However, both ions

will retain their characteristic geometries. Therefore, SF_6^- may not be efficiently converted to SF_6 neutral upon recombination with positive ions because of the additional vibrational energy imparted to the SF_6 neutral as it is formed with a configuration of much higher energy than the ground state neutral. Dissociative pathways and the total recombination energy can then combine to destroy the molecule. In a sense, this can be considered an indirect dissociative process where dissociation is not occurring upon electron attachment, but, is rather occurring with the unstable neutral generated in the recombination process. These neutrals would be no longer capable of attaching thermalized electrons. This latter explanation may also suggest why it is difficult for molecules to achieve 100% efficiency of molecular regeneration in the ECD.

For the case of C_7F_{14}, no great geometric differences between the molecule and the anion were suggested by the entropy measurements discussed above. It is reasonable to expect that for $C_7F_{14}^-$, a configuration close to that of the stable molecular species exists at the instant of electron transfer in its recombination event. The numerous vibrational states available for energy dispersion within the C_7F_{14} molecule may also be an important factor in assisting in its survival. This favors the maintenance of the C_7F_{14} species, while the total recombination energy is dissipated by collision with carrier gas molecules.

In another experiment, a number of substituted NO_2-benzenes were investigated to determine a θ value by the tandem cell technique. These compounds also are thought to be reactive by a stable resonance electron capture process. This analysis required a different chromatographic system, and also required the GC oven to be heated, whereas heating was not needed in the previous studies. Because a FF pulser was used in this study, the standing currents at the longer pulse periods deteriorated significantly as a result of increased impurities bleeding from the chromatographic system. Standing currents were monitored at all pulse periods; the larger decrease in electron population was measured and allowed for in equation (33).

The results for compounds studied at a 200 µsec pulse period are included in Table 7. A pulse period at 200 µsec was chosen for the following reasons; 1) the standing currents measured were in agreement between the two detectors, 2) the selection of a small pulse period gave the largest and most accurate determination of the Q_1/Q_2 ratio for these weakly responding compounds, although the ratios did not always satisfy the criteria that they be larger than 1.5, 3) using only one pulse period would allow for meaningful comparisons between the different compounds, 4) coulometry by tandem cell analysis was reasonably accurate at a minimum pulse period of around 200 µsec, and 5) knowledge gained from the previous trends of θ

calculations to pulse period variations could be applied to the information presented here, since these compounds followed the general trends seen with the other compounds previously studied.

Table 7 Measurements of θ and δ at 200 μsec as determined by tandem cell analysis, detector temperature 165° C.

Molecule	$\theta \times 10^{-8}$ (cm^3 sec^{-1})[a]	$\phi \times 10^{-8}$ (cm^3 sec^{-1})[b]	δ[c]
C_7F_{14}	6.2 ± 2	12.0 ± 3.0	.48 ± .3
Meta-Cl-NO2-benzene	2.8	9.6 ± 1.9	.40
Meta-CF_3-NO2-benzene	2.6	7.2 ± 1.4	.64
Para-Fl-NO2-benzene	2.2	2.4 ± 0.5	0
NO2-benzene	1.8	1.2 ± 0.2	0

[a] composite rate coefficent determined by tandem cells.

[b] electron attachment coefficient relative to C_7F_{14} as determined by HPECMS experiments of Kebarle et al.[58].

[c] efficiency of molecular regeneration by ion-ion recombination

The compounds, C_7F_{14}, meta-Cl-nitrobenzene, and meta-CF_3-nitrobenzene all exhibited a calculated value for some degree of regeneration. The two compounds, nitrobenzene and para-F-nitrobenzene, did not show a calculated value for regeneration. The Q_1/Q_2 ratios were below the 1.5 minimum previously established so the uncertainty in their measurements was quite high. The larger ratios for the first three compounds mentioned did give calculated values for some degree of regeneration and, when assuming an increasing value of θ with increases in pulse period, the degree of regeneration could be considered to be even smaller. The uncertainty in these measurements prevents any serious determination of a recombination value.

The general trend between the measurements of the substituted benzenes do agree with theory. If a similar degree of regeneration is assumed for compounds with similar structure, then the θ values determined, relative to each other, when compared with ϕ values determined by Kebarle et al.[58], are in agreement in the order of their values. The expected magnitude of relative θ values (assuming accuracy in measurement) does not correlate with the reported ϕ values, with this possibly attributed to either differences in the degree of regeneration by recombination, or the degree of dissociation in the electron capture reaction. Overall, a conclusive statement for θ and ϕ values cannot be given for this class of compounds because of the increasing

uncertainty in the tandem cell technique as the value of θ decreases. Possibly, a tandem ECD system could be designed for increased efficiencies of reactions so that compounds with electron attachment rate constants similar to those of the substituted NO_2-Benzenes could have their θ values more accurately ascertained.

SUMMARY

This investigation involved the examination of the reactive chemical dynamics affecting the response of the constant current pulsed ECD (CC-ECD). Chemical dopants, the compounds analyzed, and the instrumentation used, were carefully selected to control and measure the individual reactions occurring within the EC cell. The experiments were initially interpreted using the existing theories of the resonance electron capture process, and, as a result of this, improvements were made in theoretical models. Computer modeling of the resonance electron capture reaction showed that the steady-state approximations of the negative ion density were valid for the compounds studied in the CC-ECD. The computer modeling also suggested that non-linear calibration curves observed for weakly responding compounds were, in part, due to a difference in the recombination rates of electrons and negative ions with positive ions.

With an increased understanding of the response mechanisms involved, and the results reported, further application and accurate prediction of the ECD repsonses to a larger number of compounds becomes possible. Coulometric

analysis can be performed for more compounds if the mechanism of response is understood.

Another contribution of this study, was a reduction in the requirement for numerous calibrations by linearizing the response of the detector to analyte concentration. This was accomplished through either chemical doping and sensitization or by accounting for deviations in linearity with improved response functions.

A significant contribution of this study was the development of a new method for the analysis of low EA PAH's in the ECD by the use of alkyl chloride sensitization. This adds a new dimension to the analytical methods for the analysis of environmentally important compounds that were previously insensitive to normal EC detection.

The amine dopants, TMA and TEA, were useful in demonstrating the importance of the positive ion/electron recombination rate, and correcting the W-peak-shaped character that is often seen with the aromatic hydrocarbons. The amine dopants, with their stabilizing effect on the normally dynamic nature of positive ions within the undoped ECD, allowed the measured response to reflect more accurately the electron capture of the substance. When used in conjunction with the monochloroalkane dopants, the sensitized responses were even further improved by eliminating the effect of variations in the average positive

ion/electron recombination rate that is often seen with the aromatic hydrocarbons. Together, the two dopants provide linear calibration curves with high sensitivity to those compounds known to enhance.

In the TMA or EtCl doped ECD analysis of strongly responding compounds there were no detrimental effects seen and the normal EC signal was retained. By combining these two dopants improvements in the baseline noise of the detector was accomplished by eliminating the limited sensitized response to non-electron capturing impurities. Only beneficial effects with TMA were noted. The stabilizing effect of the amine doped positive ions and their electron recombination rate simplifies the reaction dynamics occuring within the ECD. An additional advantage of TMA doping, which applies to both weakly and, more importantly, strongly electron attaching compounds, is that the TMA dopant can prevent the loss of analyte molecules to protonation in the detector. A conclusion from this study is that TMA should be used as a permanent addition to the ECD detector gas, particularly when analyzing large aromatic hydrocarbons or in future applications of the ECD which involve theoretical computations.

The development of a theoretical model for alkylmonochloride sensitization has been useful in the prediction of those compounds that would show an enhanced response. The model also describes the limitations of the technique.

Sensitization is only possible for those compounds which produce negative ions unstable to electron detachment. This sensitization is further limited to only those unstable anions capable of reacting with the alkylchloride. This reaction is of no benefit to those strongly responding compounds which produce stable negative ions. At moderate detector temperatures there is no detrimental effect seen with the doping of monochloroalkanes, except for only a minor increase of detector baseline in the CC-ECD.

One practical application that can be envisioned for the use of the alkylchloride doping schemes presented here is in the analysis of environmental samples or fossil fuel extracts containing PAH's. After fractionation by high pressure liquid chromatography, the neutral fractions containing unsubstituted PAH's would be well suited to compound identification by alkylchloride sensitization and GC retention times, especially when quantitation of specific representative compounds is desired. For those HPLC fractions containing PAH's with NO_2 substituted groups the ECD already has high sensitivity.

In comparison, oxygen doping is also known to sensitize the response of PAH's and enhancements of up to two orders of magnitude have been reported (32,33). O_2 significantly destroys the baseline of the detector with a concurrent increase in the noise level. This noise level is often increased by as much as 10x over the normal response, thus

an enhancement value of 80 may only represent a 8x increase in the signal to noise ratio. The reagent ion, O_2^-, produced with O_2 doping, is reactive to a very large proportion of compounds. This makes the normally selective ECD capable of providing a sensitive response to many compounds in a chromatogram. In a sense, it defeats the advantage of using selective detectors for gas chromatography. Thus, O_2 doping is not recommended for those compounds that enhance by alkylchloride doping.

The chemical doping experiments reported in this study utilized an exponential diluter to introduce the dopants into the detector gas. This readily allowed modifications in dopant type and concentration. For routine application of GC-ECD chemical doping, this technique would not be desirable. The use of specially prepared gas tanks or permeation tubes would be a better adaptation for the addition of chemical dopants, particularly when automated GC systems are used.

In the study of ion-ion recombination processes with the tandem cells, it was shown that the response of the detector to resonance electron capturing compounds can be sensitive to the regeneration of the parent molecule by ion-ion recombination. The response of the ECD, known to be sensitive to the electron attachment rate, is also sensitive to the degree of this regeneration. The intensity of signal between the tandem ECD cells reflects both of these

processes and values for regeneration can be calculated when the compound's electron attachment rate is accurately known. When the efficiency of reaction with electrons is low, little effect is expected by a recombination/regeneration reaction. Since criteria for the Case I analysis scheme are similar to the criteria necessary for successful coulometry, it may be possible to exploit this relationship to further develop the tandem ECD technique for coulometric analysis. From the experiments reported in this study it has been observed that the value of θ is dependent on the instrumental variables of pulse period, detector temperature, and flow rate. If the two theories are combined, with the regeneration theory included into the criteria established for coulometry, the possibility exists that the instrumental parameters can be adjusted so that the ratio of responses in the cells yields a value, θ, that agrees with the literature value of ϕ. At these instrumental conditions we might expect accurate coulometric results. Coulometry would continue to be effective only for a Case I analysis, but these additional criteria would quickly establish whether or not a compound is susceptible to coulometric analysis and would suggest the proper operating conditions necessary for the measurement. Based on our observations, SF_6, a resonance electron capturing compound, would be expected to be a viable candidate for coulometry.

Overall, this study has produced considerable insight into the chemical reactions which can affect the response of the ECD. Chemical doping has improved the versatility of the ECD by altering the chemical selectivity and has given additional control and stabilization over the reaction dynamics within the electron capture detector. Knowledge gained from these studies, though it directly applies to improvements of the ECD, will hopefully also aid in the design and interpretation of response for other analytical instruments that also deal with ionic reactions in the gas phase.

LITERATURE CITED

LITERATURE CITED

(1) J. E. Lovelock in "Electron Capture Theory and Practice in Chromatography", Ed. by A. Zlatkis and C. F. Poole, Journal of Chromatography Library; Vol. 20, Introduction, Elsevier Publ., Amsterdam, Netherlands (1981).

(2) Rachel Carson, "Silent Spring", Houghton Mifflin Co., Boston, MA, (1962)

(3) J. E. Lovelock, Insitute of Petroleum, Gas Chromatography Discussion Group, Oxford, England, May 1957.

(4) E.S. Goodwin, R. Goulden and J. G. Reynolds, "Gas Chromatography with ECD detection for Rapid Identification of Pesticide Residues in Crops", Presented at 18th Int. Congr. on Pure and Applied Chemistry, Montreal, August 1961.

(5) J. E. Lovelock, Anal. Chem., 35, 474 (1963).

(6) J. E. Lovelock and S. R. Lipsky, J. Am. Chem. Soc., 82, 431 (1960).

(7) W. E. Wentworth, E. Chen, and J. E. Lovelock, J. Phys. Chem., 70, 445 (1966).

(8) R. J. Maggs, P. L. Joynes, A. J. Davies, and J. E. Lovelock, Anal. Chem., 43, 1966 (1971).

(9) W. B. Knighton and E. P. Grimsrud, Anal. Chem., 55, 713 (1983).

(10) E. P. Grimsrud and D. A. Miller, J. Chromatogr., 192, 117 (1980).

(11) M. A. Wizner, S. Singhawangcha, R. M. Barkley and R. E. Sievers, J. Chromatogr., 239, 145 (1982).

(12) E. P. Grimsrud, D. Miller, R. G. Stebbins, and S. H. Kim, J. Chromatogr., 197, 51 (1980).

Literature Cited - Continued

(13) E. C. Horning, D. I. Carroll, I. Dzidic, S. N. Lin, R. M. Stillwell, and J. P. Thenont, J. Chromatogr., 142, 481 (1977).

(14) E. P. Grimsrud, Anal. Chem., 50, 382 (1978).

(15) P. L. Gobby, E. P. Grimsrud, and S. W. Warden, Anal. Chem., 52, 473 (1980).

(16) E. P. Grimsrud and M. J. Connolly, J. Chromatogr., 239, 397 (1982).

(17) W. E. Wentworth and E. C. Chen, J. Chromatogr., 186, 99 (1979).

(18) M. W. Siegel and M. C. McKeown, J. Chromatogr., 122, 397 (1976).

(19) P. L. Patterson, J. Chromatogr., 134, 25 (1977).

(20) A. Zlatkis, C. K. Lee, W. E. Wentworth, and E. C. Chen, Anal. Chem., 54, 1596 (1983).

(21) E. P. Grimsrud and W. B. Knighton, Anal. Chem., 54, 565 (1982).

(22) W. E. Wentworth, R. S. Becker, and R. J. Tung, J. Phys. Chem., 71, 1652 (1976).

(23) D. C. Frost and C. A. McDowell,Frost, J. Chem. Phys., 29, 503 (1958).

(24) E. P. Grimsrud, and S. H. Kim, Anal. Chem., 13, 1305, (1979).

(25) J. E. Lovelock. R. J. Maggs, and E. R. Adlard, Anal. Chem., 43, 1971 (1962).

(26) E. P. Grimsrud, and S. W. Warden, Anal. Chem., 52, 1842 (1980).

(27) S. W. Warden, R. J. Crawford, W. B. Knighton, and E. P. Grimsrud, Anal. Chem., 57, 659 (1985).

(28) E. Alge, N. G. Adams and D Smith J. Phys. B: At. Mol. Phys., 17, 3827 (1984).

(29) D. Smith, N. G. Adams, and E. Alge, J. Phys. B: At. Mol. Phys., 17, 461 (1984).

Literature Cited - Continued

(30) L. Wojnarovits and G. Foldiak, J. Chromatogr., 206 511 (1981).

(31) M. Dressler in "Selective Gas Chromatographic Detectors", Ed. by A. Zlatkis and C. F. Poole, Journal of Chromatography Library; Vol. 36, Elsevier Publ., Amsterdam, Netherlands (1986).

(32) H. J. Van de Wiel and P. Tommassen, J. Chromatogr., 71, 1 (1972).

(33) E. P. Grimsrud and R. G. Stebbins, J. Chromatogr., 155, 19 (1978).

(34) E. P. Grimsrud, D. A. Miller, R. G. Stebbins and S. H. Kim, J. Chromatogr., 197, 51 (1980).

(35) D. A. Miller and E. P. Grimsrud, Anal. Chem., 51, 851 (1979).

(36) J. A. Campbell, E. P. Grimsrud and L. R. Hageman, Anal Chem., 55, 1335 (1983).

(37) J. A. Campbell and E. P. Grimsrud, J. Chromatogr., 243, 1 (1982).

(38) R. A. Rasmussen, L. E. Rasmussen, M. A. K. Khalil and R.W. Dalluge, J. Geophys. Res., 286, 793 (1980).

(39) M. P. Phillips, R. E. Sievers, P. D. Goldan, W. C. Kuster and F. C. Fensenfeld, Anal. Chem., 51, 1819 (1979).

(40) D. A. Miller, personal communications, Michigan Tech. Univ., Houghton, Michigan, August 1986.

(41) W. B. Knighton and E. P. Grimsrud, Anal. Chem., 54, 1892 (1982).

(42) E. P. Grimsrud, S. H. Kim, and P. L. Gobby, Anal. Chem., 51, 223 (1979).

(43) R. E. Kaiser and R. I. Rieder in "Electron Capture Theory and Practice in Chromatography", Ed. by A. Zlatkis and C. F. Poole, Journal of Chromatography Library; Vol. 20, Chapter 6, Elsevier Publ., Amsterdam, Netherlands (1981).

(44) W. B. Knighton, Ph.D. Thesis, Montana State University (1984).

Literature Cited - Continued

(45) M. W. Siegel and W. L. Fite, J. Phys. Chem., 80, 2871 (1976).

(46) E. P. Grimsrud, Anal Chem., 56, 1797 (1984).

(47) P. Kebarle, Annu. Rev. Phys. Chem., 28, 445 (1977).

(48) M. Moet-Ner, J. Phys. Chem., 84, 2716 (1980).

(49) D. Bombick, J. D. Pinkston and J. Allison, Anal. Chem., 51, 851 (1971).

(50) D. A. Miller, Ph.D. Thesis, Montana State University (1980).

(51) W. E. Wentworth and E. Chen, J. Gas Chromatogr., 41, 170 (1967).

(52) A. G. Harrison "Chemical Ionization Mass Spectrometry", Chap. 2, CRC Press, Inc., Baco Raton, Florida (1983).

(53) C. A. Valkenburg, W. B. Knighton, and E. P. Grimsrud, J. High Resolut. Chromatogr. and Chromatogr. Commun., 9, 320 (1986).

(54) D. Smith and N. G. Adams in "Physics of Ion-Ion and Electron-Ion Collisions", ed. by F. Brouillard and J. W. McGowan, p. 501, Plenum Press, New York (1983).

(55) N. G. Adams, D. Smith, E. Alge, and J. Burdon, Chem. Phys. Let., 116, 460, (1985).

(56) M. J. Connolly, W. B. Knighton, and E. P. Grimsrud, J. Chromatogr., 265, 145 (1983).

(57) W. B. Knighton and E. P. Grimsrud, J. Chromatogr., 288, 237 (1984).

(58) E. P. Grimsrud, S. Chowdhury, and P. Kebarle, J. Chem. Phys., 83, 1059, (1985).

(59) L. J. Sears, personal communication, Montana State University (November 1986).

(60) L. G. Christophorou, Chem. Rev., 76, 409 (1976).

(61) L. G. Christophorou, R. A. Mathis, D. R. McCorkle, J. Phys., 14, 1889 (1981).

Literature Cited - Continued

(62) P. S. Drzaic and J. Brauman, J. Am. Chem. Soc., 104, 13 (1982).

APPENDIX

```
50  REM  INITIAL CONDITONS
51  TEXT
52 ETHCL = 0
53  INPUT "N(ETHYL CL) = 0, O.K.? ";YL
54  IF YL = 0 THEN  INPUT "N(ETHYL CL) = ";ETHCL
56 KETHCL = 1E - 9
57  INPUT "K(ETHYL CL) = 1E-9, O.K.? ";YK
58  IF YK = 0 THEN  INPUT "K(ETHYL CL) =  ";KETHCL
60 I = 2E10
62  INPUT "I=2E+10,  O.K.? ";YM
64  IF YM = 0 THEN  INPUT "I= ";I
66 K1 = 5E - 9
67  INPUT "K1 = 5E-9,  O.K.? ";YN
68  IF YN = 0 THEN  INPUT "K1 = ";K1
70 KREV = 1E4
71  INPUT "KREV = 1E4, O.K.? ";YO
72  IF YO = 0 THEN  INPUT "KREV = ";KREV
75 WRECOMB = 500
76  INPUT "RN+ = 500,  O.K.? ";YP
77  IF YP = 0 THEN  INPUT "RN+ = ";WRECOMB
80 F0 = 0
81  INPUT "BASELINE FREQ = 0,  O.K.? ";YQ
82  IF YQ = 0 THEN  INPUT "BASELINE FREQ = ";F0
84 INCT = 2E - 6
85  INPUT "INC T = 2E-6, O.K.?";YR
86  IF YR = 0 THEN  INPUT "INC T = ";INCT
88 NSAMPLE = 1E13
89  INPUT "NSAMPLE = 1E+13, O.K.?";YS
90  IF YS = 0 THEN  INPUT "NSAMPLE = ";NSAMPLE
96  INPUT "ARE ALL INITIAL CONDITIONS OK?";SQ
98  IF SQ = 0 THEN  GOTO 50
101 J = 0
102 NE = 0
103 C1 = 0
104 T = 0
105 C2 = 0
106 NNEGA = 0
107 NANLC = 0
108 S = 4 * 10 ^ 10
110 H = 0
111 XT = 1
113  DIM X(279,2)
```

Fig. 39. Resonance ECD computer modeling program.

```
119 C1 = C1 + 1
120  REM :CALC RATES FOR N(E) AND N(A-)
122 RE = (S + KREV * NNEGA) - ((K1 * NSAMPLE + WRECOMB) * NE)
126 RANEG = K1 * NSAMPLE * NE - (KREV + WRECOMB + KETHCL * ETHCL)
    * NNEG A
130  REM : CALC NEW N(E) AND N(A-)
134 NE = NE + RE * INCT
136 NNEGA = NNEGA + RANEG * INCT
140  REM   CALC T
142 T = T + INCT
144  IF J = 1 THEN  GOTO 350
150  REM  HAS: HAS STANDING CURRENT BEEN REACHED?
152  IF NE / T >  = I THEN  GOTO 119
154  IF J = 1 THEN  GOTO 376
155  IF KREV = 0 THEN  GOTO 200
160  REM : HAS N(A-) REACHED A CONSTANT VALUE?
162  PRINT NNEGA,(1 / T - F0) / NSAMPLE,T / INCT
164  IF NNEGA <  = NANLC * 1.00001 THEN  GOTO 200
170  REM : UPDATE N(A-) LAST CYCLE
171 C2 = C2 + 1
172 NANLC = NNEGA
180  REM : PULSE RESETS T AND N(E), BUT NOT N(A-)
182 NE = 0
184 T = 0
186  GOTO 120
200  REM : PRINT RESULTS
202 F = 1 / T
203  PRINT 0
206  PRINT "F =   ";F
208 FINCR = F - F0
210  PRINT "F(0) =  ";F0
212  PRINT "RESPONSE =  ";FINCR
214  PRINT "N(SAMPLE) =  ";NSAMPLE
215  PRINT "MOLAR RESPONSE =  ";FINCR / NSAMPLE
216  PRINT 0
217  PRINT "T =  ";T
218  PRINT "N(A-) =  ";NNEGA
220  PRINT "N(E) =  ";NE
222  PRINT "INC T =  ";INCT
224  PRINT "S =  ";S
226  PRINT "K(-1) =  ";KREV
228  PRINT "K(1) =  ";K1
```

Fig. 39 - Continued

```
230  PRINT "I =  ";I
231  PRINT "NE / T = ";NE / T
232  PRINT "RN+ =  ";WRECOMB
234  PRINT "T / INC T =  ";T / INCT
236  PRINT "#C1 LOOPS =  ";C1
238  PRINT "#C2 LOOPS =  ";C2
244  IF H = 1 THEN  GOTO 390
250  INPUT "WANT N VS T ARRAY TO BE MADE?";J
252  IF J = 0 THEN  STOP
254 X(0,0) = 0
255 X(0,1) = 0
256 X(0,2) = NNEGA
258  PRINT 0,0,NNEGA
260  GOTO 172
350 X(XT,0) = T
354 X(XT,1) = NE
358 X(XT,2) = NNEGA
362  PRINT T,NE,NNEGA
366 XT = XT + 1
370  IF XT < 279 THEN  GOTO 152
371  PRINT "ARRAY TOO SMALL"
372  STOP
376  INPUT "WANT RESULTS AGAIN?";H
378  IF H = 1 THEN  GOTO 200
380  GOTO 500
390  INPUT "WANT ARRAY AGAIN?";J2
392  IF J2 = 0 THEN  GOTO 500
400  FOR LW = 0 TO XT
404  PRINT X(LW,0),X(LW,1),X(LW,2)
406  NEXT LW
408  GOTO 376
500  INPUT "WANT PLOT OF NE, NA- VS T?";LY
510  IF LY = 0 THEN  END
520  HGR
522  HCOLOR= 3
531  LET NNEG = NNEGA
532  IF NE > NNEG THEN  GOTO 540
534  LET XDIV = NNEGA
538  GOTO 544
540  LET XDIV = NE
544  FOR GD = 0 TO T / INCT
560  LET PT = X(GD,0) / INCT
565  LET PE = 159 - X(GD,1) * 159 / XDIV
```

Fig. 39 - Continued

```
565  LET PE = 159 - X(GD,1) * 159 / XDIV
570  HPLOT PT,PE
575  LET PN = 159 - X(GD,2) * 159 / XDIV
580  HPLOT PT,PN
585  NEXT GD
588  HPLOT 0,0 TO 279,0 TO 279,159 TO 0,159 TO 0,0
594  PRINT "T=";T;" I=";I;" K1=";K1;" K-1=";KREV;" NS=";NSAMPLE;" NECL="
    ;ETHCL;" INC T=";INCT
600  END
```

VARIABLE NAME	TERM	UNITS
ETCl	[ETCL]	molecules/cc
KETHCL	R_2	$cc^{-1} * sec^{-1}$
I	Standing Current	electrons/sec
K1	k_1	$cc^{-1} * sec^{-1}$
KREV	k_{-1}	$cc^{-1} * sec^{-1}$
XRECOMB	R_1	sec^{-1}
WRECOMB	R_3	sec^{-1}
FO	Baseline Frequency	sec^{-1}
NSAMPLE	[Sample]	molecules/cc
INCT	Smallest time unit for integration	seconds
NNEGA	N_{A^-}	molecules/cc
NANLC	N_{A^-} last C1 loop	molecules/cc
NE	N_{e^-}	molecules/cc
RE	dN_{e^-}/dt	rate of change
RANEG	dN_{A^-}/dt	rate of change

Fig. 39 - Continued

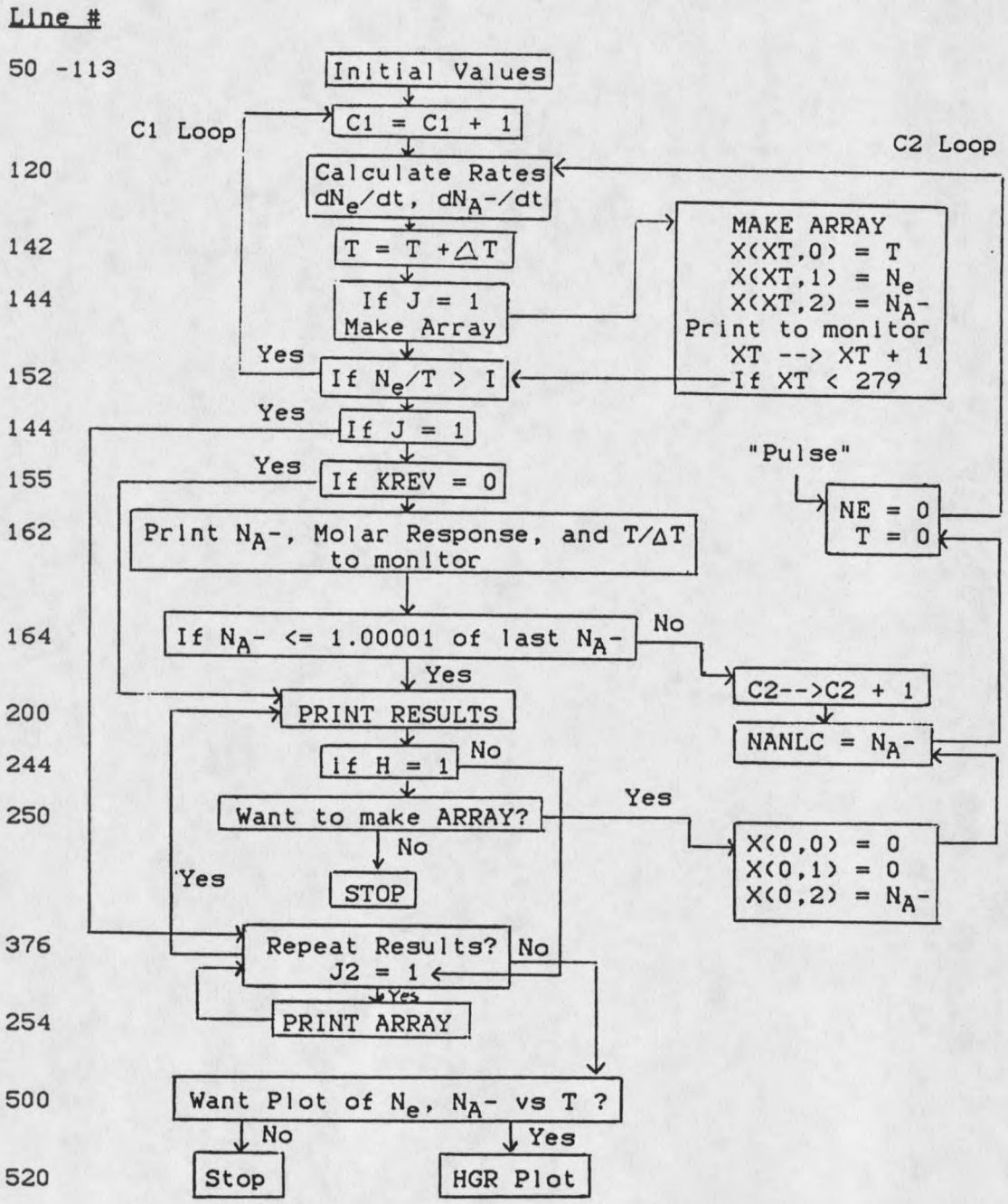

Fig. 40. Resonance ECD computer modeling flow chart.